P-N Bond Forming Reactions For The Synthesis of Phosphines

by

Matthew Wainwright

A **Doctoral Thesis** submitted
in partial fulfilment for the award of

Doctor of Philosophy of Loughborough University

Department of Chemistry,
Loughborough University,
Loughborough,
Leicestershire,
LE11 3TU.

Dedicated to my Mum and Dad.

Abstract

The reactions of dialkylureas and thioureas with chlorodiphenylphosphine yielded ligands of the type {Ph$_2$PN(R)}$_2$C=E, where R = Me or Et and E = O or S. Reaction of the ligands {Ph$_2$PN(Me)}$_2$C=O and {Ph$_2$PN(Et)}$_2$C=O with Pt(II), Pd(II) and Mo(0) resulted in the formation of square planar and octahedral chelate complexes, while {Ph$_2$PN(Et)}$_2$C=O also acted as a bridging ligand when reacted with Au(I). The coordination chemistry of {Ph$_2$PN(Me)}$_2$C=S was less predictable and reaction of the ligand with Pd(II) resulted in P-N bond cleavage and the formation of a five-membered heterocycle.

The ligand Cl$_2$PN(Et)N(Et)PCl$_2$ was readily synthesised from the reaction of 1,2-diethylhydrazine dihydrochloride and phosphorus trichloride. Subsequent reactions of the ligand with alcohols and Grignard reagents resulted in the formation of a range of aryloxy- and aryl-substituted phosphorus (III) hydrazides. Spectroscopic and single crystal X-ray crystallographic studies showed that the ligands reacted with Pt(II) and Pd(II) to form square planar, five-membered P,P' chelate rings.

Ligands of the type R$_2$PN(C$_2$H$_4$)$_2$NPR$_2$ and R$_2$PN(C$_5$H$_{10}$)NPR$_2$ were synthesised by the reactions of piperazine and homopiperazine with R$_2$PCl, where R$_2$ = Ph$_2$, -OC$_6$H$_4$O- and -OC$_2$H$_4$O-. Reaction of the ligands with Pt(II), Pd(II) and Mo(0) resulted in the formation of seven- and eight-membered P,P' chelate rings, while further reactions with Au(I) and Ru(II) resulted in the ligands acting as bidentate bridging ligands. Single crystal X-ray crystallographic studies on *cis*-[PdCl$_2$\{Ph$_2$PN(C$_2$H$_4$)$_2$NPPh$_2$\}] showed that the ligand forms an umbrella-like structure around the metal centre.

Results of tests performed to determine the ability of a number of the above ligands to promote the palladium catalysed formation of polyketone from CO and ethene were poor and in each case little or no polymeric material was produced

Acknowledgements

Contents

List of Figures

List of Tables

Abbreviations.

The following abbreviations are used throughout this thesis.

Å	Angstrom Unit, 10^{-10} m
^{t}Bu	t-butyl, $-C(CH_3)_3$
cat.	Catalyst
cm^{-1}	wavenumber
cod	cycloocta-1,5-diene, C_8H_{12}
^{o}	degrees
^{o}C	degrees centigrade
dmso	dimethyl sulfoxide, $(CH_3)_2SO$
dppe	diphenylphosphinoethane, $Ph_2P(CH_2)_2PPh_2$
dppm	diphenylphosphinomethane, $Ph_2PCH_2PPh_2$
E	chalcogen
Et	ethyl, $-C_2H_5$
FAB	fast atom bombardment
FT	Fourier transform
GC	Gas Chromatography
HFIPA	1,1,1,3,3,3-hexafluoroisopropyl alcohol
HOTf	Trifluoromethane sulfonic acid
HOTs	*p*-toluene sulfonic acid
Hz	Hertz
IR	infra-red
J	coupling constant, Hz
Mass Spec.	Mass Spectrometry
Me	methyl, $-CH_3$
MeO	Methoxy
m/z	mass-to-charge ratio
NMR	nuclear magnetic resonance
Ph	phenyl, $-C_6H_5$
PhO	phenoxy, $-OC_6H_5$
pip	piperidine

ppm	parts per million
^{i}Pr	i-propyl, -CH(CH$_3$)$_2$
thf	tetrahydrofuran, C$_4$H$_8$O
tht	tetrahydrothiophene
X	Halide

General Experimental Conditions.

Unless stated otherwise, all reactions were performed under an atmosphere of oxygen-free nitrogen using standard Schlenk procedures. All glassware was oven dried at 100 °C or flame dried under vacuum before use.

All solvents and reagents were purchased from Aldrich, Strem or Fisher and used as received In addition toluene, thf, Et_2O and petroleum ether (60-80) were distilled from sodium-benzophenone under nitrogen, and CH_2Cl_2 from CaH_2. $CDCl_3$ (99+ atom % D) was used as supplied.

^{31}P NMR (36.2, 101.25 MHz) were recorded on JEOL FX90Q and BRUKER AC250 spectrometers. Chemical shifts are reported relative to 85 % H_3PO_4 in H_2O on both spectrometers. Infra-red spectra were recorded as KBr discs on a Perkin Elmer System 2000 FTIR spectrometer. Microanalyses were carried out by the service at Loughborough University. FAB^+ mass spectra were recorded by the EPSRC mass spectrometry service at Swansea

Chapter 1

Introduction

1.1 *An introduction to the chemistry of phosphine ligands*

In the last three decades considerable progress has been made in the use of transition metal complexes in homogeneous catalysis [1,2] The preparation of stable complexes of transition metals in low oxidation states depends to a large extent on the use of strong π-acceptor ligands and throughout inorganic and organometallic chemistry few ligands have been as widely employed as tertiary mono- and di-phosphines [3-11] Ligand systems containing phosphines linked by alkyl chains, such as $Ph_2PCH_2CH_2PPh_2$ [bis(diphenylphosphino)ethane (dppe)] and $Ph_2PCH_2PPh_2$ [bis(diphenylphosphino)methane (dppm)], have been extensively studied due to their ability to coordinate to metal centres through the lone pair of electrons at one or both of the phosphorus centres.[12-14] However compared with the vast body of data accumulated on diphosphines in which the phosphorus nuclei are linked by a carbon atom or chain, considerably less has appeared on ligands where the backbone of the molecule comprises a heteroatom or group. Recently interest in diphosphazane ligands, $X_2PN(R)PX_2$, has grown rapidly as substituents on both phosphorus and nitrogen can be easily varied, resulting in changes in the P-N-P bond angle, the coordination behaviour of the ligands and the structural features of the resulting complexes.[15-18] Of these ligands $Ph_2PNHPPh_2$ [bis(diphenylphosphino)amine (dppa)], which is isoelectronic to dppm, has received the most attention[19] as it demonstrates a similar coordinative versatility to the methylene compound. Despite the recent interest in ligands of the type $X_2PN(R)PX_2$, the chemistry of the hydrazine analogues, $X_2PN(R)N(R)PX_2$, has remained largely unexplored and is limited to a few reports.[20-23]

1.2 *Phosphine derivatives of urea and thiourea*

The principal route to diphosphinoamines is the condensation of chlorophosphines with primary amines, or their trimethylsilyl derivatives, for example

the synthesis of dppa from the condensation of hexamethyldisilazane with chlorodiphenylphosphine (Equation 1.1).[19]

$$2Ph_2PCl + NH(SiMe_3)_2 \longrightarrow Ph_2PNHPPh_2 + 2Me_3SiCl$$

Equation 1.1
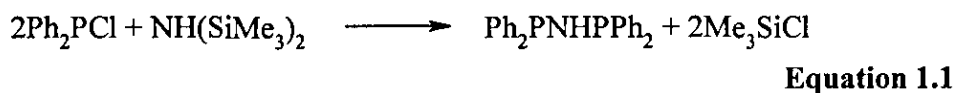
By a similar methodology, phosphorus-substituted derivatives of urea and thiourea can be prepared. The following brief overview of phosphorus-containing derivatives of urea and thiourea will concentrate on the chemistry of acyclic mono- and diphosphine derivatives.

1.2.1 *Urea derivatives*

The syntheses of diphosphines based on a urea skeleton were first reported in the mid 1960's, and were derived by condensation of isocyanates with diphenylphosphinic amide[24] or via phosphorus-substituted carbodiimides[25] (Equations 1.2 and 1 3).

Equation 1.2

$$Ph_2P(X)Cl + Ag_2CN_2 \xrightarrow{- 2AgX} Ph_2P(X)-N\!\!=\!\!\!=\!\!C\!\!=\!\!\!=\!\!N-P(X)Ph_2$$

X = lone pair, O or S

H_2O (X = O) or
H_2O_2 (X = lone pair)

Equation 1.3

14
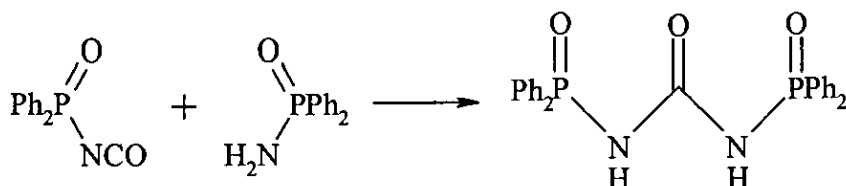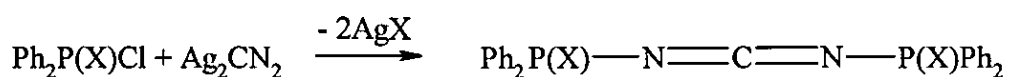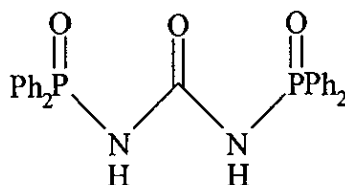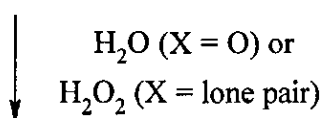
After these initial reports the field became dormant until interest in the compounds was rekindled in the 1980's when silylated starting materials became the precursor of choice. Schmutzler reported the synthesis of numerous diphosphine derivatives of urea from the reactions of chlorophosphines with N,N'-bis(trimethylsilyl)-N,N'-bis(dimethyl)urea (Equation 1.4).[26-31]

R = R' = F or Ph

R = Ph, Et, Me, ^{t}Bu or ^{i}Pr; R' = Cl   **Equation 1.4**

R = Ph; R' = ^{t}Bu
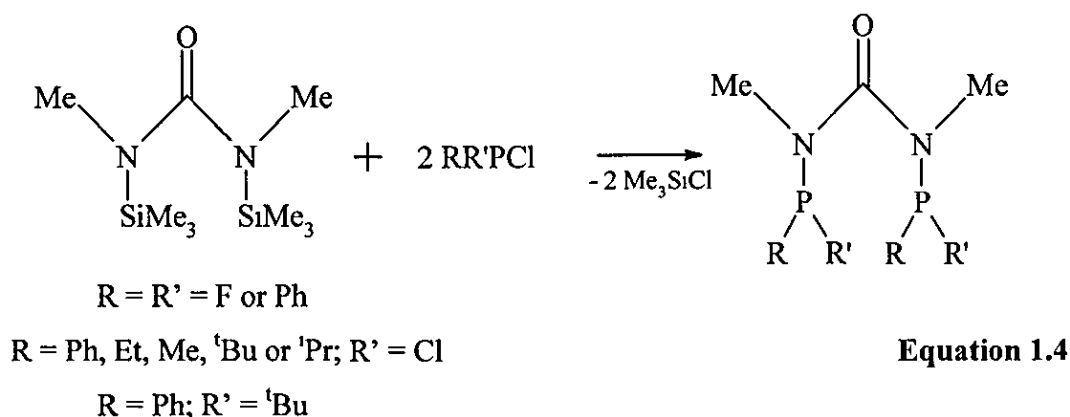
Experiments conducted between (Me$_3$Si)N(Me)C(O)(Me)N(SiMe$_3$) and PhPCl$_2$ in an NMR tube at − 45 °C show evidence of a two-step reaction[28] Upon warming the sample ^{31}P-{^{1}H} NMR studies show two strong signals, one representing the starting material PhPCl$_2$ and the other an intermediate product, and one weak signal representing the expected diphosphine product. However, in a spectrum recorded five minutes later at room temperature only the product Ph(Cl)PN(Me)C(O)(Me)NP(Cl)Ph was observed. On the basis of the above evidence Schmutzler *et al* suggested the following pathway for the reaction (Figure 1.1).

Schmutzler also reported that dehalogenation of the P-chloro substituted compounds with the bis(trimethylsilyl) ester of oxalic acid leads to mixed-valence heterocycles containing a P-P bond (Equation 1.5).[28,29]

R = Me, Et, ^{i}Pr or Ph   **Equation 1.5**

15
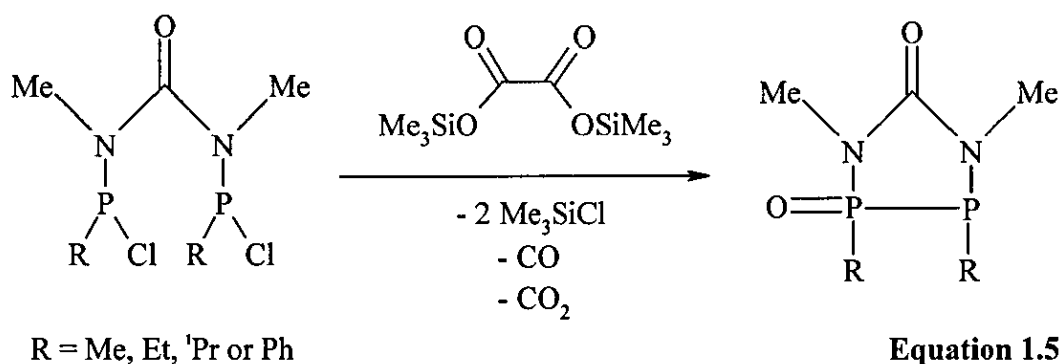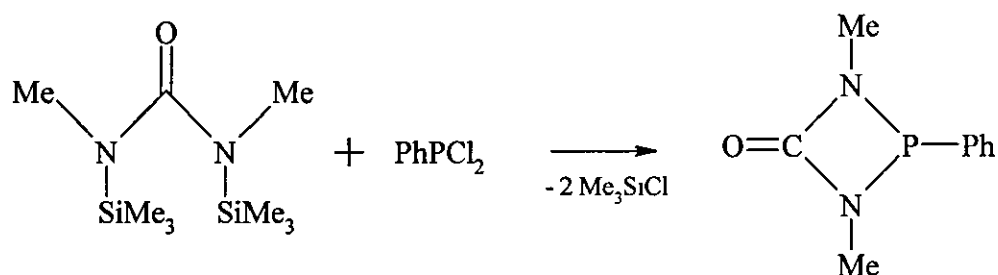
In a second step, insertion of $PhPCl_2$ into the P-N bond is suggested to occur
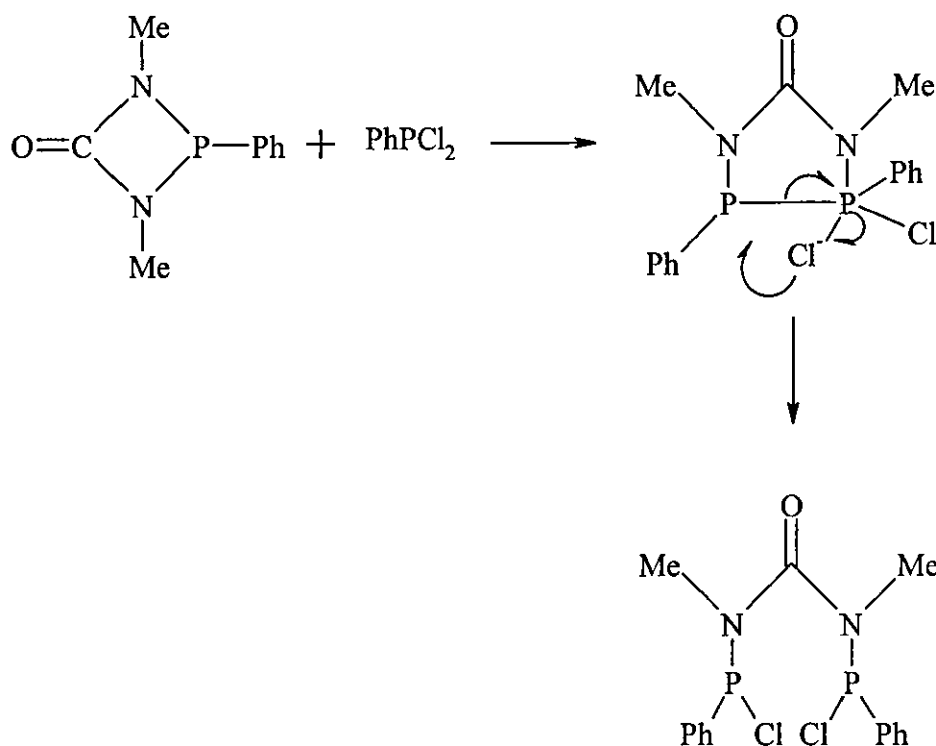
Figure 1.1 Reaction pathway for the synthesis of Ph(Cl)PN(Me)C(O)(Me)NP(Cl)Ph.

Reports of diphosphine derivatives of ureas are not only limited to examples involving N,N'-dimethyl substituted ureas. The reactions of F_2PCl with various N,N'-bis(trimethylsilyl)ureas at –30 to –25 °C have led to the synthesis of several N,N'-dialkyl diphosphines (Equation 1.6).[30]
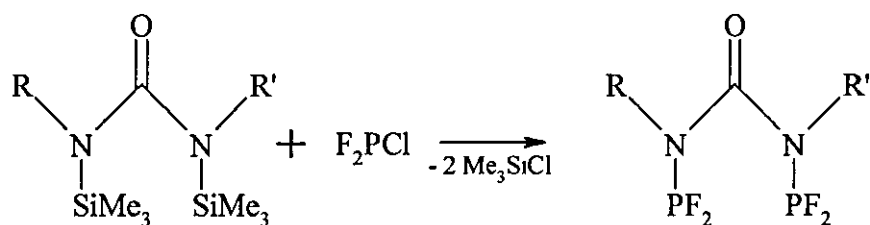
$$R = R' = H; \quad R = R' = Me; \quad R = Me, R' = Et, \qquad \textbf{Equation 1.6}$$
$$R = Me, R' = c\text{-}C_6H_{11}$$

More recently Woollins has described the synthesis of $\{Ph_2PN(H)\}_2CO$ via the reaction of chlorodiphenylphosphine with N,N'-bis(trimethylsilyl)urea.[32] Air- and moisture-tolerant $\{Ph_2PN(H)\}_2CO$ was found to be readily soluble only in Me_2SO, an observation which was attributed to the possibility of strong intermolecular hydrogen bonding between the carbonyl group and amine protons of adjacent molecules in the solid state. Oxidation of the ligand by hydrogen peroxide, sulfur or selenium leads to the phosphorus (V) derivatives $Ph_2P(E)NHC(O)NHP(E)Ph_2$ (E = O, S or Se).

1.2.2 *Coordination chemistry of diphosphine derivatives of ureas*

Examples of metal complexes containing linear diphosphine derivatives of ureas are rare. The diflurophosphine-substituted urea $\{F_2PN(Me)\}_2CO$ has been shown to form simple P,P' chelates when reacted with Ni^0, Rh^I and Ir^I [30,33] and the analogous ligand $\{F_2PN(H)\}_2CO$ forms six-membered chelate rings when reacted with Ni^0 and Mo^0 (Equations 1.7 and 1 8) [30] The reaction of $\{Ph_2PN(H)\}_2CO$ with $[ML_2(cod)]$ (L = Cl or Me, M = Pt or Pd) also proceeds smoothly with the displacement of cod and formation of the expected P,P' chelates (Equation 1.9) [32] The crystal structure of cis-$[PdCl_2\{Ph_2PNHCONHPPh_2\}]$ reveals the expected square planar geometry around the palladium centre and shows a puckered pseudo-boat-like six-membered PdP_2N_2C ring. The backbone of the ligand is involved in a pair of hydrogen bonds to adjacent molecules to form dimer pairs of molecules (Figure 1.2).[32]

17

Equation 1.7

R = H or Me
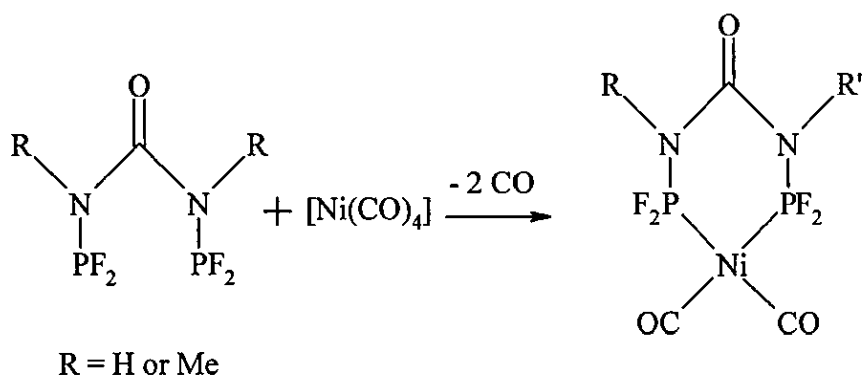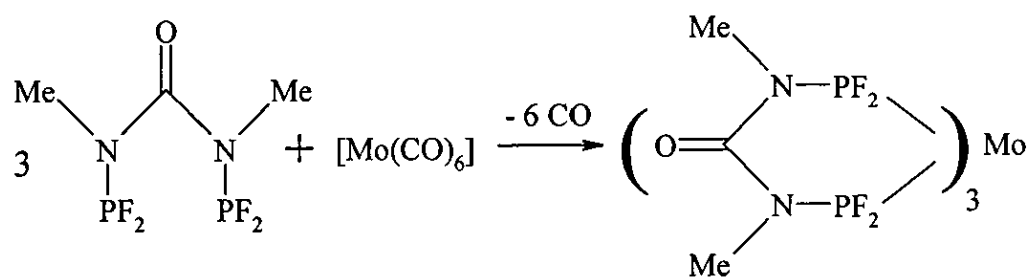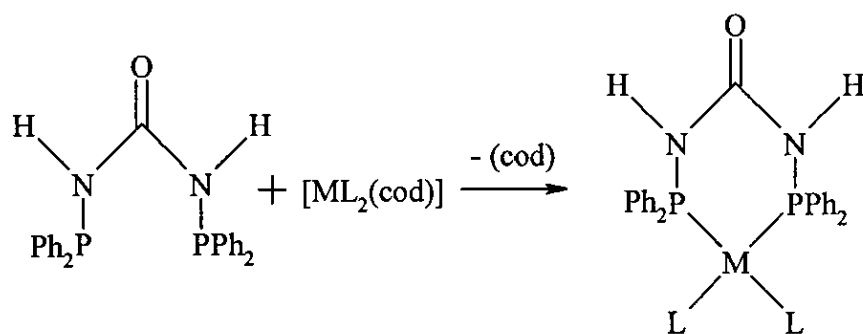
Equation 1.8

M = Pt or Pd; L = Cl or Me

Equation 1.9

In contrast to the above ligands, $\{(Bu^t)(Ph)PNMe\}_2CO$ displays a wider range of coordination modes (Equations 1.10, 1 11 and 1.12).[31]

(a)   (b)
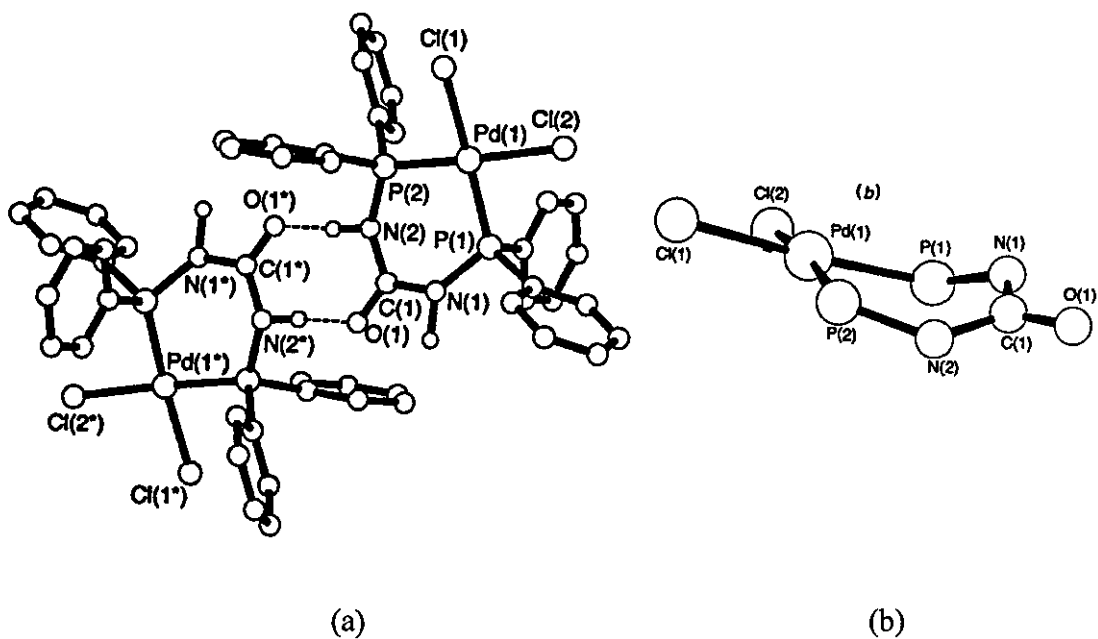
Figure 1.2 Crystal structure of cis-[PdCl$_2${Ph$_2$PNHCONHPPh$_2$}] (a) showing the dimer pair formation and (b) the core illustrating the pseudo-boat conformation of the ring [31]

Equation 1.10

Equation 1.11

M = Cr, Mo or W

Equation 1.12

19
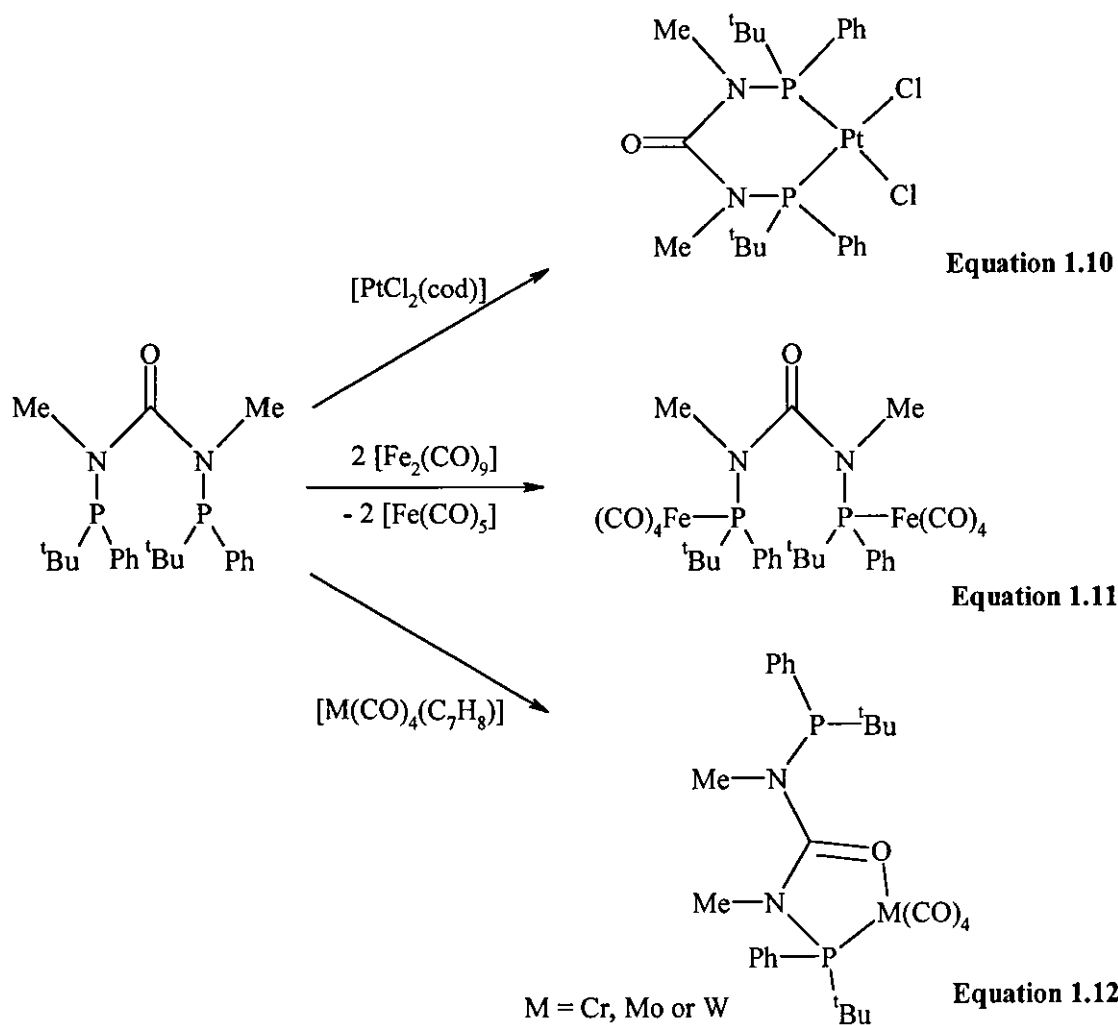
1.2.3 *Thiourea derivatives*

The chemistry of diphosphine–substituted thioureas remains relatively unexplored to date. Schmutzler reported that the monosulfide $Ph_2P-P(S)Ph_2$ was the only phosphorus-containing product from the reactions between Ph_2PCl and thiourea and Ph_2PCl and N,N'-bis(trimethylsilyl)thiourea (Equation 1.13) and proposed the formation of the product was due to carbodiimide elimination from the C=N isomer (Equation 1.14).[34]
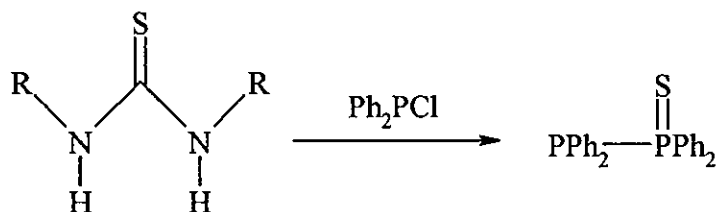
R = H or SiMe₃   **Equation 1.13**
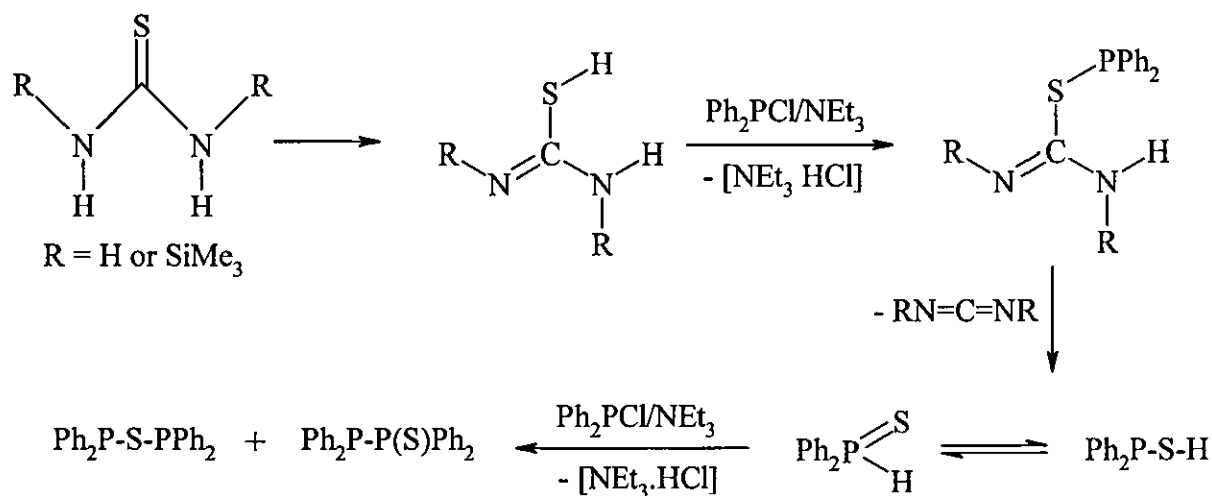
Equation 1.14

This theory was however disproved by Bhattacharyya *et al* who showed that at room temperature reaction of Ph_2PCl with thiourea in thf proceeds according to Equation 1.15 to give $Ph_2PNHC(S)NHPPh_2$.[32] Precipitation of $[NEt_3H]Cl$ accompanies the consumption of the insoluble thiourea and the supernatant solution turns green as the reaction proceeds. Removal of the salt by filtration, evaporation of the thf *in vacuo* and trituration of the resultant oil with ethanol gives the diphosphine in typically 46 %
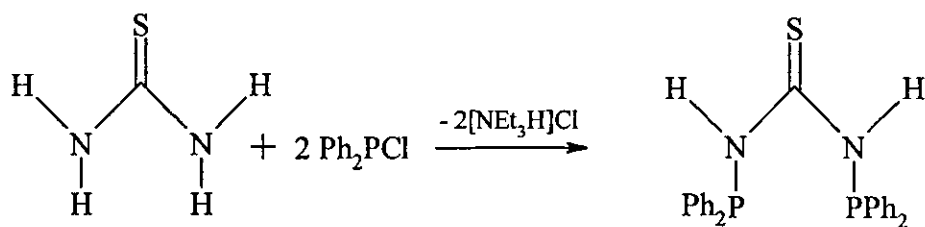
Equation 1.15

yield. Concentration of the ethanol filtrates leads to the isolation of more soluble by-products, of which $Ph_2P\text{-}P(S)Ph_2$ is the most abundant Bhattacharyya *et al* reported two minor differences between their synthetic procedure and the one employed by Schmutzler. Firstly, a shorter reaction time was employed (45 minutes *vs* 5 hours) and secondly addition of the chlorophosphine was performed at room temperature, as opposed to at -20 °C. Allowing a hot saturated Me_2SO solution of $Ph_2PNHC(S)NHPPh_2$ to cool slowly to room temperature gave crystals of $Ph_2PNHC(S)NHPPh_2.Me_2SO$ suitable for X-ray analysis (Figure 1.3).
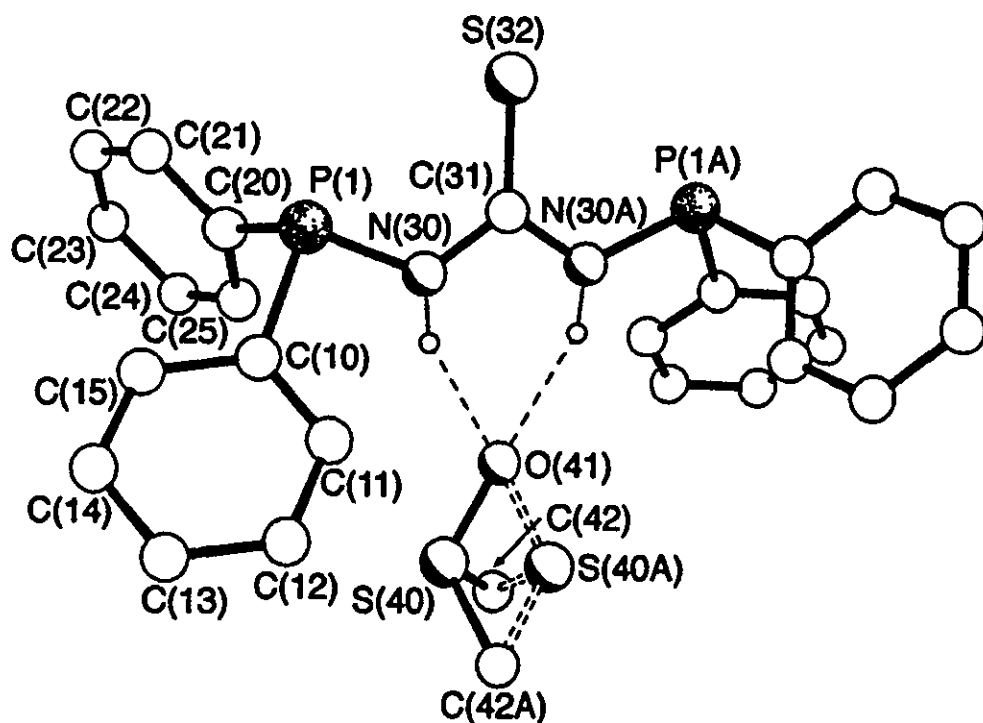
Figure 1.3 Crystal structure of $Ph_2PNHC(S)NHPPh_2 \ Me_2SO$.[32]

The molecule possesses crystallographic C_2 symmetry about the C-S bond and the PN(CS)NP backbone of the structure is planar (maximum deviation from the plane 0 003 Å). As with the analogous urea compound, $Ph_2PNHC(O)NHPPh_2$, oxidation of $Ph_2PNHC(S)NHPPh_2$ by sulfur proceeds in refluxing toluene to give the disulfide $Ph_2P(S)NHC(S)NHP(S)Ph_2$, however, unlike the urea compound, reaction of the thiourea derivative with H_2O_2 or selenium failed to give the respective dioxidised compounds Woollins also reported the synthesis of a mono-substituted derivative via the reaction of thiourea with one equivalent of Ph_2PCl.[35] Oxidation of $H_2NC(S)NHPPh_2$ is readily achieved with sulfur and selenium to give the compounds $H_2NC(S)NHP(S)Ph_2$ and $H_2NC(S)NHP(Se)Ph_2$ [36]

Schmutzler was more successful with substituted thioureas and was able to synthesise a number of mono- and bis-substituted derivatives of N,N'-dimethylthiourea via reaction with one or two equivalents of different chlorophosphines (Equation 1.16 and 1.17).[37,38]
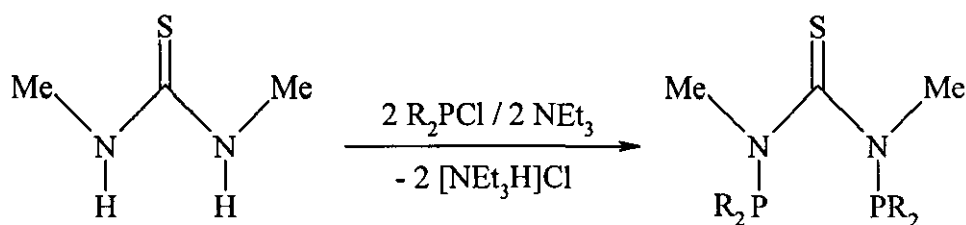
$R_2 = Ph_2$, $(OMe)_2$ or $-OCH_2CH_2O-$ **Equation 1.16**
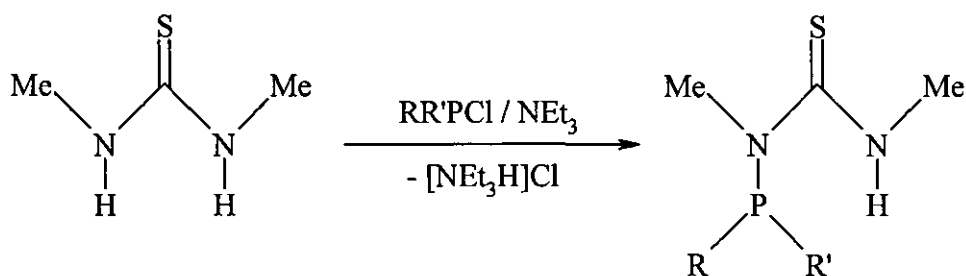
R = R' = Me; R = R' = OMe; R = Me, R' = Ph;   **Equation 1.17**
R = R' = ^{i}Pr; R = R' = O^{i}Pr; R = ^{t}Bu, R' = Ph;
R = R' = Ph; R-R' = -OCH$_2$CH$_2$O-

Schmutzler and co-workers also reported the synthesis of unsymmetrical diphosphine derivatives of N,N'-dimethylthiourea via reaction of $Ph_2PN(Me)C(S)N(Me)H$ with F_2PCl and Me_2PCl (Equation 1.18).[39]
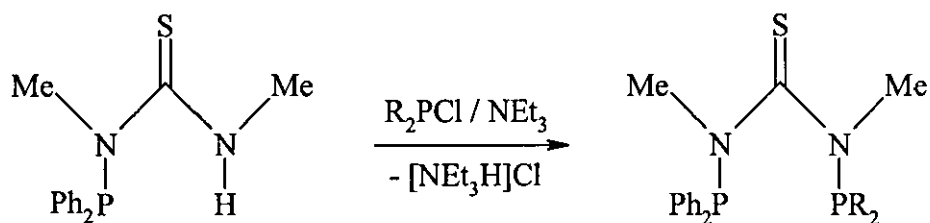
R = F or Me   **Equation 1.18**

1.2.4 *Coordination chemistry of phosphine derivatives of thiourea*

Of the above examples of mono- and bis-substituted phosphine derivatives of thiourea the only reports of metal complexes containing such ligands are those involving $H_2NC(S)NHPPh_2$ and $H_2NC(S)NHP(S)Ph_2$.[35,36] The reaction of two equivalents of the ligand $H_2NC(S)NHPPh_2$ with $[PtCl_2(cod)]$ results in the formation of the bis-chelate metal complex $[Pt\{H_2NC(S)NHPPh_2\}_2]^{2+}$ $2Cl^-$ (Equation 1.19).[35]
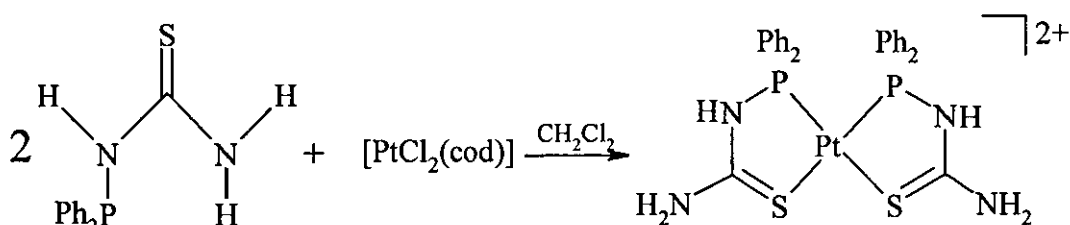
                                                                              Equation 1.19

The X-ray crystal structure of the complex confirms that the two ligands are bonded to the platinum atom by the sulfur and phosphorus groups to give five-membered Pt-S-C-N-P rings. Reaction of the oxidised ligand $H_2NC(S)NHP(S)Ph_2$ with KOtBu in thf at room temperature gives $K[H_2NC(S)NP(S)Ph_2]$ which in turn reacts with Zn^{II} and Pt^{II} salts to yield bis-chelate metal complexes (Equations 1 20 and 1.21 and Figures 1.4 and 1.5). Surprisingly, reaction of $H_2NC(S)NHP(S)Ph_2$ with $[PtCl_2(cod)]$ failed to give the expected six-membered chelate complex $[PtCl_2\{H_2NC(S)NHP(S)Ph_2\}]$ and instead resulted in the bis-chelate

23

[Pt{H₂NC(S)NHP(S)Ph₂}{H₂NC(S)NP(S)Ph₂}]Cl containing one neutral and one deprotonated ligand. The crystal structure of the complex shows that the two chelates are bound to the platinum atom by the four sulfur donor atoms, forming two six-membered rings in the *trans* configuration (Figure 1.6).

$$ZnCl_2 + 2\ K[H_2NC(S)NP(S)Ph_2] \longrightarrow [Zn\{H_2NC(S)NP(S)Ph_2\}_2] + 2\ KCl$$

Equation 1.20

$$[PtCl_2(cod)] + 2\ K[H_2NC(S)NP(S)Ph_2] \longrightarrow [Pt\{H_2NC(S)NP(S)Ph_2\}_2] + 2\ KCl$$
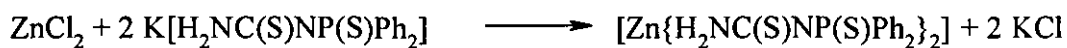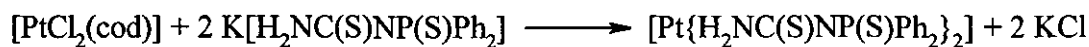
Equation 1.21
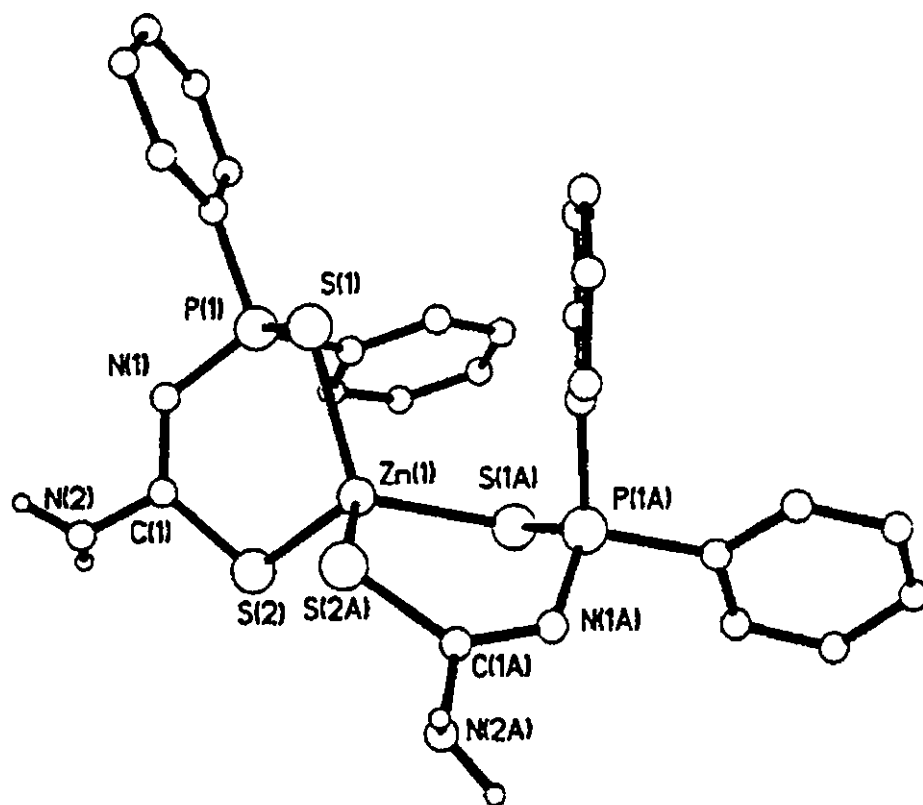
Figure 1.4 Crystal structure of [Zn{H₂NC(S)NP(S)Ph₂}₂].[36]

24
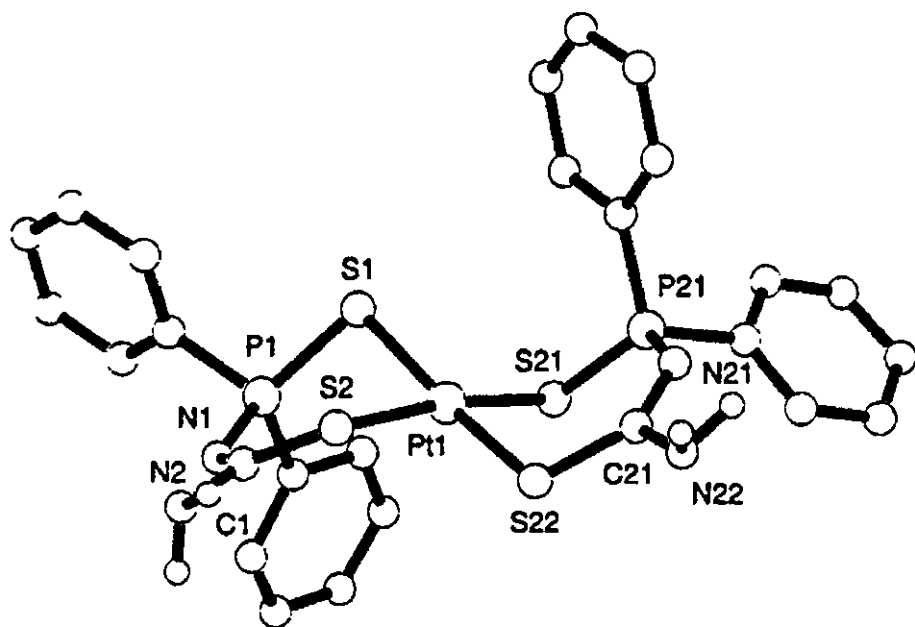
Figure 1.5 Crystal structure of *cis*-[Pt{H₂NC(S)NP(S)Ph₂}₂] [36]
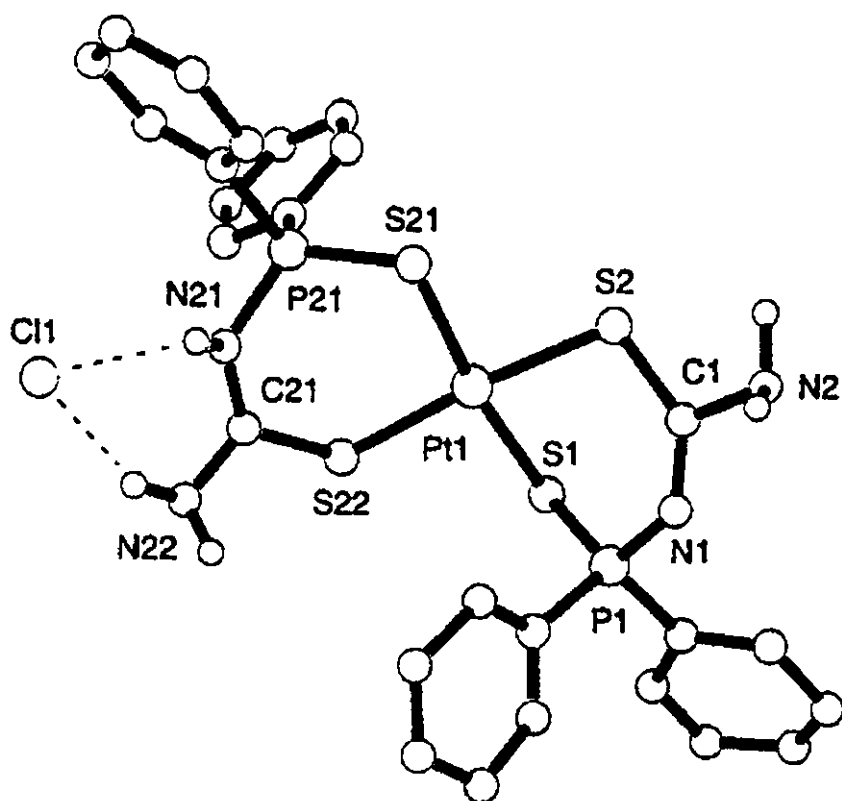
Figure 1.6 Crystal structure of *trans*-
[Pt{H₂NC(S)NHP(S)Ph₂}{H₂NC(S)NP(S)Ph₂}]Cl [36]

1.3 *Phosphine derivatives of hydrazine*

As mentioned earlier the chemistry of phosphorus-nitrogen compounds containing phosphorus-hydrazine backbones has received little attention when compared to ligands of the type $X_2PN(R)PX_2$.[20-23] The following brief overview summarises the developments in the chemistry of P(III) hydrazides.

1.3.1 *Synthesis of phosphorus(III) hydrazides*

The synthesis of acyclic phosphorus (III) hydrazides was pioneered in the 1970's by Gilje *et al*[21] and Nöth *et al*[40] who reported the synthesis of 1,2-bis(dichlorophosphino)dimethylhydrazine through (i) the condensation of PCl_3 with 1,2-dimethylhydrazine at -196 °C and (ii) the reaction of the cage compound $P[N(Me)N(Me)]_3P$ with PCl_3, both methods giving the product in 15-20 % yield. Despite these reports there was little interest in the field until Katti *et al.*, continuing their studies of main group metal hydrazides,[41-46] reported the development of a one-step, straightforward and high-yield synthetic route to $Cl_2PN(Me)N(Me)PCl_2$. The new route involved the treatment of PCl_3 with 1,2-dimethylhydrazine dihydrochloride (Equation 1.22).[47]

$$H(Me)NN(Me)H.2HCl + excess\ PCl_3 \longrightarrow Cl_2PN(Me)N(Me)PCl_2 + 4HCl$$
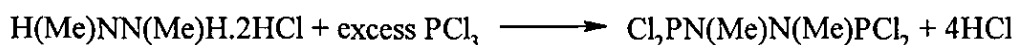
Equation 1.22

Phosphorus trichloride was used as both solvent and reactant, and the mixture was refluxed for 36 hours to obtain the desired product as a colourless viscous oil in 92 % yield. $Cl_2PN(Me)N(Me)PCl_2$ can then be used as a chloro precursor and undergoes facile nucleophilic substitution reactions with alkoxides and Grignard reagents to produce a broad range of alkoxy-, aryloxy- and aryl-substituted phosphine hydrazides (Figure 1.7).[48,49]

26
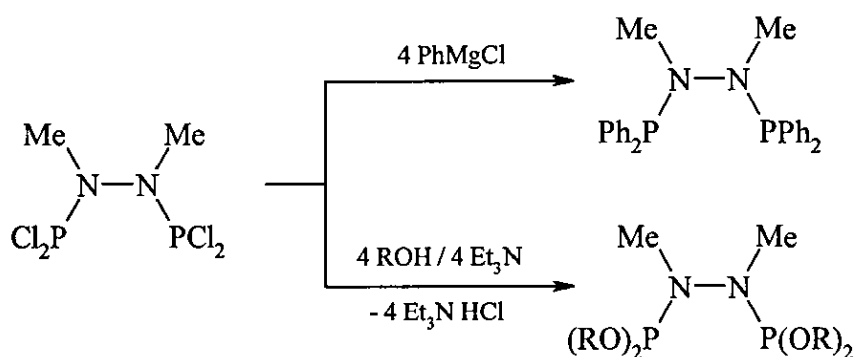
$R = Me$; Et; CH_2CF_3; $(CH_2)_7CH_3$;

$CH_2CH=CH_2$; ^iPr; Ph, C_6H_4Br-p

or o-$C_6H_4(CH_2CH=CH_2)$

Figure 1.7 Diphosphine derivatives of N,N'-dimethylhydrazine

Reddy *et. al.* reported that the cyclic phosphorus hydrazides $RP[N(Me)N(H)]_2PR$ (R = Et, Ph and ^tBu) can be prepared by the reaction of $RPCl_2$ with four equivalents of methylhydrazine (Equation 1.23).[50]

$$RPCl_2 + 4\ MeHNNH_2 \longrightarrow$$

$R = Et$, Ph or ^tBu
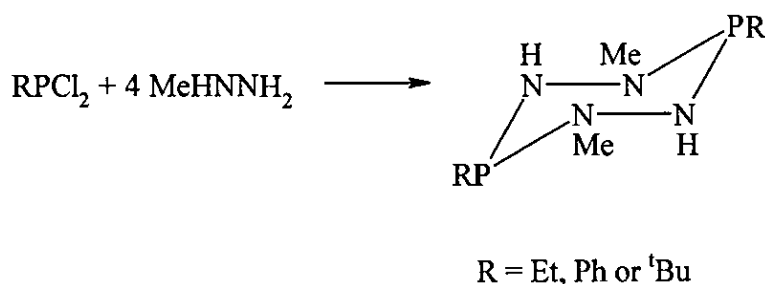
Equation 1.23

^{31}P-$\{^1H\}$ NMR spectroscopy indicates that the Ph and ^tBu derivatives exist in the chair conformations in solution, yet the ethyl analogue exists in both the chair and boat conformations. Reddy *et al* also reported that $PhP[N(Me)N(H)]_2PPh$ can be used as a synthon for the synthesis of novel tetraphosphines via reactions with phosphorus (III) halides (Figure 1.8)[51] The new tetraphosphine represents the first

example of a compound that combines the phosphinoamine, [P-N-P], and phosphorus (III) hydrazide, [P-N-N-P], functionalities in a single molecular framework.
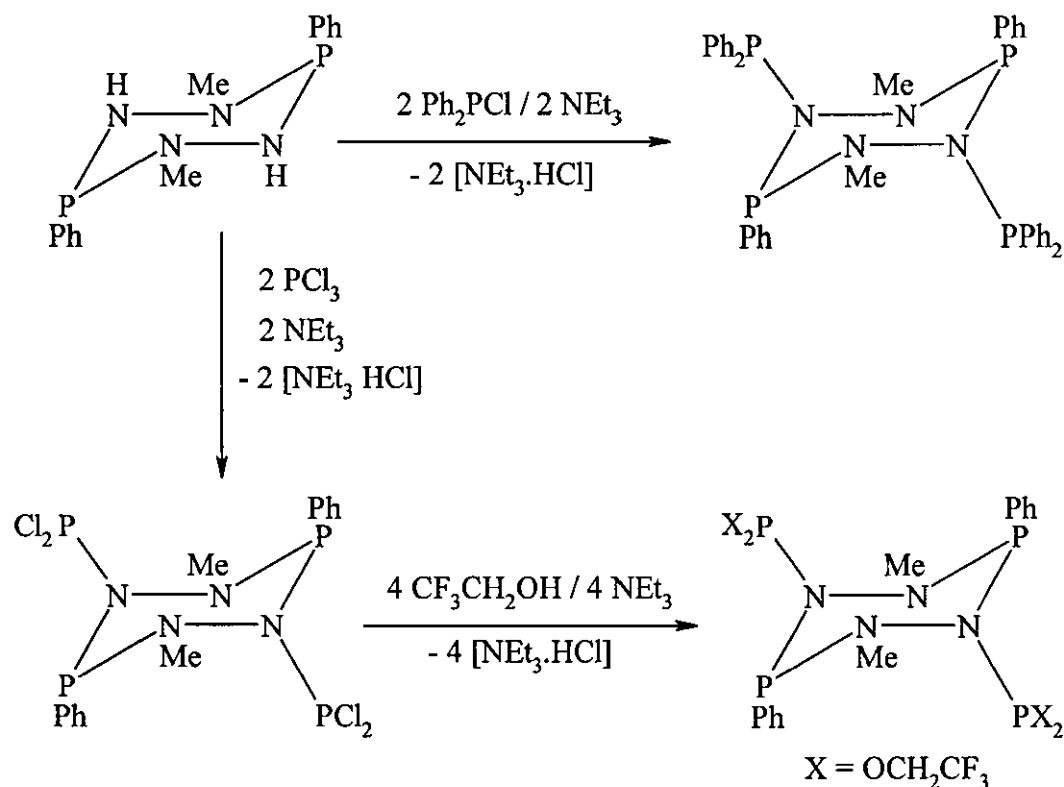
Figure 1.8 Synthesis of novel tetraphosphines.

The reaction of Ph$_2$PCl with [PhPN(Me)N(H)]$_2$ in the presence of Et$_3$N at 25 °C results in the new heterocyclic phosphorinane [PhPN(Me)N(PPh$_2$)]$_2$ in 84 % yield The alkoxy derivative, [PhPN(Me)N(P(OCH$_2$CF$_3$)$_2$)]$_2$ was synthesised by the treatment of [PhPN(Me)N(H)]$_2$ with PCl$_3$ in the presence of Et$_3$N to produce the intermediate [PhPN(Me)N(PCl$_2$)]$_2$ followed by reaction with CF$_3$CH$_2$OH. Both compounds were isolated as air-stable, white crystalline solids.[50]

1.3.2 *Coordination chemistry of phosphorus (III) hydrazides*

Katti and co-workers reported that the phosphorus (III) hydrazides described in Figure 1.7 react cleanly with Group 6 metal carbonyls to produce mono-nuclear Mo^0 and W^0 complexes (Equation 1.24).[23,47]
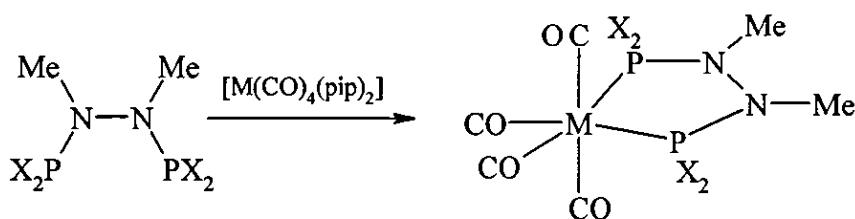
$$M = \text{Mo or W}; \quad X = OCH_2CF_3 \text{ or OPh}$$

Equation 1.24

IR spectroscopic data for the complexes and X-ray crystallographic data (for M = W, X = OPh) confirmed the *cis* nature of the carbonyl ligands around the Mo^0 and W^0.

Reactions of [X$_2$PN(Me)N(Me)PX$_2$] with Pt^{II} and Pd^{II} also proceed smoothly to yield a range of *P,P'* chelate complexes (Equation 1.25).[23,47,48] Reaction of equimolar quantities of ligand with [PtCl$_2$(cod)] or [PdCl$_2$(PhCN)$_2$] results in the formation of the complexes in good yield. The X-ray crystal structures of [PtCl$_2${(RO)$_2$PN(Me)N(Me)P(OR)$_2$}], R = Ph or o-C$_6$H$_4$(CH$_2$CH=CH$_2$), confirm that in each case the platinum is in the expected square planar environment and the ligand chelates in a *cis* nature to form a five-membered metallacycle (Figure 1 9)[48]
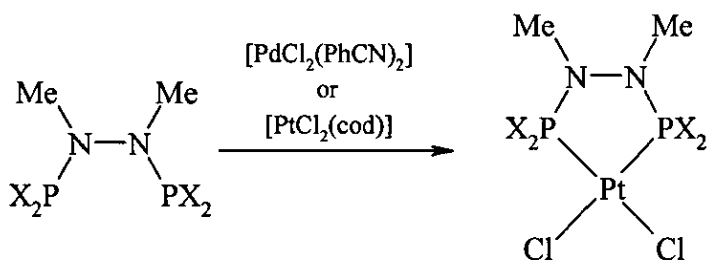
$X = Cl, OCH_2CF_3, O^iPr, OPh, OC_6H_4Br\text{-}p$ M = Pt or Pd

     or o-C$_6$H$_4$(CH$_2$CH=CH$_2$)   **Equation 1.25**

29
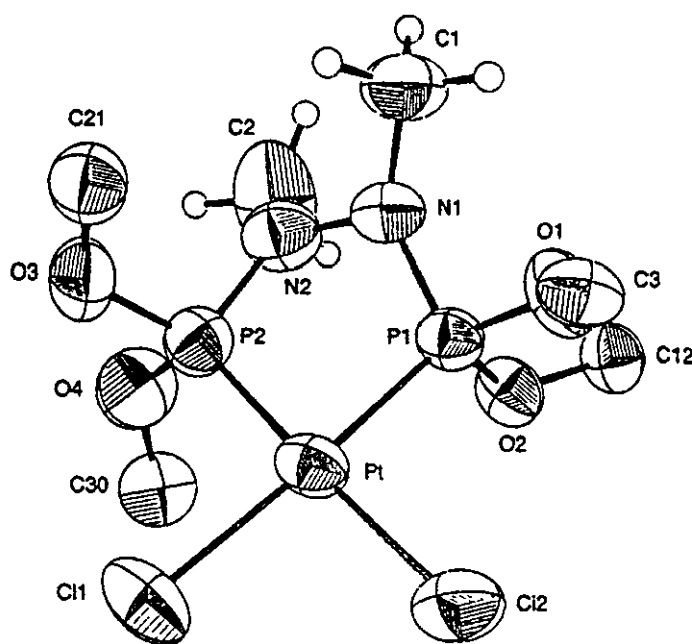
Figure 1.9 Crystal structure of *cis*-[PtCl$_2$\{(RO)$_2$PN(Me)N(Me)P(OR)$_2$\}], R = *o*-C$_6$H$_4$(CH$_2$CH=CH$_2$), (Phenyl ring atoms are omitted for clarity).[48]

The ligands [(RO)$_2$PN(Me)N(Me)P(OR)$_2$] (where R = CH$_2$CF$_3$ or Ph) react with [RhCl(CO)$_2$]$_2$ to produce chloro-bridged dimers in near quantitative yields (Figure 1.10).[14] The chloride bridge in the dimers can be readily cleaved upon reactions with triaryl phosphines or arsines and the five-membered P-N-N-P-Rh rings retained (Figure 1.10). The resulting compounds can be thought of as 'hybrids' to the Wilkinson catalyst [RhCl(PPh$_3$)$_3$] and variations of the substituents on the phosphorus-hydrazine backbone may afford complexes for potential catalytic applications.[23]
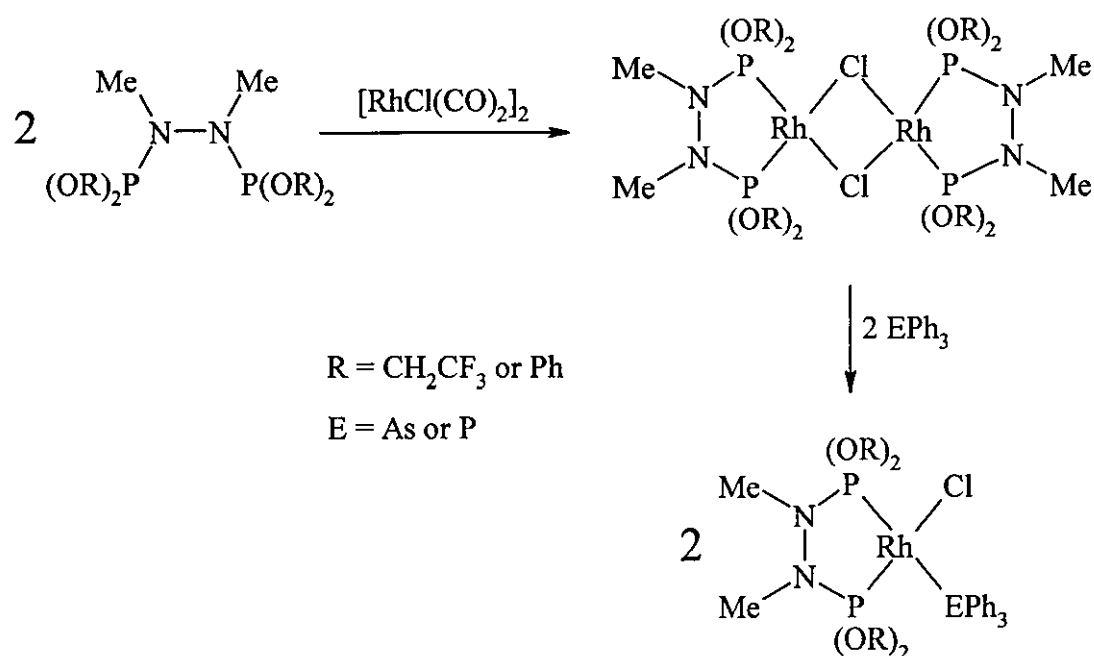
Figure 1.10 Reaction of [(RO)$_2$PN(Me)N(Me)P(OR)$_2$] (R = CH$_2$CF$_3$ or Ph)

Cyclic phosphorus hydrazides can be used as functionalised phosphines for reactions with transition metal precursors. The presence of two trivalent phosphorus centres in the compounds RP[N(Me)N(H)]$_2$PR (R = Et and Ph) presents the possibility of using them as bidentate ligands Both compounds react smoothly with two equivalents of [Mo(CO)$_4$(pip)$_2$] to give the binuclear complexes [{Mo(CO)$_4$(pip)}$_2${μ-[RPN(Me)N(H)]$_2$}] (Equation 1 26).[50]
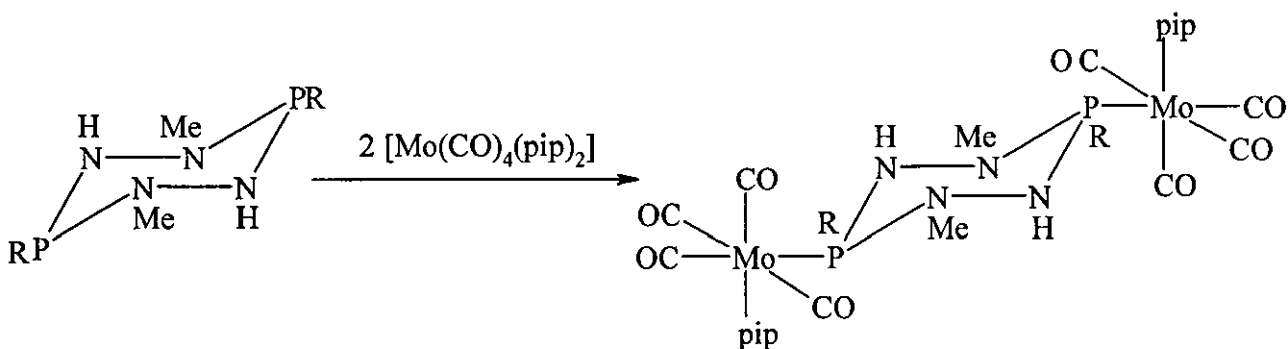
R = Et or Ph

Equation 1.26

Reddy *et al* reported that the tetraphosphine ligands [PhPN(Me)N(PPh$_2$)]$_2$ and [PhPN(Me)N(P(OCH$_2$CF$_3$)$_2$)]$_2$ react successfully with a number of transition metals compounds to yield four-membered metallacyclic complexes (Equations 1.27 and 1.28).[51]
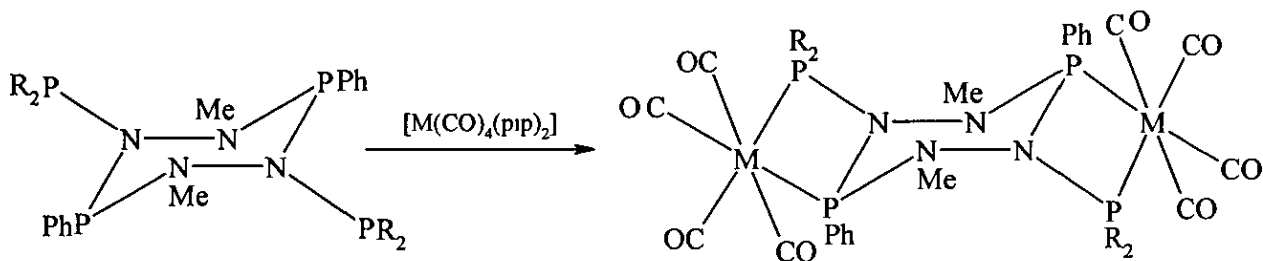
M = Mo or W; R = Ph or OCH$_2$CF$_3$ **Equation 1.27**
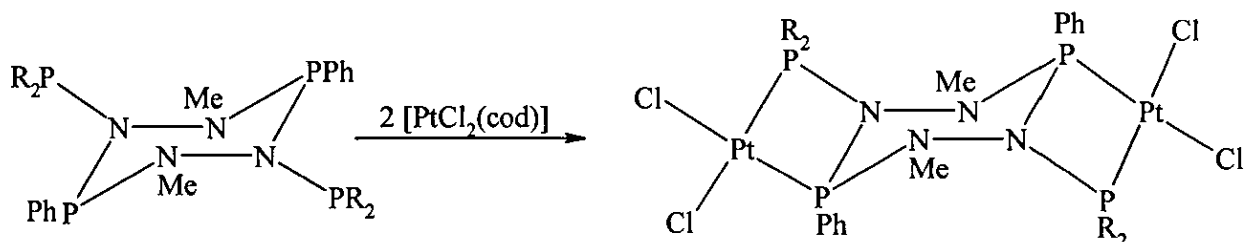
R = OCH$_2$CF$_3$ **Equation 1.28**

The X-ray crystal structure of [{W(CO)$_4$}$_2$\{μ-[PhPN(Me)N(P(OCH$_2$CF$_3$)$_2$)]$_2$\}] confirms that the preferred mode of coordination of the ligand is via the P-N-P functionality

1.4 *Phosphine derivatives of piperazine*

Reports of reactions involving piperazine [HN(C$_2$H$_4$)$_2$NH] and Ph$_2$PCl are limited to a few examples[52,53]. It was reported in a Japanese patent that the reaction of piperazine with Ph$_2$PCl, in benzene, results in the mono-substituted product Ph$_2$PN(C$_2$H$_4$)$_2$NH.[53] However, when repeating the reaction Thomas *et al* reported that the compound formed is the bis-substituted product Ph$_2$PN(C$_2$H$_4$)$_2$NPPh$_2$ and not Ph$_2$PN(C$_2$H$_4$)$_2$NH.[52] No coordination chemistry was described for the bis-substituted product Ph$_2$PN(C$_2$H$_4$)$_2$NPPh$_2$.

1.5 *Development of the use of tertiary phosphine ligands in the transition metal-catalysed copolymerisation of CO and ethene*

As mentioned at the start of the chapter, considerable process has been made recently in the use of transition metal complexes in homogeneous catalysis, for example, olefins (*e g* ethylene and propylene) are readily polymerised by a variety of homogeneous catalysts to give polyolefins (*e g* polyethylene and polypropylene), while spectacular improvements in catalyst activity have been reported for the rhodium catalysed carbonylation of methanol[54]. Another area of homogeneous catalysis which has received considerable interest from both academia and industry over the last decade is the alternating copolymerisation of carbon monoxide and ethene (Equation 1.29).[55,56,57]

$$= \; + \; CO \; \xrightarrow{cat} \; \left(\!\! \begin{array}{c} O \\ \| \\ \end{array} \!\!\! \right)_n$$
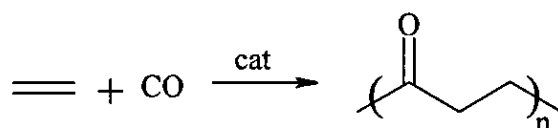
<div align="right">**Equation 1.29**</div>

These copolymers are of interest for four reasons.[55] Firstly, as a monomer carbon monoxide is particularly plentiful and inexpensive, and secondly, the presence of the carbonyl group in the backbone makes these copolymers photodegradable.[58] A third reason is that, because of the ease with which the carbonyl group can be chemically modified, the polyketones serve as excellent starting materials for other classes of functionalized polymers. In fact, approximately two dozen polymers incorporating a variety of functional groups have been previously synthesised from the CO/ethene coploymer.[59] Finally, specific interest in the alternating CO/ethene copolymer stems from its high mechanical strength, which results from its high crystallinity.[60]

Nickel was the first transition metal used to catalyse the copolymerisation of CO and ethene. In the late 1940s, Reppe and Magin[61,62] showed that $K_2Ni(CN)_4$ in water produced low-melting point oligomers of ethene and CO in addition to diethyl ketone and propionic acid. In the early 1970s Shell Development succeeded[63,64] in improving the catalyst by the addition of strong acids such as HOTf and HOTs in solvents such as HFIPA. They were able to obtain a polymer with a relatively high molecular weight, but the yield of polymer per gram of catalyst remained low.

Palladium catalysts for alternating polyketone formation were first reported by Gough at ICI in 1967[65,66] and consisted of bis(tertiaryphosphine)palladium dichloride complexes which yielded polyketone at a rate of around 300 g (g of Pd)$^{-1}$ h^{-1}. However these catalysts required severe operating conditions (250 °C, 2000 bar) and the yield of polymer per gram of palladium was low. It was not until the 1980s that advances occurred which opened the way for efficient synthesis of polyketone. Firstly, Sen and co-workers[67,68] published work which showed that certain tertiary phosphine palladium complexes containing the weakly coordinating tetrafluoroborate anion in dichloromethane produced polyketone under very mild conditions. Secondly, at Shell Research cationic palladium complexes containing tertiary phosphine ligands and weakly coordinating anions were studied in methanol as catalysts for the methoxycarbonylation of ethene to give methyl propionate. A surprising and remarkable change in selectivity was observed, by Drent and co-workers, when the triphenylphosphine ligands were replaced by cis-chelating bidentate phosphine ligands. Under the same conditions, no methyl propionate product was formed, instead high molecular-weight, perfectly alternating (CO/ethene) polyketone was formed at very high rates (ca 6000 g (g of Pd)$^{-1}$ h^{-1}. These catalysts proved very active and yields (in g of polymer/g of palladium) above 10^6 were achieved under economically attractive, mild reaction conditions (85 °C, 45 bar).[56,69-72] It was subsequently discovered that variation of the bidentate ligand results in significant changes in both the reaction rate and the molecular weight of the product, for example, the reaction rate achieved when using dppp as the diphosphine is approximately six times that achieved when dppe is the chelate.[73] As a consequence of this discovery, a great number of studies on the synthesis and coordination chemistry of many different ligand systems have taken place over the past two decades. Initial investigations centred on ligands containing a P-C-P framework and more recently there has also been considerable interest in ligands containing P-N-P linkages The ease of the formation of the P-N bond, through reaction of chlorophosphines with amines, offers scope for the synthesis of many different chelating ligands and subtle variations of the substituents on both the P and N atoms can have a marked effect on the electronic and steric properties of any resulting metal complexes.

1.6 *The mechanism for the palladium-catalysed copolymerisation of CO and ethene*

1.6.1 *Propagation*

It is thought that the catalytically active species in polyketone formation is a d^8 square-planar cationic complex L_2PdP^+, where L_2 represents the bidentate ligand and P^+ is the growing polymer chain. The fourth coordination site at palladium may be filled by an anion, a solvent molecule, a carbonyl group of the chain (*vide infra*), or a monomer molecule.

The two alternating propagation steps are migratory insertion of CO into the palladium-alkyl bond (Equation 1.30)[74] and migratory insertion of ethene into the resulting palladium-acyl bond (Equation 1.31).[73] Propagation errors (double CO or ethene insertion) are not observed.

$$L_2PdCH_2CH_2P^+ \xrightarrow{\ CO\ } L_2PdCOCH_2CH_2P^+$$

Equation 1.30

$$L_2PdCOP^+ \xrightarrow{\ C_2H_4\ } L_2PdCH_2CH_2COP^+$$
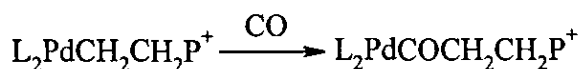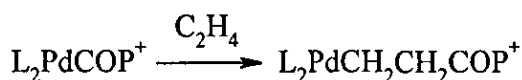
Equation 1.31

1.6.2 *Initiation and termination*

End group analysis of the CO/ethene copolymer by ^{13}C NMR has demonstrated the presence of 50 % ester ($-COOCH_3$) and 50 % ketone ($-COCH_2CH_3$) groups while GC and MS analyses of the oligomer fractions show, in addition to the expected keto-ester product (**2**), the presence of diester (**3**) and diketones (**4**) compounds.

$$CH_3CH_2-(-COCH_2CH_2-)_n-COOCH_3 \qquad n \geq 0$$

2 keto-ester

$$CH_3O-(-COCH2CH2-)_n-COOCH_3 \qquad n \geq 1$$

3 diester

$$CH_3CH_2-(-COCH_2CH_2-)_n-COCH_2CH_3 \qquad n \geq 0$$

4 diketone

35
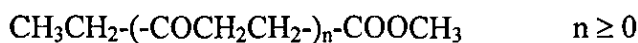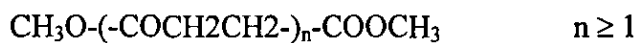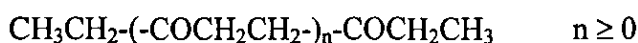
At low temperatures ($\leq 85\ ^\circ$C), the majority of the products are keto-esters with small quantities of diesters and diketones, however, significantly larger quantities of the latter two products are observed when the temperature of the reaction is increased. This observation has been explained[13c2] by assuming two initiation and two termination mechanisms for polyketone formation. The first initiation mechanism produces ester end groups and starts with a palladium carbomethoxy species,[13,18c2] which can be formed either by CO insertion in a palladium methoxide or by direct attack of methanol on coordinated CO (Equation 1.32).

$$CO \nearrow \quad L_2PdCO^{2+} \quad \overset{CH_3OH}{\underset{H^+}{\diagup}}$$

$$L_2Pd^{2+}$$
$$\qquad \qquad \qquad L_2PdCOOCH_3^+ \xrightarrow{\ C_2H_4\ } L_2PdCH_2CH_2COOCH_3^+ \longrightarrow \longrightarrow$$

$$CH_3OH \searrow \qquad \nearrow CO$$
$$\qquad L_2PdOCH_3^+$$
$$H^+$$
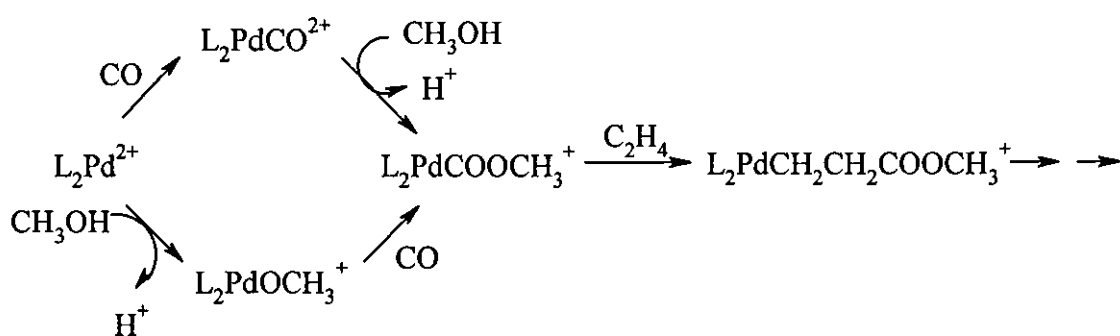
Equation 1.32

Alternatively, a chain can start by insertion of ethene in a palladium hydride,[56,57,59] producing a ketone end group. Ethene insertion in a palladium hydride and CO insertion in the resulting ethyl complex are both rapid and reversible; it is thought that the second ethene insertion (in the Pd acyl) is reversible[76] and 'traps' the acyl to start the chain (Equation 1 33).

$$L_2PdH^+ \xrightleftharpoons{\ C_2H_4\ } L_2PdCH_2CH_3^+ \xrightleftharpoons{\ CO\ } L_2PdCOCH_2CH_3^+$$

$$\xrightarrow{\ C_2H_4\ } L_2PdCH_2CH_2COCH_2CH_3^+ \longrightarrow \longrightarrow$$
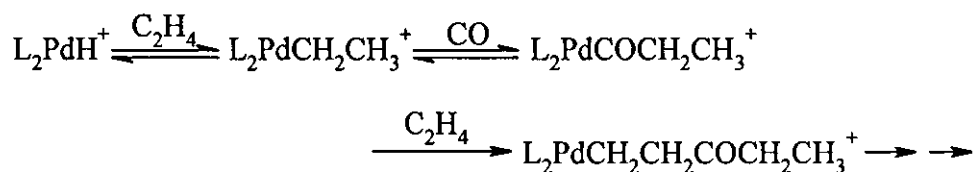
Equation 1.33

Two relevant termination mechanisms have been proposed for the CO/ethene polymerisation reaction. One mechanism, protolysis of the palladium-alkyl bond, produces a saturated ketone end group (Equation 1.34)

$$L_2PdCH_2CH_2COP^+ \xrightarrow{\ CH_3OH\ } L_2PdOCH_3^+ + CH_3CH_2COP$$
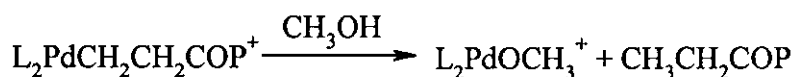
<div align="right">**Equation 1.34**</div>

A second mechanism, the alcholysis of the palladium-acyl bond, gives an ester end group (Equation 1.35)

$$L_2PdCOP^+ \xrightarrow{\ CH_3OH\ } L_2PdH^+ + PCOOCH_3$$
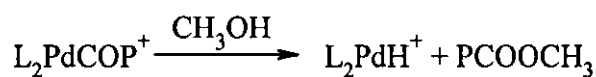
<div align="right">**Equation 1.35**</div>

Figure 1.1 summarises the formation of the three possible polymeric products of types **2, 3** and **4** by the two initiation-propagation-termination cycles **A** and **B**. Both cycles produce keto-ester molecules but the cycles are connected by two 'cross' termination steps which give diester and diketone products
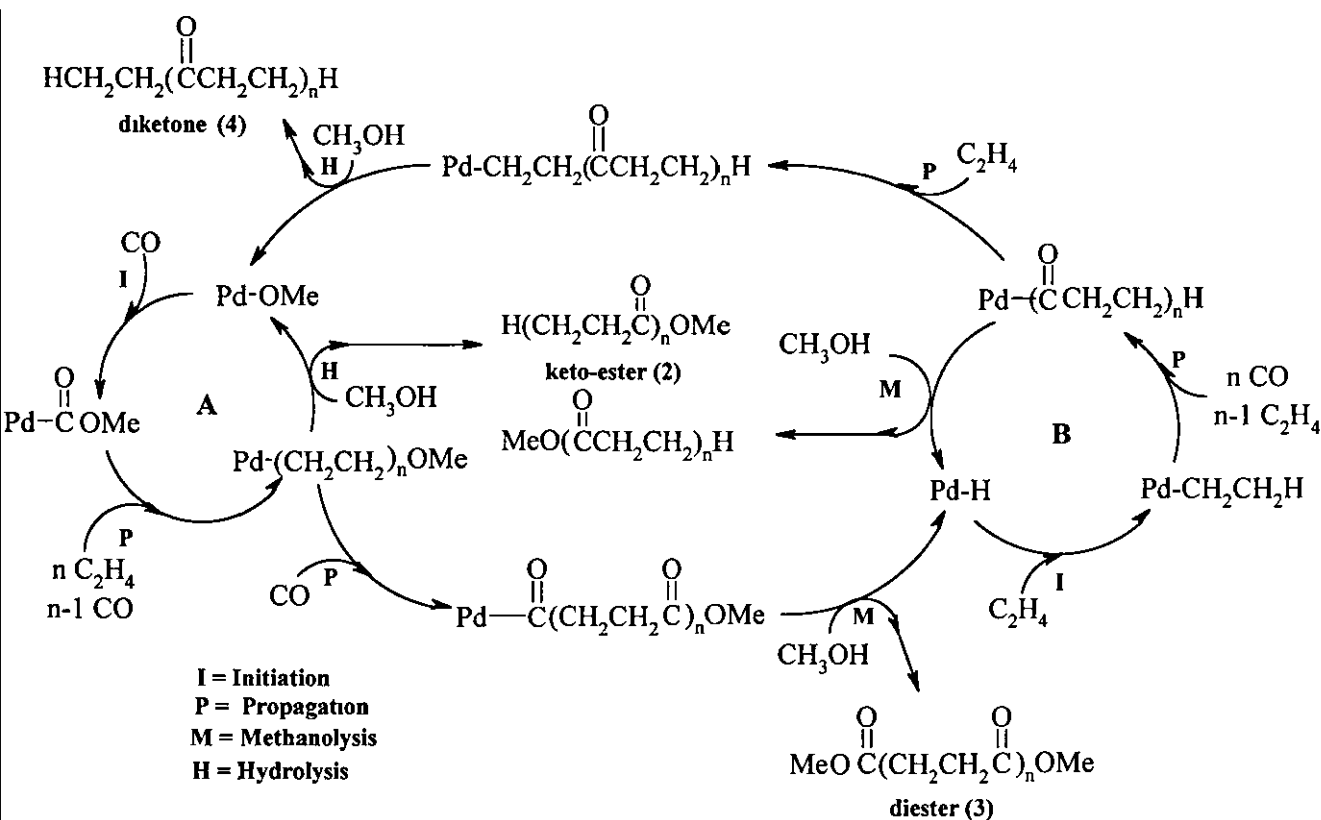
Figure 1.1 Proposed mechanism of CO/ethene copolymerisation.

1.6 *Aims of this work.*

The chemistry of the types of phosphorus-nitrogen compounds described in this chapter remains relatively unexplored and therefore, in collaboration with BP Chemicals Ltd, we decided to investigate more fully the synthesis and coordination chemistry of these types of ligands and their possible applications in catalytic systems. Our initial studies concentrated on the formation of ligands containing a P-N-C(E)-N-P (E = O or S) backbone via reaction of urea- and thiourea-based compounds with chlorophosphines. In particular, the coordination chemistry of these systems had received very little attention and offered great scope for further detailed investigation. We also studied the synthesis of ligands based around a P-N-N-P backbone and their subsequent reactions with different metal centres to give five-membered chelate rings. Although there were a number of reports involving the reactions of diphosphine derivatives of *N,N'*-dimethylhydrazine, the synthesis and coordination chemistry of phosphine derivatives of other dialkylhydrazines remained unexplored. Finally, we studied the reactions of piperazine and homopiperazine with various chlorophosphines. Very little had been reported concerning such reactions and therefore the opportunity presented itself for an in-depth investigation into the ability of these compounds to act as bidentate ligands.

We describe here our studies on the synthesis and coordination chemistry of a number of ligands of the above types and the catalytic properties of selection of the compounds.

Chapter 2

The Preparation and Coordination Chemistry of Phosphorus (III) Derivatives of Dialkyl Ureas and Thioureas.

2.1 *Introduction*

As discussed in Chapter 1, after initial investigations in the 1960's[24,25], research into the study of diphosphines based on a urea and thiourea backbone became dormant until interest was rekindled in the 1980's.[26-31] The mild reaction conditions required in the synthesis of these ligands, resulting from the use of silylated compounds, coupled with the inexpensive nature of the starting materials ensures that the products remain economically viable, while the substituent groups on both the phosphorus and the nitrogen atoms can be easily varied, offering excellent control of the steric and electronic properties of the ligands. The presence of the C=O and C=S functionalities also offers sites which can be chemically modified to alter the properties of the compounds. Here we report on the extension of the work of Woollins and Schmutzler to include the coordinative properties of known ligands, as well as the synthesis and coordination chemistry of new diphosphine derivatives of dialkylureas and thioureas.

Results and Discussion

2.2 *Ligand synthesis of diphosphine derivatives of dialkyl ureas*

Both Woollins[32] and Schmutzler[26-31] have reported the synthesis of diphosphine derivatives of ureas from silylated starting materials (Equations 1.4 and 1.6). We have discovered that the synthesis of {Ph$_2$PN(Me)}$_2$CO **1** is also possible from the reaction of *N,N'*-dimethylurea with two equivalents of Ph$_2$PCl, in the presence of NEt$_3$, in dichloromethane (Equation 2.1).

$$\text{Me-N(H)-C(O)-N(H)-Me} + 2Ph_2PCl \xrightarrow{NEt_3,\ CH_2Cl_2} \text{Me-N(PPh_2)-C(O)-N(PPh_2)-Me} + 2NEt_3.HCl$$
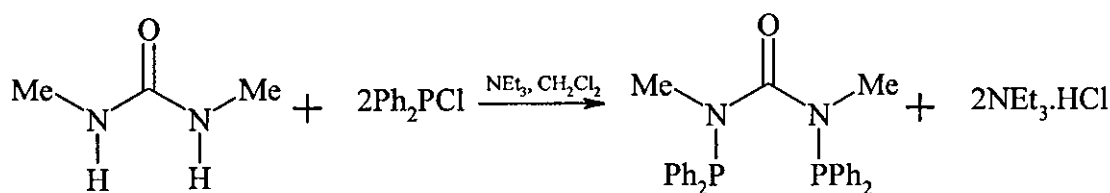
1

Equation 2.1

Slow addition of a dichloromethane solution of {HN(Me)}$_2$CO and NEt$_3$ to a dichloromethane solution of Ph$_2$PCl at room temperature results in a viscous, pale yellow solution. ^{31}P-{^1H} NMR studies conducted immediately after completion of the addition of the urea show that the reaction mixture contains three phosphorus containing species, the starting material Ph$_2$PCl, at δ(P) 82.9, the desired product **1**, at δ(P) 54.7, and presumably the mono-substituted product {Ph$_2$PN(Me)C(O)N(Me)H} at δ(P) 46.4. We can be confident in this assignment as the value of its' chemical shift, δ(P) 46.4, and it's position relative to the bis-substituted product are analogous to the values for mono-substituted products of similar, related thiourea systems.[37] Stirring of the reaction mixture overnight results in the loss of the species at δ(P) 82.9 and δ(P) 46.4 and leaves **1** as the only phosphorus-containing species. Removal of the solvent *in vacuo*, leaves an off white solid residue which is washed with water to remove NEt$_3$.HCl. Collection of the solid by suction filtration and drying over P$_4$O$_{10}$ *in vacuo* results in the product, **1**, as a white solid in 56 % yield Air- and moisture-tolerant, **1** is readily soluble in both dichloromethane and thf. Elemental analysis is in good agreement with the calculated values (Table 2.4) and FAB$^+$ mass spectrometry shows the expected parent-ion peak (m/z 456 [M]$^+$). The IR spectrum of **1** contains strong bands which can be assigned to ν(CO), ν(CN) and ν(PN) (Table 2.1).

The analogous diethyl urea ligand, {Ph$_2$PN(Et)}$_2$CO **2**, can be synthesised in a similar manner to **1**. Reaction of *N,N'*-diethylurea with two equivalents of Ph$_2$PCl, in the presence of NEt$_3$, in dichloromethane gives the desired product **2** (Equation 2.2). As for **1**, slow addition of a dichloromethane solution of the urea to a dichloromethane solution of Ph$_2$PCl results in a viscous, yellow solution containing three phosphorus species.

Et–N(H)–C(=O)–N(H)–Et + 2Ph$_2$PCl $\xrightarrow{\text{NEt}_3,\ \text{CH}_2\text{Cl}_2}$ Et–N(PPh$_2$)–C(=O)–N(PPh$_2$)–Et + 2NEt$_3$.HCl

<div align="center">
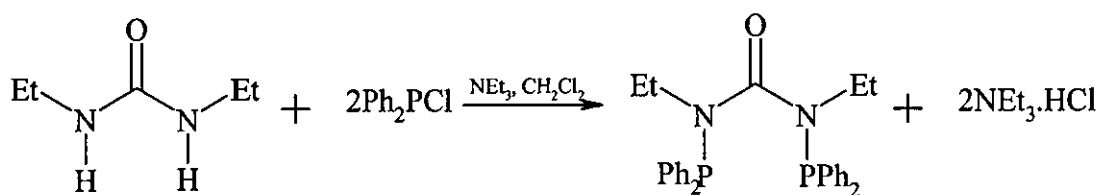
2   **Equation 2.2**

</div>

^{31}P-$\{^{1}$H$\}$ NMR studies on the reaction mixture again show peaks corresponding to the chlorophosphine, bis-substituted product and mono-substituted product. The time taken for the reaction to proceed to completion and leave only the bis-substituted product **2** is significantly longer than the reaction time required in the formation of **1**. Stirring was continued for 1 week during which time the peaks at δ(P) 82.9 and δ(P) 45.4, corresponding to Ph$_2$PCl and the mono-substituted product respectively, slowly reduced in intensity to leave only a peak corresponding to {Ph$_2$PN(Et)}$_2$CO, at δ(P) 56.4 ppm. The product can be isolated in the same manner as **1**, via removal of solvent and washing with water to leave **2** as a white solid in 40 % yield. Like **1**, the product is both air- and moisture-tolerant and readily soluble in both thf and dichloromethane. The product gave satisfactory elemental analysis results (Table 2 4) and FAB^{+} mass spectrometry showed the expected parent-ion peak (m/z 484 [M]$^{+}$). The IR spectrum of **2** contains strong bands which can be assigned to ν(CO), ν(CN) and ν(PN) (Table 2.1)

2.3 *Bidentate chelating coordination chemistry of {Ph$_2$PN(R)}$_2$CO, R = Me, Et*

As discussed in Chapter 1, Schmutzler and co-workers have reported the synthesis of phosphine derivatives of *N,N'*-dimethylurea.[26-31] However, reports of metal complexes containing these ligands are rare, especially where the ligands act as *P,P'* chelates. Therefore, using the ligands **1** and **2**, we have investigated their complexation chemistry more fully via reactions with various metal compounds

The reactions of **1** and **2** with equimolar quantities of [PtCl$_2$(cod)] in dichloromethane proceed according to Equation 2.3 to yield the *P,P'*-chelates cis-[PtCl$_2$\{\{Ph$_2$PN(Me)\}$_2$CO\}], **3**, and cis-[PtCl$_2$\{\{Ph$_2$PN(Et)\}$_2$CO\}], **4** as 6-membered metallacycles.
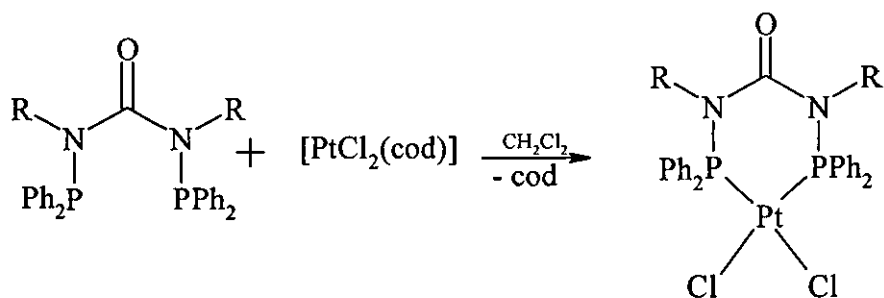
$$R = Me \ (3), \ Et \ (4)$$

Equation 2.3

Addition of the solid diphosphines **1** and **2** to dichloromethane solutions of [PtCl$_2$(cod)], followed by addition of diethyl ether, results in the formation of the products **3** and **4**, as white solids in yields of 79 and 58 % respectively. The ^{31}P-{^{1}H} NMR spectra of **3** and **4** show singlets, at δ(P) 53 4 and δ(P) 56.7 respectively, each with satellites from the ^{1}J coupling to ^{195}Pt. The magnitude of the couplings [$^{1}J(^{195}Pt-^{31}P) 3792 Hz for **3** and 3910 Hz for **4**] are in agreement with reported values for similar diphosphine urea chelates containing a phosphorus trans to chloride in Pt(II) systems [77] FAB^{+} mass spectrometry studies on **3** display the parent-ion peak and a peak corresponding to the loss of a chloride ion (m/z 722 [M]$^{+}$ and 687 [M - Cl]$^{+}$). The same studies on **4** fail to show the parent-ion peak but do show a peak corresponding to the loss of a chloride ion (m/z 715 [M - Cl]$^{+}$). The IR spectra of **3** and **4** show bands which can be assigned to ν(CO), ν(CN) and ν(PN) (Table 2.1), which are at a higher frequency than the values observed for the free ligands **1** and **2** and indicate an increase in bond order upon complexation. Elemental analyses are in good agreement with calculated values (Table 2 4). Colourless crystals of **3** and **4**, suitable for X-ray crystallography, were grown by layering dichloromethane solutions of **3** and **4** with diethyl ether. Single crystal X-ray studies confirm the *cis* chelate geometry of the ligands and that the molecules are square planar at the platinum (Figures 2.1 and 2.2). Selected bond lengths and angles are shown in Tables 2.2 and 2.3. The molecules have approximate C$_2$ symmetry and the bite angles are close 90° [90.7 (2) for **3** and 88.8 (3) for **4**] indicating that this size ring is very well suited to square planar coordination. In **3** the six-membered PtP$_2$N$_2$C ring is hinged about P(2)-N(1) by 45° while in **4** the same ring is hinged about P(1)-N(2) by 51°. In both molecules the

42

exocyclic urea oxygen atom is effectively in the plane of its' substituents. The internal angles of both **3** and **4** are all close to trigonal and it is noticeable in both molecules that the C-N bond lengths within the PtP_2N_2C ring are significantly shorter than N-Me/N-Et bond lengths, indicating some degree of delocalisation across the $N_2C=O$ groups. In both complexes the P-N bond lengths (1.716 (6) and 1.749 (8) Å for **3** and 1.725 (3) and 1.714 (3) Å for **4**) are similar to those observed in related compounds.[32,77]

Table 2.1 Selected IR data (cm^{-1}) for compounds **1-8**

Compound	Formula	ν (CO)	ν (CN)	ν (PN)
1	$\{Ph_2PN(Me)\}_2CO$	1646	1432	961
2	$\{Ph_2PN(Et)\}_2CO$	1649	1432	992
3	cis-$[PtCl_2\{\{Ph_2PN(Me)\}_2CO\}]$	1672	1435	973
4	cis-$[PtCl_2\{\{Ph_2PN(Et)\}_2CO\}]$	1669	1436	997
5	cis-$[PtMe_2\{\{Ph_2PN(Me)\}_2CO\}]$	1626	1434	983
6	cis-$[PtMe_2\{\{Ph_2PN(Et)\}_2CO\}]$	1652	1436	994
7	cis-$[PtCl(Me)\{\{Ph_2PN(Me)\}_2CO\}]$	1637	1433	984
8	cis-$[PtCl(Me)\{\{Ph_2PN(Et)\}_2CO\}]$	1658	1436	996
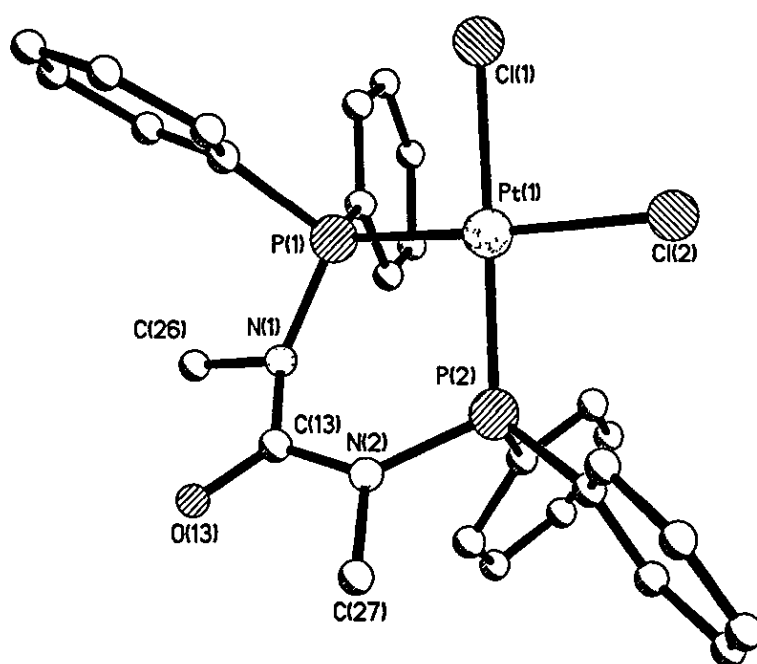
Figure 2.1 Solid state structure of cis-$[PtCl_2\{\{Ph_2PN(Me)\}_2CO\}]$ **3**.
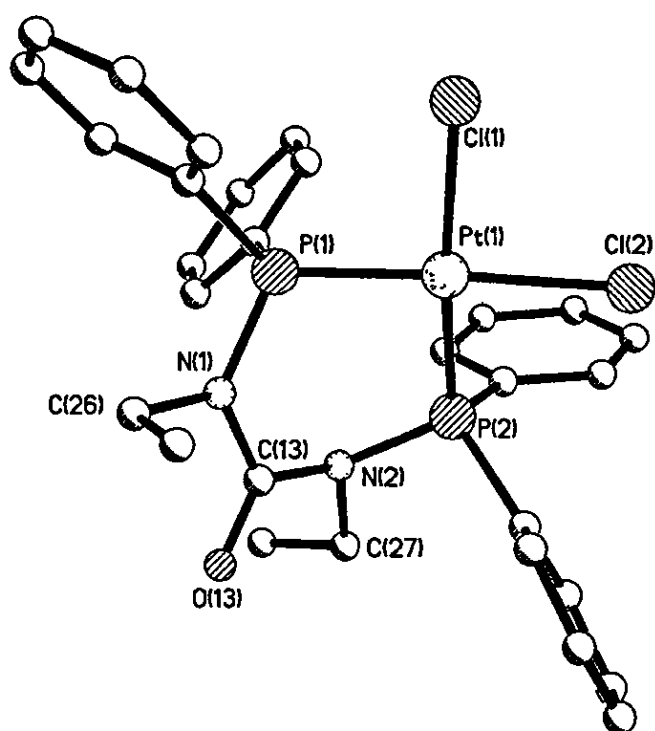
Figure 2.2 The solid state structure of *cis*-[PtCl$_2$\{\{Ph$_2$PN(Et)\}$_2$CO\}] **4**.

Table 2.2 Selected bond lengths (Å) for compounds **3** and **4**.

Bond	3	4
P(1)-Pt(1)	2.207 (4)	2 2141 (8)
P(2)-Pt(1)	2.2054 (13)	2 2157 (8)
Pt(1)-Cl(1)	2.3567 (13)	2.3414(9)
Pt(1)-Cl(2)	2.362 (4)	2.3595 (9)
N(1)-P(1)	1.716 (6)	1.725 (3)
N(2)-P(2)	1.749 (8)	1.714 (3)
N(1)-C(13)	1.413 (10)	1.385 (5)
N(2)-C(13)	1.360 (12)	1.411 (5)
N(1)-C(26)	1.499 (8)	1.488 (5)
N(2)-C(27)	1.485 (8)	1.500 (5)
C(13)-O(13)	1.222 (11)	1 217 (5)

Table 2.3 Selected bond angles (°) for compounds **3** and **4**.

Bonds	3	4
P(1)-Pt(1)-P(2)	90 7 (2)	88.8 (3)
N(1)-P(1)-Pt(1)	114.9 (2)	111.0 (11)
N(2)-P(2)-Pt(1)	112.0 (3)	114.8 (11)
Cl(1)-Pt(1)-Cl(2)	89.4 (14)	87.9 (4)
Cl(1)-Pt(1)-P(1)	86.9 (14)	95.5 (3)
Cl(2)-Pt(1)-P(2)	92.7 (2)	87.7 (3)
P(1)-N(1)-C(13)	125.1 (6)	122.5 (2)
P(2)-N(2)-C(13)	123.5 (6)	120.6 (2)
N(1)-C(13)-N(2)	119.8 (8)	117.8 (3)
N(1)-C(13)-O(13)	118.8 (9)	121.0 (4)
N(2)-C(13)-O(13)	121.1 (9)	121.1 (4)
C(13)-N(2)-C(27)	116.1 (7)	112.5 (3)
C(13)-N(1)-C(26)	111.7 (6)	115.1 (3)

Both $\{Ph_2PN(Me)\}_2CO$ and $\{Ph_2PN(Et)\}_2CO$ also react successfully with $[PtMe_2(cod)]$ to produce P,P' chelates. Addition of the solid diphosphines **1** and **2** to dichloromethane solutions of $[PtMe_2(cod)]$ results in cis-$[PtMe_2\{\{Ph_2PN(Me)\}_2CO\}]$, **5**, and cis-$[PtMe_2\{\{Ph_2PN(Et)\}_2CO\}]$, **6** respectively (Equation 2.4).
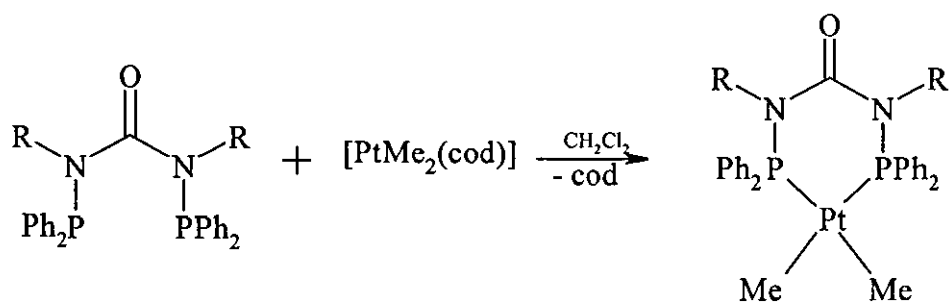
R = Me (**5**), Et (**6**)

Equation 2.4

45

Cis-[PtMe₂{{Ph₂PN(Me)}₂CO}] and *cis*-[PtMe₂{{Ph₂PN(Et)}₂CO}] were both isolated as white solids in 65 % yields after stirring the reaction mixtures for 1-2 hours and then adding light petroleum. FAB^+ mass spectrometry studies on **5** and **6** show the respective parent-ion peaks as well as peaks corresponding to $[M - CH_3]^+$ fragments (m/z 681 $[M]^+$ and 666 $[M - CH_3]^+$ for **5**, m/z 710 $[M]^+$ and 695 $[M - CH_3]^+$ for **6**) The ^{31}P-$\{^1H\}$ NMR spectra of both compounds show singlets, at δ(P) 74.9 and δ(P) 77.7 respectively, which are considerably further downfield than the values observed for **3** and **4**, with satellites from coupling to ^{195}Pt. The magnitude of the $^1J(^{195}Pt$-$^{31}P)$ couplings (1944 for **5** and 1997 for **6** Hz) are much smaller than those associated with the analogous dichloro species **3** and **4**, and are consistent with values previously reported for similar complexes where phosphorus is *trans* to a methyl group.[32] Elemental analysis of **5** and **6** gave satisfactory results (Table 2 4) and the IR spectra of each showed the expected bands for ν(CO), ν(CN) and ν(PN) (Table 2.1).

Table 2.4 Elemental analysis data for complexes **1-8** (calculated values in parentheses).

Compound	Formula	C	H	N
1	{Ph₂PN(Me)}₂CO	69 6 (71.0)	5.3 (5.7)	5 5 (6.1)
2	{Ph₂PN(Et)}₂CO	70.8 (71.2)	6.2 (6 2)	5.3 (5.8)
3	[PtCl₂{{Ph₂PN(Me)}₂CO]	42 8 (44.9)	3.4 (3.6)	3.6 (3 8)
4	[PtCl₂{{Ph₂PN(Et)}₂CO]	45.2 (46.4)	4.2 (4 0)	3.9 (3.7)
5	[PtMe₂{{Ph₂PN(Me)}₂CO]	47.3 (50.1)	4.9 (5.1)	4.0 (4.2)
6	[PtMe₂{{Ph₂PN(Et)}₂CO]	52.7 (52.4)	5.8 (5 1)	4.0 (3.9)
7	[PtCl(Me){{Ph₂PN(Me)}₂CO]	47.5 (47.9)	4.0 (4 2)	3.7 (3.9)
8	[PtCl(Me){{Ph₂PN(Et)}₂CO}]	48.2 (49.3)	4.0 (4.5)	3.1 (3.8)

Reactions of **1** and **2** with [PtCl(Me)(cod)] proceed, according to Equation 2.5, with the displacement of cod and formation of *cis*-[PtCl(Me){{Ph₂PN(Me)}₂CO}], **7** and *cis*-[PtCl(Me){{Ph₂PN(Et)}₂CO}], **8** respectively. Addition of the solid diphosphines **1** and **2** to dichloromethane solutions of [PtCl(Me)(cod)] followed by addition of diethyl ether results in the products, **7** and **8**, as white solids in 67 and 63 % yields respectively. The ^{31}P-$\{^1H\}$ NMR spectrum of **7** shows an AX type spectrum
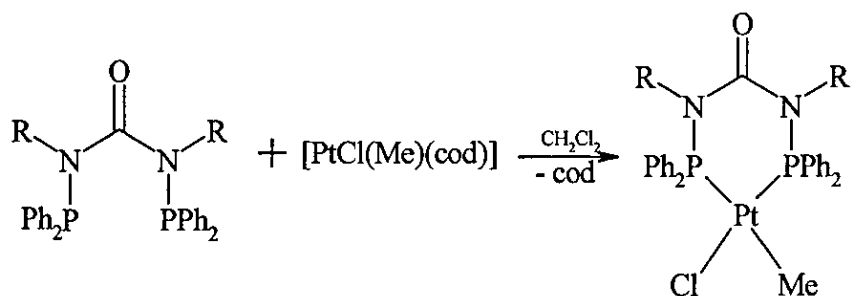
R = Me (7), Et (8)

Equation 2.5

(Figure 2.3) due to the chemical inequivalence of the phosphorus centres. Both peaks in the spectrum are of equal magnitude and both show satellites due to coupling to ^{195}Pt. The phosphorus *trans* to the chloride in the complex can be assigned to the peak at δ(P) 61.4 due to the larger $^{1}J(^{195}\text{Pt-}^{31}\text{P})$ coupling associated with it (4509 Hz). Consequently the phosphorus *trans* to the methyl group is assigned to the peak at δ(P) 74.1 and has a smaller $^{1}J(^{195}\text{Pt-}^{31}\text{P})$ coupling of 1819 Hz. The value of the $^{2}J(\text{PP})$ coupling is 30 Hz which is in agreement with previously reported values for similar systems.[32]
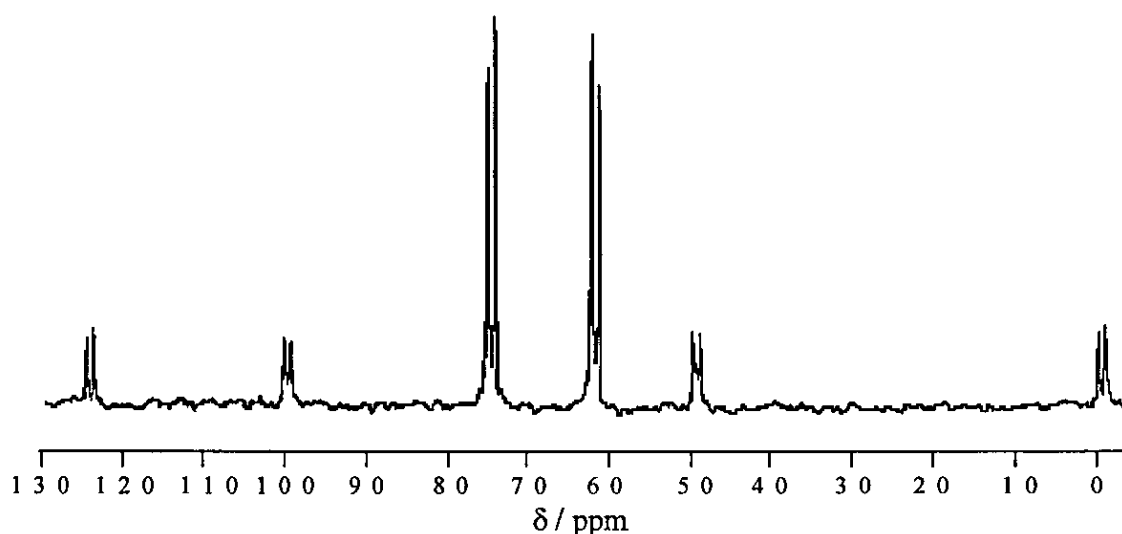
Figure 2.3 ^{31}P-$\{^{1}\text{H}\}$ NMR spectrum of *cis*-[PtCl(Me){{Ph$_2$PN(Me)}$_2$CO}] 7

47

The FAB$^+$ mass spectrum of 7 show the expected parent-ion peak (m/z 701 [M]$^+$) and a fragmentation pattern corresponding to the loss of a methyl group and a Cl atom (m/z 686 [M - CH$_3$]$^+$ and 666 [M - Cl]$^+$). Elemental analysis is in agreement with calculated values (Table 2.4) and the IR spectrum shows bands corresponding to v(CO), v(CN) and v(PN) (Table 2.1) ^{31}P-{^{1}H} NMR studies on 8 show a spectrum with a similar AX type pattern to that observed for 7, the phosphorus centre *trans* to the chloride having a chemical shift of δ(P) 64.2 and a $^1J(^{195}$Pt-^{31}P) coupling of 4596 Hz. The chemical shift of the phosphorus centre *trans* to the methyl group, as in 7, is slightly further downfield at a value of δ(P) 77.1, again with a significantly smaller $^1J(^{195}$Pt-^{31}P) coupling of 1891 Hz. FAB$^+$ mass spectrometry shows the peaks reported for 7 (m/z 730 [M]$^+$, 715 [M-CH$_3$]$^+$ and 694 [M-Cl]$^+$) and elemental analysis is in good agreement with calculated values (Table 2.1) The IR spectrum of 8 shows bands which can be assigned to v(CO), v(CN) and v(PN) (Table 2.4)

Palladium complexes involving {Ph$_2$PN(Me)}$_2$CO and {Ph$_2$PN(Et)}$_2$CO acting as bidentate *P,P'* chelates are also successfully formed when the diphosphines 1 and 2 are reacted with [PdCl$_2$(cod)]. As with the platinum analogues 3 and 4, addition of the solid ligands 1 and 2 to dichloromethane solutions of [PdCl$_2$(cod)], followed by the addition of diethyl ether, results in the 6-membered chelate species *cis*-[PdCl$_2${Ph$_2$PN(Me)}$_2$CO}] 9 and *cis*-[PdCl$_2${Ph$_2$PN(Et)}$_2$CO}] 10 respectively (Equation 2 6).
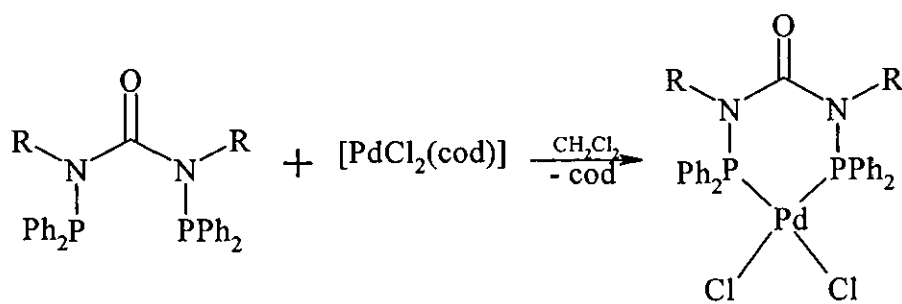
R = Me (9), Et (10)

Equation 2.6

Isolation of 9 and 10 results in the products as a yellow solid in 73 % yields and ^{31}P-{^{1}H} NMR studies show a singlets at δ(P) 76 2 and 80.1 respectively. FAB$^+$ mass spectrometry does not show the expected parent-ion peaks but instead fragmentation

patterns consistent with the loss of chloride atoms (m/z 598 [M - Cl]$^+$ and 563 [M - 2Cl]$^+$ for **9** and m/z 626 [M-Cl]$^+$ and 591 [M-2Cl]$^+$ for **10**). Peaks due to ν(CO), ν(CN) and ν(PN) are evident in the IR spectra (Table 2.5) and elemental analysis is in agreement with calculated values for both compounds (Table 2.12). Yellow crystals of cis-[PdCl$_2$\{Ph$_2$PN(Me)\}$_2$CO\}] and cis-[PdCl$_2$\{Ph$_2$PN(Et)\}$_2$CO\}] suitable for X-ray crystallography were grown by layering dichloromethane solutions of the compounds with diethyl ether. The solid state structures of cis-[PdCl$_2$\{\{Ph$_2$PN(Me)\}$_2$CO\}] and cis-[PdCl$_2$\{\{Ph$_2$PN(Et)\}$_2$CO\}] are shown in Figures 2 4 and 2.5 and selected bond lengths and angles are shown in Tables 2 6 and 2.7. The molecules have approximate non-crystallographic C$_2$ symmetry and similar geometry about the metal to **3** and **4** Perhaps the most surprising difference is an enlargement of the P-N-C angles in **9** and **10** relative to those in **3** and **4**, for which there is no ready explanation. In **9** the PdP$_2$N$_2$C ring is effectively planar and co-planar with the coordination sphere. The same ring in **10** is puckered, though not hinged like the examples in **3** and **4**, with C(13) and O(13) in the same plane as the coordination sphere and N(1) and N(2) lying 0.5 Å above and below the plane respectively. As with compounds **3** and **4** the P-N bond lengths in **9** and **10** (1.697 (2) and 1.704 (2) Å for **9** and 1.707 (4) and 1.712 (4) Å for **10**) are typical for these type of compounds[77] and, once again, the C-N bond lengths within the PtP$_2$N$_2$C rings of both molecules are significantly shorter than N-Me/N-Et bond lengths, indicating some degree of delocalisation across the N$_2$C=O groups. The Pd-Cl and Pd-P bond lengths in **9** and **10** are in agreement with values previously reported for cis-[PdCl$_2$\{\{Ph$_2$PN(H)\}$_2$CO\}] and are all single in character.[32]

Table 2.5 Selected IR data (cm^{-1}) for compounds **9, 10, 13, 14** and **15**.

Compound	Formula	ν (CO)	ν (CN)	ν (PN)
9	cis-[PdCl$_2$\{Ph$_2$PN(Me)\}$_2$CO\}]	1648	1435	991
10	cis-[PdCl$_2$\{Ph$_2$PN(Et)\}$_2$CO\}]	1670	1436	996
13	cis-[Mo(CO)$_4$\{Ph$_2$PN(Me)\}$_2$CO\}]	1643	1433	962
14	cis-[Rh(cod)\{Ph$_2$PN(Et)\}$_2$CO][ClO$_4$]	1664	1437	996
15	[(AuCl)$_2$\{Ph$_2$PN(Et)\}$_2$CO\}]	1655	1436	997
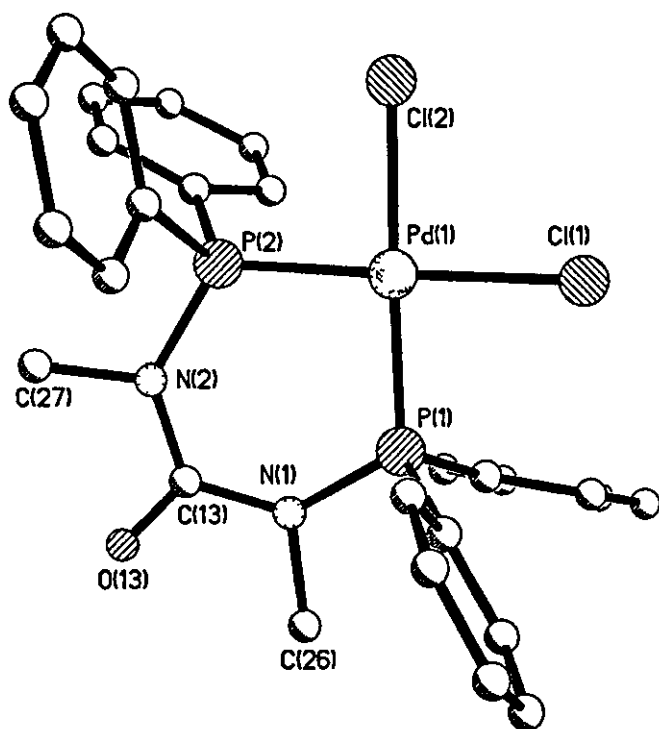
Figure 2.4 The solid state structure of *cis*-[PdCl$_2$\{\{Ph$_2$PN(Me)\}$_2$CO\}] **9**.
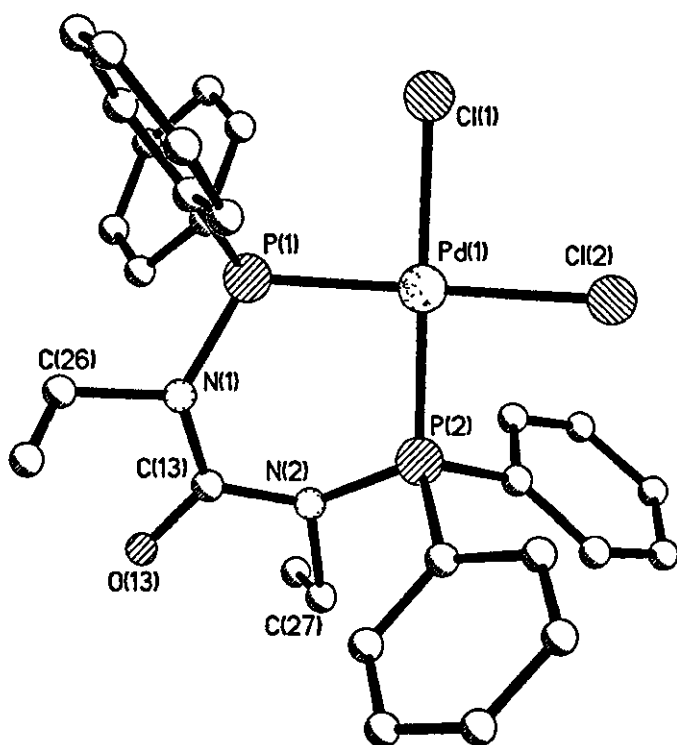
Figure 2.5 The solid state structure of *cis*-[PdCl$_2$\{\{Ph$_2$PN(Et)\}$_2$CO\}] **10**.

Table 2.6 Selected bond lengths (Å) for compounds **9** and **10**.

Bond	9	10
P(1)-Pd(1)	2 2003 (8)	2.2165 (13)
P(2)-Pd(1)	2.2072 (8)	2.2135 (13)
Pd(1)-Cl(1)	2.3476 (8)	2.3545 (13)
Pd(1)-Cl(2)	2.3418 (9)	2.3577 (13)
N(1)-P(1)	1.697 (2)	1.707 (4)
N(2)-P(2)	1.704 (2)	1.712 (4)
N(1)-C(13)	1 380 (4)	1.382 (6)
N(2)-C(13)	1.377 (4)	1.397 (6)
N(1)-C(26)	1.494 (4)	1 506 (6)
N(2)-C(27)	1.486 (4)	1.504 (6)
C(13)-O(13)	1.224 (3)	1.215 (6)

Table 2.7 Selected bond angles (°) for compounds **9** and **10**.

Bonds	9	10
P(1)-Pd(1)-P(2)	94.76 (3)	91.47 (5)
N(1)-P(1)-Pd(1)	118.19 (9)	115.93 (14)
N(2)-P(2)-Pd(1)	118.41 (9)	116.05 (14)
Cl(1)-Pd(1)-Cl(2)	91.47 (3)	90 28 (5)
Cl(1)-Pd(1)-P(1)	86.84 (3)	89 26 (5)
Cl(2)-Pd(1)-P(2)	86.98 (3)	89.22 (5)
P(1)-N(1)-C(13)	132.6 (2)	126.2 (3)
P(2)-N(2)-C(13)	131.5 (2)	117.2 (3)
N(1)-C(13)-N(2)	122.9 (3)	120.2 (4)
N(1)-C(13)-O(13)	118.6 (3)	120.7 (4)
N(2)-C(13)-O(13)	118.5 (3)	119.1 (4)
C(13)-N(2)-C(27)	112.8 (2)	113.2 (4)
C(13)-N(1)-C(26)	112.4 (4)	112.9 (4)

Compounds **9** and **10** demonstrate that the ligands {Ph$_2$PN(Me)}$_2$CO (**1**) and {Ph$_2$PN(Et)}$_2$CO (**2**) can act as simple metal chelates and form six-membered ring systems when reacted with [PdCl$_2$(cod)]. However, reaction of the two ligands with palladium acetate fails to result in the expected chelate systems. Instead P-N bond cleavage takes place and the reaction involves the formation of a [Ph$_2$PO]$^-$ ligand which is incorporated into a Pd$_2$P$_2$O$_2$ heterocycle (Equation 2.7).
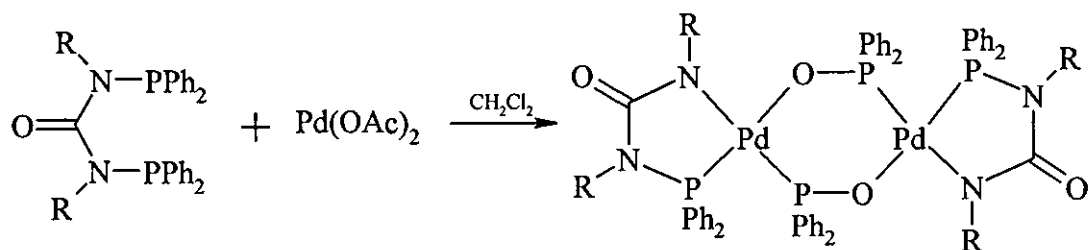
R = Me (**11**), Et (**12**)

Equation 2.7

Addition of the solid diphosphine **1 a** to dichloromethane solution of [Pd(OAc)$_2$] followed by addition of diethyl ether results in [Pd{OPPh$_2$}{N(Me)C(O)N(Me)PPh$_2$}]$_2$ (**11**) as a yellow solid in a low yield of 31 % The ^{31}P-{^{1}H} NMR spectrum of **11** shows two broad singlet peaks at δ(P) 84 4 and δ(P) 71 2 We assign the phosphorus in the [Ph$_2$PO]$^-$ ligand to the species further downfield at δ(P) 84.4 due to its' proximity to the electronegative oxygen atom and consequently the phosphorus in the PNCNPd ring is assigned to the peak at δ(P) 71 2. FAB$^+$ mass spectrometry shows the parent-ion peak (m/z 1158 [M]$^+$) and a peak corresponding to [Pd{OPPh$_2$}{N(Me)C(O)N(Me)PPh$_2$}]$^+$ (m/z 579) and the IR spectrum shows peaks which can be assigned to ν(CO) (1630 cm^{-1}), ν(CN) (1434 cm^{-1}) and ν(PN) (995 cm^{-1}). Elemental analysis is in good agreement with calculated values Yellow crystals suitable for X-ray crystallography were grown by layering a dichloromethane solution of **11** with diethyl ether. Figure 2.6 shows the solid state structure of [PdOPh$_2${N(Me)C(O)N(Me)PPh$_2$}]$_2$ and Tables 2 8 and 2.9 show selected bond lengths and angles. The structure of **11** reveals the square planar palladium centres as spiro in the tricyclic system. The PdPN$_2$C rings are close to planar [maximum deviations for the two rings are 0.01 Å for N(2) and –0.05 Å for N(31)] with the C=O and the NMe groups being effectively coplanar with the PdPN$_2$C rings. The internal

nitrogen angles in the PdPN$_2$C ring are close to trigonal, whilst the angle at the phosphorus is slightly reduced from a perfect tetrahedral angle. The central Pd$_2$P$_2$O$_2$ ring adopts a chair geometry with the central Pd$_2$P$_2$O$_2$ core having two PdOP planes inclined by ca. 138°. Within this ring the P-O bond lengths [P(2)-O(2) 1.536 (4) and P(32)-O(32) 1.539 (3) Å] are appropriate for a coordinated [Ph$_2$PO]⁻ anion and similar to those reported for a Pd$_2$P$_2$O$_2$ ring[78] but slightly shorter than those reported for [(Ph$_3$P)Pt(Ph$_2$PO)$_2$Pt(PPh$_3$)].[79]
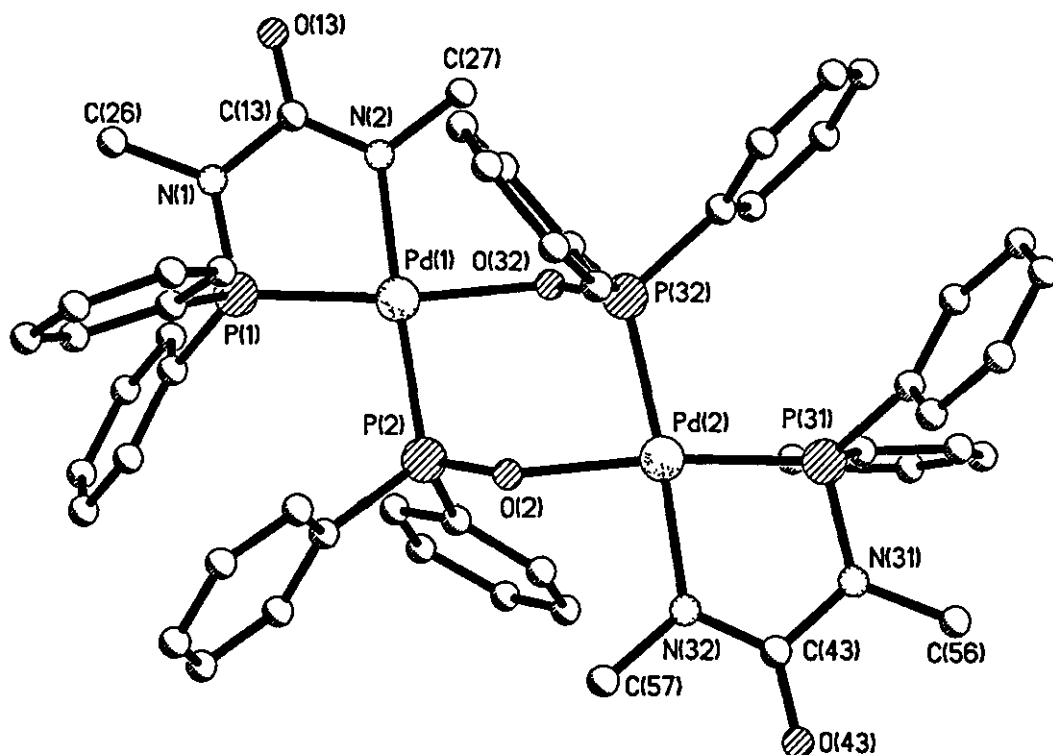
Figure 2.6 Solid state structure of [Pd{OPPh$_2$}{N(Me)C(O)N(Me)PPh$_2$}] **11**.

Using the same method employed in the preparation of **11**, [Pd{OPPh$_2$}{N(Et)C(O)N(Et)PPh$_2$}]$_2$, **12** was isolated as a yellow solid in 51 % yield. The ^{31}P-{^{1}H} NMR spectrum again shows two broad peaks. As expected the peak assigned to the [Ph$_2$PO]⁻ ligand, at δ(P) 84.5, has the same chemical shift as in the dimethyl analogue **11**, with the phosphorus in the PNCNPd ring having a chemical shift of δ(P) 69 5. FAB⁺ mass spectrometry shows the peaks corresponding to the species observed for **11**, namely the parent-ion peak (m/z 1214) and a peak corresponding to [Pd{OPPh$_2$}{N(Et)C(O)N(Et)PPh$_2$}]⁺ (m/z 607) and the IR

53

Table 2.8 Selected bond lengths (Å) for compound **11.**

Bond	Length	Bond	Length
Pd(1)-N(2)	2.083 (4)	Pd(2)-N(32)	2.059 (4)
Pd(1)-P(1)	2.2043 (14)	Pd(2)-P(31)	2.1985 (14)
Pd(1)-O(32)	2.092 (3)	Pd(2)-O(2)	2.075 (3)
Pd(1)-P(2)	2.2764 (14)	Pd(2)-P(31)	2.2600 (14)
P(1)-N(1)	1.674 (5)	P(31)-N(31)	1 676 (5)
N(1)-C(13)	1.424 (7)	N(31)-C(43)	1.414 (7)
C(13)-N(2)	1.323 (7)	C(43)-N(32)	1 328 (7)
C(13)-O(13)	1.235 (6)	C(43)-O(43)	1 240 (6)
P(2)-O(2)	1.536 (4)	P(32)-O(32)	1.539 (3)

Table 2.9 Selected bond angles (°) for compound **11.**

Bond	Angle	Bond	Angle
P(1)-Pd(1)-N(2)	81.81 (13)	P(31)-Pd(2)-N(32)	81 90 (13)
Pd(1)-P(1)-N(1)	102.6 (2)	Pd(2)-P(31)-N(31)	102.3 (2)
P(1)-N(1)-C(13)	119.4 (3)	C(43)-N(31)-P(31)	119.2 (3)
N(1)-C(13)-N(2)	114.6 (5)	N(31)-C(43)-N(32)	114 2 (5)
C(13)-N(2)-Pd(1)	121.6 (4)	C(43)-N(32)-Pd(2)	121 9 (4)
Pd(1)-P(2)-O(2)	113.9 (2)	Pd(2)-P(32)-O(32)	112.8 (2)
Pd(1)-O(32)-P(32)	128 4 (7)	Pd(2)-O(2)-P(2)	134.8 (2)

spectrum contains peaks at 1620, 1435, 1103 and 996 cm^{-1} assignable to ν(CO), ν(CN), ν(PO) and ν(PN) respectively. Elemental analysis is in good agreement with calculated values. Layering of a dichloromethane solution of **12** with diethyl ether produces yellow crystals which are suitable for X-ray crystallography. The solid state structure of **12.CH$_2$Cl$_2$** is shown in Figure 2.7 and selected bond lengths and angles are shown in Tables 2.10 and 2.11.
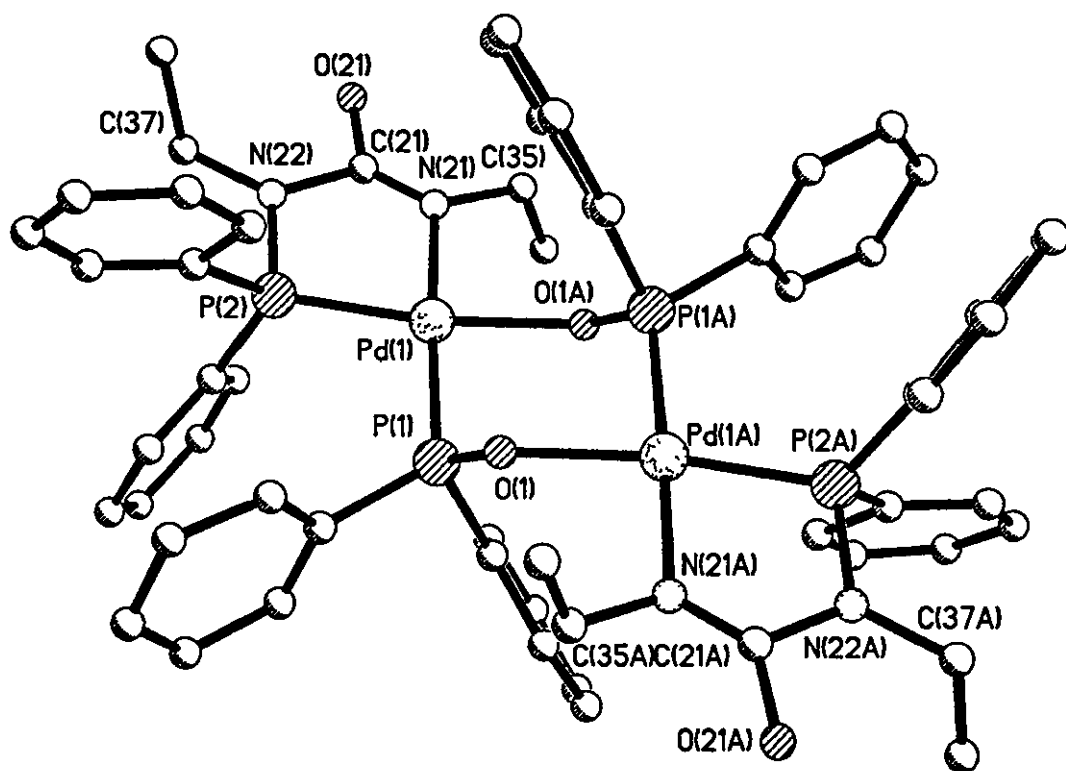
Figure 2.7 Solid state structure of $[Pd\{OPPh_2\}\{N(Et)C(O)N(Et)PPh_2\}]_2.CH_2Cl_2$.

Table 2.10 Selected bond lengths (Å) for compounds **12** CH_2Cl_2

Bond	Length	Bond	Length
Pd(1)-N(21)	1.990 (11)	P(2)-N(22)	1.639 (12)
Pd(1)-P(1)	2.221 (4)	N(22)-C(21)	1.43 (2)
Pd(1)-O(1A)	2.051 (9)	C(21)-N(21)	1 21 (2)
Pd(1)-P(2)	2.160 (5)	C(21)-O(21)	1.28 (2)

Table 2.11 Selected bond angles (°) for compound **12** CH_2Cl_2.

Bond	Angle	Bond	Angle
P(2)-Pd(1)-N(21)	80.6 (4)	C(21)-N(21)-Pd(1)	124 3 (12)
Pd(1)-P(2)-N(22)	103 2 (5)	Pd(1)-P(1)-O(1)	112.7 (4)
P(2)-N(22)-C(21)	114 0 (12)	N(21)-Pd(1)-O(1A)	92.9 (5)
N(22)-C(21)-N(21)	115.7 (130)	P(1)-Pd(1)-O(1A)	84.6 (4)

55

The reaction of {Ph$_2$PN(Me)}$_2$CO (1) with [Mo(CO)$_4$(pip)$_2$] in dichloromethane results in the displacement of the piperidine molecules and the formation of the *P,P'* chelate complex cis-[Mo(CO)$_4${Ph$_2$PN(Me)C(O)N(Me)PPh$_2$}], 13 (Equation 2.8).
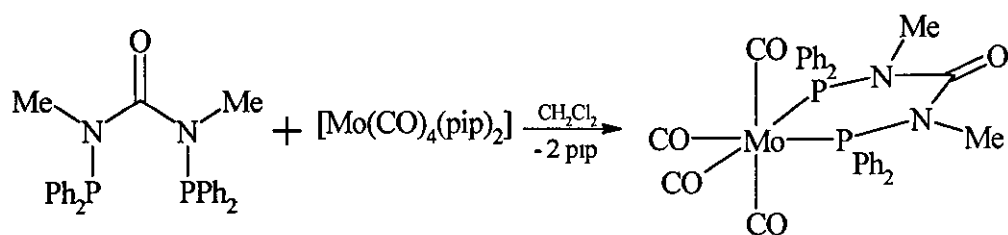
13

Equation 2.8

[Mo(CO)$_4$(pip)$_2$] was suspended in dry dichloromethane and **1** added as a solid. The reaction mixture was heated to reflux for 15 minutes, cooled, and the solvent volume reduced *in vacuo* to *ca.* 5.0 cm^3 The addition of methanol to the solution gave **13** as a yellow solid in 71 % yield. The ^{31}P-{^{1}H} NMR spectrum of **13** show a singlet at δ(P) 101.9, a downfield shift of approximately 50 ppm from the free ligand **1** and at a considerably higher frequency than the Pt(II) and Pd(II) complexes of **1** and **2**. The IR spectrum shows the expected peaks associated with ν(CO), ν(CN) and ν(PN) of the ligand (Table 2.5) as well as four distinct bands in the region 2100-1800 cm^{-1} due to the carbonyl ligands These peaks are consistent with the *cis* binding of the ligand and the terminal nature of the carbonyl groups. Elemental analysis is in good agreement with calculated values (Table 2.12) and the FAB$^+$ mass spectrum shows the parent-ion peak and the sequential loss of four carbonyl groups (m/z 664 [M]$^+$, 636 [M - CO]$^+$, 608 [M - 2CO]$^+$, 680 [M - 3CO]$^+$ and 652 [M - 4CO]$^+$) Yellow crystals of **13**, suitable for X-ray crystallography, were obtained by layering a dichloromethane solution of **13** with diethyl ether. The solid state structure of **13** is shown in Figure 2 8 and selected bond lengths and angles are shown in Table 2 13. The molecule displays octahedral geometry at the molybdenum with some contraction of the P(1)-Mo(1)-P(2) angle [80.7 (2)°]. The Mo-C distances differ as a consequence of the *trans* ligand, with Mo-C(31) and Mo-C(34) (*trans* to P) being shorter [ca. 2.00 Å] than Mo-C(32) and Mo-C(33) (*trans* to carbonyl) [ca.2.03 Å]. Unlike **9** the MoP$_2$N$_2$C ring is non-planar,

56

being hinged by 55° along the N(2)-P(1) vector. Within the MoP$_2$N$_2$C ring the P-N and C-N bond lengths are close to those reported for similar systems.[80]

Table 2.12 Elemental analysis data for complexes **9**, **10**, **13**, **14** and **15** (calculated values in parentheses).

Compound	Formula	C	H	N
9	[PdCl$_2$\{Ph$_2$PN(Me)\}$_2$CO]	50.9 (51.2)	3 8 (4.1)	3.9 (4.4)
10	[PdCl$_2$\{Ph$_2$PN(Et)\}$_2$CO]	50.8 (52.6)	4.4 (4.5)	3.8 (4 2)
13	[Mo(CO)$_4$\{Ph$_2$PN(Me)\}$_2$CO]	55.4 (56 0)	3.8 (3.9)	4.1 (4.2)
14	[Rh(cod)\{Ph$_2$PN(Et)\}$_2$CO]ClO$_4$	57.7 (58.9)	5.1 (5 3)	3 4 (3 5)
15	[(AuCl)$_2$\{Ph$_2$PN(Et)\}$_2$CO\}	36.9 (36 6)	3.6 (3.2)	3 2 (2.9)
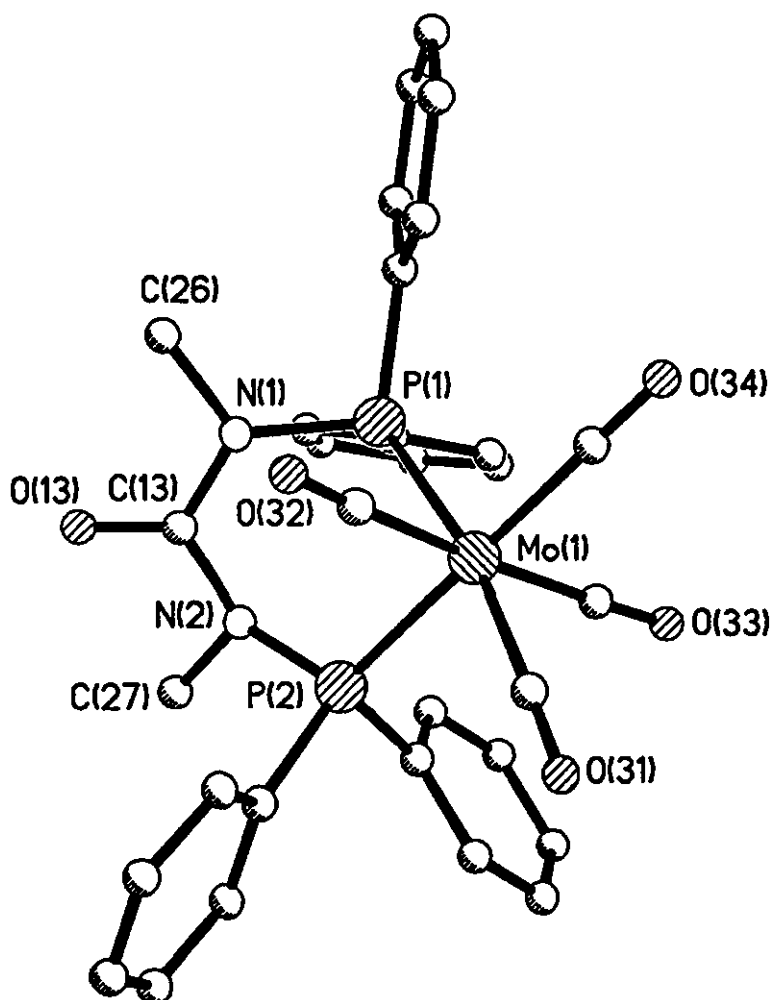
Figure 2.8 Solid state structure of *cis*-[Mo(CO)$_4$\{Ph$_2$PN(Me)C(O)N(Me)PPh$_2$\}] **13**

Table 2.13 Selected bond lengths (Å) and bond angles (°) for **13**.

Bond	Length	Bond	Angle
Mo(1)-P(1)	2.4849 (7)	P(1)-Mo(1)-P(2)	80.72 (2)
Mo(1)-P(2)	2.4808 (6)	Mo(1)-P(1)-N(1)	107.69 (7)
P(1)-N(1)	1.743 (2)	Mo(1)-P(2)-N(2)	116 23 (7)
P(2)-N(2)	1.731 (2)	P(1)-N(1)-C(13)	123.0 (2)
N(1)-C(13)	1.379 (3)	P(2)-N(2)-C(13)	124.4 (2)
N(2)-C(13)	1.411 (3)	N(2)-C(13)-N(1)	118.6 (2)
Mo(1)-C(31)	2 003 (3)	C(31)-Mo(1)-P(1)	170.25 (8)
Mo(1)-C(32)	2.024 (3)	C(31)-Mo(1)-P(2)	90.70 (8)
Mo(1)-C(33)	2.037 (3)	C(34)-Mo(1)-P(1)	97.54 (9)
Mo(1)-C(34)	2 001 (3)	C(34)-Mo(1)-P(2)	176.29 (8)

The reaction of two equivalents $\{Ph_2PN(Et)\}_2CO$ (**2**) with $[RhCl(cod)]_2$ in acetone proceeds according to Equation 2.9 to yield the P,P' chelate product cis-$[Rh(cod)\{Ph_2PN(Et)CON(Et)PPh_2\}][ClO_4]$, **14**.
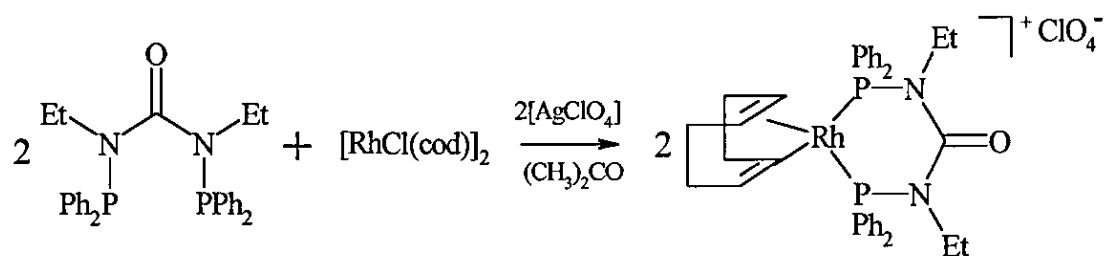
14

Equation 2.9

Addition of solid $\{Ph_2PN(Et)\}_2CO$ to a stirred solution of $[RhCl(cod)]_2$ and $Ag[ClO_4]$ followed by the addition of diethyl ether results in **14** as a brown solid in 58 % yield. The ^{31}P-$\{^1H\}$ NMR spectrum of **14** show a single phosphorus-containing species at $\delta(P)$ 90.3 with a $^1J(^{103}Rh$-$^{31}P)$ coupling of 167 Hz and the FAB^+ mass spectrum shows a peak corresponding to $[Rh(cod)\{Ph_2PN(Et)CON(Et)PPh_2$-$P,P'\}]^+$ (m/z 695). Elemental analysis is in agreement with calculated values (Table 2.12) and the IR spectrum shows peaks associated with $\nu(CO)$, $\nu(CN)$ and $\nu(PN)$ (Table 2.5).

2.4 *Bidentate bridging coordination chemistry of {Ph₂PN(Et)}₂CO.*

Compounds **3-10**, **13** and **14** demonstrate the ability of the ligands {Ph₂PN(Me)}₂CO and {Ph₂PN(Et)}₂CO to act as bidentate P,P' chelates and form six-membered metallacycles. As described in Chapter 1 Schmutzler and co-workers have also previously reported that {(Ph)(ᵗBu)PN(Me)}₂CO can act as a bidentate bridging ligand between two metal centres when reacted with [Fe₂(CO)₉].[31] We have also demonstrated that {Ph₂PN(Et)}₂CO can act as bidentate bridging ligand when reacted with [AuCl(tht)] to form the complex [Ph₂P{AuCl}N(Et)C(O) N(Et)P{AuCl}Ph₂], **15** (Equation 2.10).
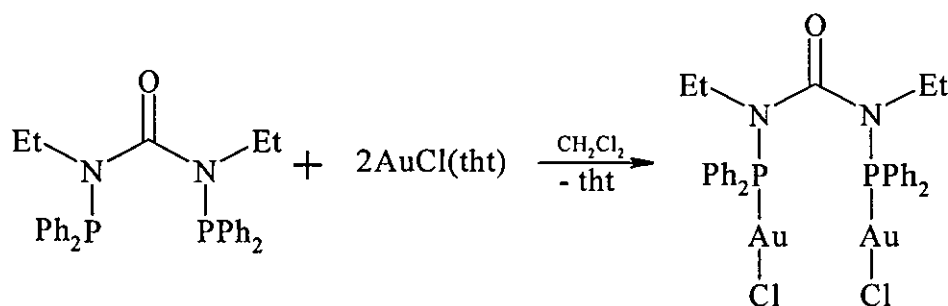
15

Equation 2.10

Addition of solid {Ph₂PN(Et)}₂CO to a dichloromethane solution of two equivalents of [AuCl(tht)] followed by addition of diethyl ether results in **15** as white solid in 72 % yield. The complex displays a singlet at δ(P) 75.7 in its ³¹P-{¹H} NMR spectrum and elemental analysis is in good agreement with calculated values (Table 2 12) The FAB⁺ mass spectrum shows a parent-ion peak and a peak corresponding to the loss of a chloride ion (m/z 948 [*M*]⁺ and 913 [*M* - Cl]⁺) and the IR spectrum shows peaks which can be assigned to ν(CO), ν(CN) and ν(PN) (Table 2.5) Layering of a chloroform solution of **15** with diethyl ether results in colourless crystals of [Ph₂P{AuCl}N(Et)C(O)N(Et)P{AuCl}Ph₂].CHCl₃ suitable for X-ray crystallography. The solid state structure of **15** is shown in Figure 2.9 and selected bond lengths and angles are shown in Table 2.14. The structure of **15** confirms that the molecule contains two Au centres. The overall W-shaped molecule has approximately non-crystallographic two fold axis about the C(13)-O(13) bond, though the backbone is

non-planar; N(1) and N(2) lie -0 45 and +0.21 Å from the N(1)-C(13)-O(13)-N(2) mean plane. The P-Au-Cl angles are close to linear, as expected, and there is no evidence of any delocalisation in P_2N_2C chain. P-N, P-Au and Au-Cl bond lengths are all comparable to those observed in similar compounds.[81]
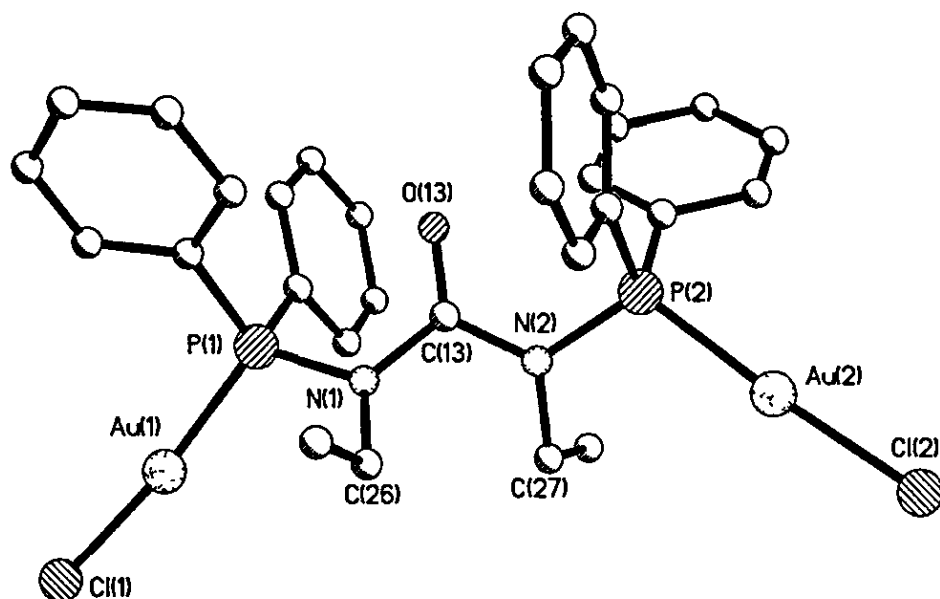
Figure 2.8 Solid state structure of [Ph$_2$P{AuCl}N(Et)C(O)N(Et)P{AuCl}Ph$_2$].CHCl$_3$.

Table 2.14 Selected bond lengths (Å) and angles (°) for **15.CHCl$_3$**

Bond	Length	Bond	Angle
Au(1)-Cl(1)	2 316 (2)	P(1)-Au(1)-Cl(1)	171.29 (6)
P(1)-Au(1)	2.239 (2)	N(1)-P(1)-Au(1)	114.1 (2)
P(1)-N(1)	1.709 (5)	C(26)-N(1)-P(1)	120 6 (4)
N(1)-C(26)	1.475 (7)	C(13)-N(1)-P(1)	117.3 (4)
N(1)-C(13)	1.415 (7)	N(1)-C(13)-O(13)	121.5 (5)
C(13)-O(13)	1.213 (6)	N(1)-C(13)-N(2)	116.3 (5)
C(13)-N(2)	1.389 (7)	N(2)-C(13)-O(13)	122.2 (5)
N(2)-C(27)	1.492 (7)	C(13)-N(2)-P(2)	118.3 (4)
N(2)-P(2)	1.706 (5)	C(27)-N(2)-P(2)	118.9 (4)
P(2)-Au(2)	2.243 (2)	N(2)-P(2)-Au(2)	110.1 (2)
Au(2)-Cl(2)	2.298 (2)	P(2)-Au(2)-Cl(2)	174.48 (7)

2.5 *Ligand synthesis of diphosphine derivatives of dialkyl thioureas*

Woollins[32] and Schmutzler[37, 38] have reported the synthesis of diphosphine derivatives of thioureas, the latter showing that {Ph$_2$PN(Me)}$_2$CS can be formed from the reaction of *N,N'*-dimethylthiourea and two equivalents of chlorodiphenylphosphine. We have discovered that the analogous reaction involving *N,N'*-diethylthiourea results in the ligand {Ph$_2$PN(Et)}$_2$CS. Schmutzler did not report any coordination chemistry for the {Ph$_2$PN(Me)}$_2$CS ligand. We have therefore synthesised {Ph$_2$PN(Me)}$_2$CS according to the published literature method and reacted the ligand with [PtCl$_2$(cod)].

The reaction of *N,N'*-diethyl thiourea with 2 equivalents of Ph$_2$PCl in thf and diethyl ether proceeds according to Equation 2.11 to yield {Ph$_2$PN(Et)}$_2$CS, **16**.
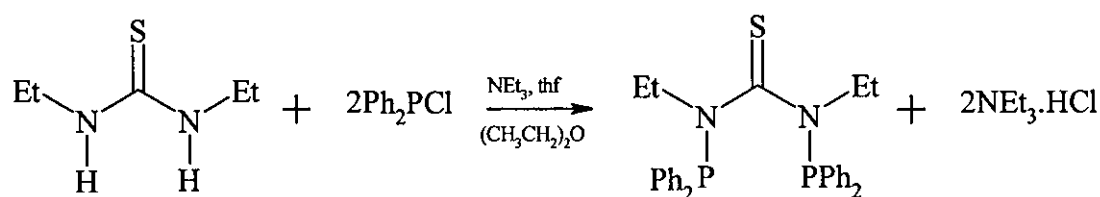
16

Equation 2.11

Slow addition of a diethyl ether solution of Ph$_2$PCl to a stirred thf/diethyl ether solution of {HN(Et)}$_2$CS and NEt$_3$ at -5°C results in the immediate precipitation of NEt$_3$.HCl. *In-situ* ^{31}P-{^{1}H} NMR studies conducted immediately after the addition of the chlorophosphine show the presence of two phosphorus containing species. A pair of doublets at δ(P) 45.8 and δ(P) −12.2 are attributed to the monosulfide Ph$_2$P-P(S)Ph$_2$ [^1J(^{31}P-^{31}P) 253 Hz] reported previously by Schmutzler[34] and discussed in Chapter 1. The major phosphorus containing species occurs at δ(P) 44.3 and we can be confident in assuming that this is the mono-substituted product Ph$_2$PN(Et)C(S)N(Et)H as its chemical shift is very similar to that reported by Schmutzler[37] for the analogous mono-substituted product Ph$_2$PN(Me)C(S)N(Me)H. Further addition of Ph$_2$PCl eventually results in the loss of this peak and the formation of the desired bis-substituted product at δ(P) 66 9. Removal of the NEt$_3$.HCl by suction filtration and reduction of the solvent volume *in vacuo* results in the precipitation of the product. Isolation of the product by suction filtration results in {Ph$_2$PN(Et)}$_2$CS, **16**, as a white

solid in low yield (26 %). Air- and moisture-tolerant **16** is readily soluble in dichloromethane and thf and elemental analysis is in good agreement with calculated values. FAB$^+$ mass spectrometry failed to show the expected parent-ion peak but did show a peak that can be attributed to the loss of a sulfur atom (m/z 468 [M-S]$^+$). The IR spectrum shows peaks which can be assigned to ν(CS) (1234 cm^{-1}), ν(CN) (1435 cm^{-1}) and ν(PN) (997 cm^{-1}).

2.6 *Reaction of {Ph$_2$PN(Me)}$_2$CS with [PtCl$_2$(cod)].*

Reports of metal complexes containing ligands of the type {Ph$_2$PN(R)}$_2$CE (E = O, S) are rare. Schmutzler reported the synthesis of {Ph$_2$PN(Me)}$_2$CS but did not describe any complexation chemistry for the ligand [38] Here we describe the reaction of {Ph$_2$PN(Me)}$_2$CS with [PtCl$_2$(cod)].

The ligand {Ph$_2$PN(Me)}$_2$CS was prepared according to literature methods[38] and reacted with equimolar quantities of [PtCl$_2$(cod)] in thf. The reaction fails to give the expected *P,P'* chelate system and instead proceeds according to Equation 2.12 with P-N bond cleavage, to give the novel five-membered heterocycle **17**.

17
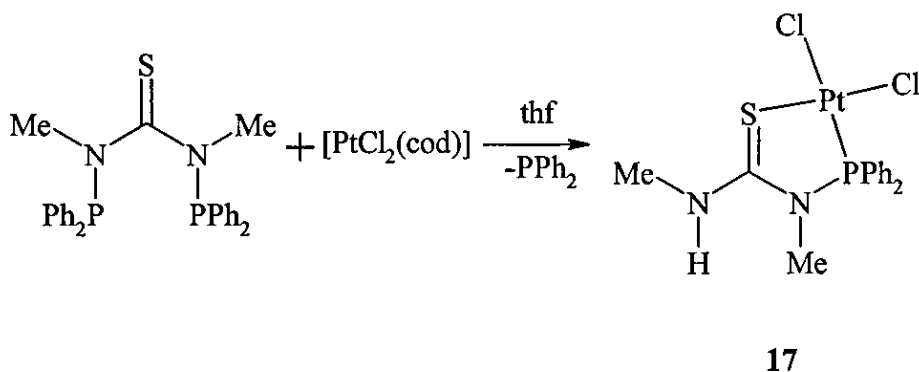
Equation 2.12

The ^{31}P-{^{1}H} NMR spectrum of **17** shows a singlet with satellites from coupling to ^{195}Pt. The product has a chemical shift of δ(P) 78 3 and the magnitude of the coupling [^{1}J(^{195}Pt-^{31}P) 3967 Hz] is once again in agreement with previously reported values for platinum (II) complexes where phosphorus is *trans* to chloride.[32] FAB$^+$ mass spectrometry failed to show the expected parent-ion peak but did show a peak corresponding to the loss of a chloride ion (m/z 519 [*M* - Cl]$^+$). Colourless crystals of **17** suitable for X-ray crystallography were grown by layering a chloroform/dmso
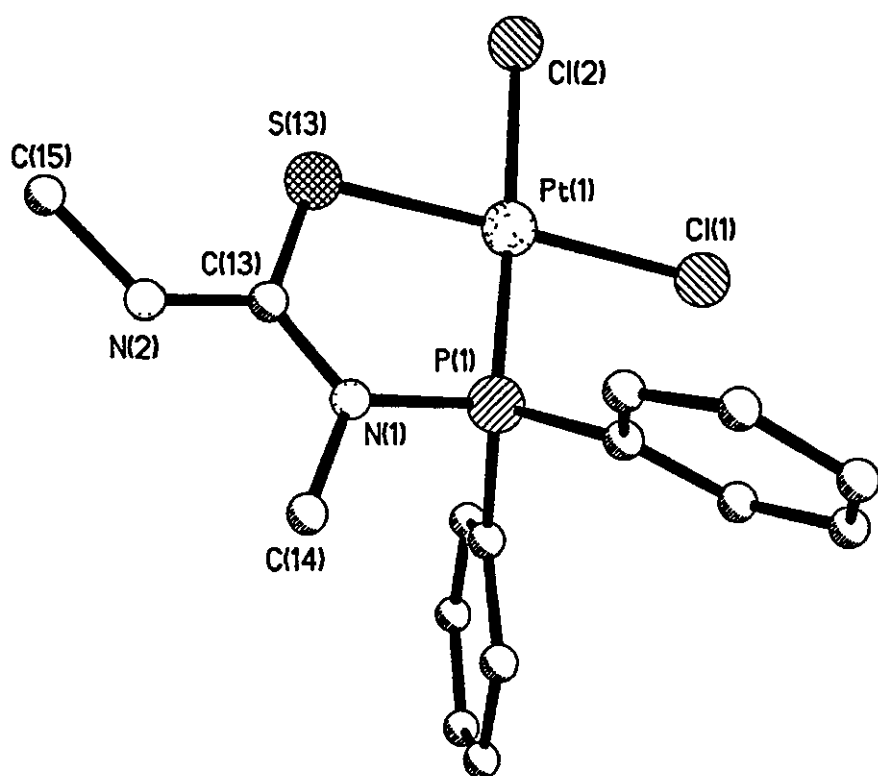
Figure 2.10 Solid state structure of [PtCl$_2$\{(Ph$_2$)PN(Me)CSN(Me)H-
P,*S*\}].dmso.CHCl$_3$.

Table 2.15 Selected bond lengths (Å) and bond angles (°) for **17** dmso.CHCl$_3$.

Bond	Length	Bond	Angle
Pt(1)-Cl(1)	2.324 (4)	Cl(1)-Pt(1)-Cl(2)	91 10 (14)
Pt(1)-Cl(2)	2.387 (3)	P(1)-Pt(1)-S(13)	88.02 (13)
Pt(1)-P(1)	2.188 (3)	Pt(1)-P(1)-N(1)	106.8 (4)
Pt(1)-S(13)	2.256 (4)	P(1)-N(1)-C(13)	118.7 (8)
P(1)-N(1)	1.739 (10)	P(1)-N(1)-C(14)	120.7 (9)
N(1)-C(14)	1 49 (2)	N(1)-C(13)-S(13)	121.7 (10)
N(1)-C(13)	1.34 (2)	C(13)-S(13)-Pt(1)	104.0 (5)
C(13)-S(13)	1.737 (13)	C(13)-N(1)-C(14)	120.2 (11)
C(13)-N(2)	1 34 (2)	N(2)-C(13)-S(13)	119.3 (10)
N(2)-C(15)	1.49 (2)	C(15)-N(2)-C(13)	123.4 (14)

solution of the product with diethyl ether. The solid state structure of **17**.dmso.CHCl₃ is shown in Figure 2.10 and selected bond lengths and angles are shown in Table 2.15 According to a recent review there are very few fully characterised examples of 5-membered 'true' heterocycles (i e. heterocycles in which every ring atom is different), though there is a report of a related PtSNCP heterocycle.[82,83] The X-ray structure of **17** reveals square planar coordination of the platinum with the five-membered PtPNCS ring being almost perfectly planar (maximum deviation from the PtPNCSCl₂ plane is 0.11 Å for S(13), with N(2),C(14) and C(15) lying 0 05, 0.18 and –0.06 Å from this plane). The bond lengths and angles within **17** are in the expected range. The Pt-Cl distances vary as a function of the trans element, within the five-membered PtPNCS heterocycle the P-N and C-N bonds are effectively single bonds whilst C(13)-S(13) is slightly longer than a formal C=S double bond.

2.7 *Conclusions*

Ligands of the type {Ph₂PN(R)}₂C=E (where R = Me or Et and E = O or S) can be readily synthesised via reactions of dialkylureas or thioureas with chlorodiphenylphosphine. Reactions of the compounds {Ph₂PN(Me)}₂C=O and {Ph₂PN(Et)}₂C=O with Pt(II), Pd(II), Mo(0) and Rh(I), results in the ligands acting as *P,P'* chelates and formation of six-membered ring systems, while {Ph₂PN(Et)}₂C=O acts as a bridging ligand when reacted with Au(I). Different substituents on the nitrogen atoms appear to have little influence on bond lengths and angles within the metal complexes. The coordination chemistry of {Ph₂PN(Me)}₂C=S is less predictable and results in P-N bond cleavage and the formation of a five-membered heterocycle when reacted with Pd(II). Studies of the chemistry of these types of ligands are still far from extensive. A great deal of scope exists for further investigation into the reactions of various urea and thiourea derivatives with different chlorophosphines and, subsequently, the coordination chemistry of any ligands produced. In particular, the coordinative properties of diphosphine derivatives of thioureas remain relatively unexplored.

Experimental

General experimental conditions and instrumentation were as set out on page 12. The complexes [AuCl(tht)] (tht = tetrahydrothiophene),[84] [MCl$_2$(cod)] (M = Pt or Pd; cod = cycloocta-1,5-diene),[85,86] [PtMeX(cod)] (X = Cl or Me),[87] [Mo(CO)$_4$(pip)$_2$],[88] and [{Rh(μ-Cl)(cod)}$_2$],[89] were prepared using literature procedures. Chlorodiphenylphosphine and triethylamine were distilled prior to use. N,N'-dimethylurea, N,N'-diethylurea, N,N'-diethylthiourea, P$_2$O$_5$, AgClO$_4$ and reagent grade KBr were used without further purification. Pd(OAc)$_2$ was kindly donated by BP Chemicals Ltd.

[Ph$_2$PN(Me)]$_2$CO 1. A solution of N,N'-dimethylurea (2.00 g, 22.6 mmol) and triethylamine (4.59 g, 6.5 cm^3, 45 4 mmol) in dichloromethane (20.0 cm^3) was added dropwise over a period of 3 h to a stirred solution of chlorodiphenylphosphine (9.94 g, 8.2 cm^3, 35 mmol) in dichloromethane (10.0 cm^3). Stirring was continued for 24 h. The solvent was removed *in vacuo* and diethyl ether (20.0 cm^3) added. The white solid was collected by suction filtration, washed with water to remove triethylamine hydrochloride and dried over P$_4$O$_{10}$ *in vacuo*. Yield: 5.76 g, 56 % Microanalysis: Found (Calcd for C$_{27}$H$_{26}$N$_2$OP$_2$) C 70.5 (71.0), H 5.0 (5 7), N 5.5 (6.1) %. ^{31}P-{^{1}H} NMR (CDCl$_3$): δ(P) 54 6 IR (KBr disc, cm^{-1}): 3050s, 2969s, 2932s, 1646vs, 1479s, 1432vs, 1422vs, 1408s, 1311s, 1183m, 1150m, 1116m, 1088s, 1067s, 1013s, 997s, 961vs, 819vs, 770m, 746vs, 694vs, 586s, 548m, 523s, 505s, and 493s FAB mass spectrum: m/z 456, [M^+].

[Ph$_2$PN(Et)]$_2$CO 2. A solution of N,N'-diethylurea (2 00 g, 17.2 mmol) and triethylamine (3 63 g, 5.0 cm^3, 35 0 mmol) in dichloromethane (20 0 cm^3) was added dropwise over a period of 4 h to a stirred solution of chlorodiphenylphosphine (7.57 g, 6.2 cm^3, 35.0 mmol) in dichloromethane (10.0 cm^3). Stirring was continued for 48 h. The solvent was removed *in vacuo* and diethyl ether (20.0 cm^3) added. The white solid was collected by suction filtration, washed with water to remove triethylamine hydrochloride and dried over P$_4$O$_{10}$ *in vacuo*. Yield: 3.35 g, 9 %. Microanalysis: Found (Calcd for C$_{29}$H$_{30}$N$_2$OP$_2$) C 70.8 (71.2), H 6.2 (6.2), N 5.3 (5 8) % ^{31}P-{^{1}H} NMR (CDCl$_3$): δ(P) 56.1. IR (KBr disc, cm^{-1}): 3054s, 2969s, 2931s, 1649vs, 1478s,

1432vs, 1378s, 1363s, 1318s, 1263vs, 1181m, 1134m, 1087s, 1041s, 992s, 936m, 783m, 749vs, 694vs and 493s. FAB mass spectrum. *m/z* 484, [M^+].

cis-[PtCl$_2${Ph$_2$PN(Me)CON(Me)PPh$_2$}] 3. To a solution of [PtCl$_2$(cod)] (0.033 g, 0.08 mmol) in dichloromethane (5.0 cm^3) was added solid [Ph$_2$PN(Me)]$_2$CO (0.040 g, 0.08 mmol) and the colourless solution stirred for *ca* 1 h. The solution was concentrated under reduced pressure to *ca.* 1.0 cm^3 and diethyl ether (10.0 cm^3) added. The white product was collected by suction filtration. Yield: 0.050 g, 79 %. Microanalysis: Found (Calcd for C$_{27}$H$_{26}$Cl$_2$N$_2$OP$_2$Pt) C 42 8 (44.9), H 3.4 (3.6), N 3.6 (3.8) %. ^{31}P-{^{1}H} NMR (CDCl$_3$): δ(P) 53 4, $^1J(^{195}$Pt-^{31}P) 3792 Hz.. IR (KBr disc, cm^{-1}): 3061s, 2960s, 2692s, 1672vs, 1484m, 1435s, 1315m, 1261w, 1182m, 1141m, 1092s, 1036m, 973m, 810w, 777w, 750s, 690m, 635w, 578w, 539s, 515s, 498m, 315w and 296m. FAB mass spectrum: *m/z* 722, [M]$^+$.

cis-[PtCl$_2${Ph$_2$PN(Et)CON(Et)PPh$_2$}] 4. To a solution of [PtCl$_2$(cod)] (0 038 g, 0.10 mmol) in dichloromethane (5.0 cm^3) was added solid [Ph$_2$PN(Et)]$_2$CO (0.050 g, 0.10 mmol) and the colourless solution stirred for *ca* 2 h. The solution was concentrated under reduced pressure to *ca* 1 0 cm^3 and diethyl ether (10 0 cm^3) added The white product was collected by suction filtration. Yield: 0.045 g, 58 %. Microanalysis: Found (Calcd for C$_{29}$H$_{30}$Cl$_2$N$_2$OP$_2$Pt) C 45.2 (46 4), H 4 2 (4.0) N 3.9 (3.7) % ^{31}P-{^{1}H}NMR (CDCl$_3$): δ(P) 56.7, $^1J(^{195}$Pt-^{31}P) 3910 Hz. IR (KBr disc, cm^{-1}): 3052s, 2977s, 2677s, 1669vs, 1478w, 1436vs, 1310s, 1249vs, 1186s, 1098vs, 1025w, 997s, 790w, 775w, 746s, 729w, 692vs, 628s, 611w, 542s, 521vs, 502w, 483s, 320s and 295s. FAB mass spectrum: *m/z* 715, [M – Cl]$^+$.

cis-[PtMe$_2${Ph$_2$PN(Me)CON(Me)PPh$_2$}] 5. To a solution of [PtMe$_2$(cod)] (0.044g, 0.13 mmol) in dichloromethane (10.0 cm^3) was added solid [Ph$_2$PN(Me)]$_2$CO (0 060 g, 0.13 mmol) and the colourless solution stirred for *ca* 3 h. The solution was concentrated under reduced pressure to *ca* 1.0 cm^3 and light petroleum (b p 60-80 °C) (10.0 cm^3) added. The white product was collected by suction filtration Yield: 0 058 g, 65 %. Microanalysis: Found (Calcd for C$_{29}$H$_{32}$N$_2$OP$_2$Pt) C 47 3 (50.1) H 4 9 (5.1), N 4.0 (4.2) % ^{31}P-{^{1}H} NMR (CDCl$_3$): δ(P) 74 9, $^1J(^{195}$Pt-^{31}P) 1944 Hz. IR (KBr disc, cm^{-1}): 3050s, 2942s, 2875s, 1626vs, 1482s, 1434vs, 1414s, 1295vs,

1100vs, 983s, 840s, 747vs, 710s, 696vs, 622s, 607s, 564vs, 539s, 517s, 494s, 474s and 302w. FAB mass spectrum: m/z 681, $[M]^+$.

cis-[PtMe$_2$\{Ph$_2$PN(Et)CON(Et)PPh$_2$\}] 6. To a solution of [PtMe$_2$(cod)] (0.034g, 0.10 mmol) in dichloromethane (5 0 cm^3) was added solid [Ph$_2$PN(Et)]$_2$CO (0.050 g, 0.10 mmol) and the colourless solution stirred for *ca* 2 h The solution was concentrated under reduced pressure to *ca* 1.0 cm^3 and light petroleum (b p. 60-80 °C) (10.0 cm^3) added. The white product was collected by suction filtration Yield: 0.046 g, 63 %. Microanalysis: Found (Calcd for C$_{31}$H$_{36}$N$_2$OP$_2$Pt) C 52.7 (52.4), H 5 8 (5.1), N 4 0 (3 9) %. ^{31}P-\{^{1}H\} NMR (CDCl$_3$)· δ(P) 77.7, $^1J(^{195}$Pt-^{31}P) 1997 Hz IR (KBr disc, cm^{-1}): 3057s, 2970s, 2933s, 2878s, 2801s, 1652vs, 1481s, 1458s, 1436vs, 1382s, 1324s, 1249vs, 1178s, 1097vs, 994s, 776s, 746vs, 696vs, 624s, 603s, 541s, 525vs, 475s, 449s, 348w, 303w and 224s. FAB mass spectrum m/z 710, $[M]^+$.

cis-[PtMe(Cl)\{Ph$_2$PN(Me)CON(Me)PPh$_2$\}] 7. To a solution of [PtMe(Cl)(cod)] (0.054g, 0.15 mmol) in dichloromethane (10.0 cm^3) was added solid [Ph$_2$PN(Me)]$_2$CO (0.070 g, 0 15 mmol) and the colourless solution stirred for *ca.* 1 h. The solution was concentrated under reduced pressure to *ca* 1 0 cm^3 and diethyl ether (10.0 cm^3) added The white product was collected by suction filtration Yield 0 075 g, 67 % Microanalysis: Found (Calcd for C$_{28}$H$_{29}$ClN$_2$OP$_2$Pt) C 47 5 (47.9), H 4.0 (4.2), N 3.7 (3.9) %. ^{31}P-\{^{1}H\} NMR (CDCl$_3$)· δ(P) (P$_A$ *trans* to CH$_3$) 74 1, $^1J(^{195}$Pt-^{31}P$_A$) 1819 Hz, δ(P) (P$_B$ *trans* to Cl) 61.4, $^1J(^{195}$Pt-^{31}P$_B$) 4509 Hz, $^2J(^{31}$P$_A$-^{31}P$_B$) 30 Hz. IR (KBr disc, cm^{-1}): 2949s, 2885s, 1637vs, 1481s, 1433vs, 1290vs, 1184s, 1101vs, 1027w, 984s, 844w, 747s, 713s, 694s, 624s, 610s, 566s, 546s, 512s, 493s, 476s and 303s. FAB mass spectrum: m/z 701, $[M]^+$.

cis-[PtMe(Cl)\{Ph$_2$PN(Et)CON(Et)PPh$_2$\}] 8. To a solution of [PtMe(Cl)(cod)] (0 036g, 0 10 mmol) in dichloromethane (5 0 cm^3) was added solid [Ph$_2$PN(Et)]$_2$CO (0 050 g, 0.10 mmol) and the colourless solution stirred for *ca* 2 h The solution was concentrated under reduced pressure to *ca* 1.0 cm^3 and diethyl ether (10.0 cm^3) added. The white product was collected by suction filtration. Yield: 0.049 g, 63 %. Microanalysis Found (Calcd for C$_{30}$H$_{33}$ClN$_2$OP$_2$Pt) C 48.2 (49.3), H 4.0 (4 5), N 3.1 (3.8) %. ^{31}P-\{^{1}H\} NMR (CDCl$_3$): δ(P) (P$_A$ *trans* to CH$_3$) 77 1, $^1J(^{195}$Pt-^{31}P$_A$) 1891 Hz,

δ(P) (P$_B$ *trans* to Cl) 64.2, $^1J(^{195}$Pt-^{31}P$_B$) 4596 Hz, $^2J(^{31}$P$_A$-^{31}P$_B$) 31 Hz. IR (KBr disc, cm^{-1}): 3056s, 2970s, 2883s, 1658vs, 1481s, 1458s, 1436vs, 1382s, 1324s, 1246vs, 1179s, 1098s, 996s, 776s, 747vs, 695vs, 624s, 606s, 545s, 522vs, 478s, 301w, 237s and 230s. FAB mass spectrum. *m/z* 730, [*M*]$^+$.

cis-[PdCl$_2$\{Ph$_2$PN(Me)CON(Me)PPh$_2$\}] 9. To a yellow solution of PdCl$_2$(cod) (0.033 g, 0.08 mmol) in dichloromethane (10.0 cm^3) was added solid [Ph$_2$PN(Me)]$_2$CO (0.040 g, 0.08 mmol) and the yellow solution stirred for *ca* 3 h. The solution was concentrated under reduced pressure to *ca* 1.0 cm^3 and diethyl ether (10.0 cm^3) added. The yellow product was collected by suction filtration Yield: 0 040 g, 73 %. Microanalysis: Found (Calcd for C$_{27}$H$_{26}$Cl$_2$N$_2$OP$_2$Pd) C 50 9 (51.2), H 3.8 (4.1), N 3.9 (4.4) % ^{31}P-\{^{1}H\} NMR (CDCl$_3$): δ(P) 76.2. IR (KBr disc, cm^{-1}): 3059s, 1648vs, 1481s, 1435vs, 1296vs, 1185s, 1102vs, 991s, 850s, 749s, 716s, 689s, 624s, 608s, 570s, 511s, 490s, 326s and 304s FAB mass spectrum: *m/z* 598, [*M* - Cl]$^+$.

cis-[PdCl$_2$\{Ph$_2$PN(Et)CON(Et)PPh$_2$\}] 10. To a yellow solution of [PdCl$_2$(cod)] (0.029 g, 0.10 mmol) in dichloromethane (5.0 cm^3) was added solid [Ph$_2$PN(Et)]$_2$CO (0 050 g, 0.10 mmol) and the yellow solution stirred for *ca* 1 h. The solution was concentrated under reduced pressure to *ca* 1.0 cm^3 and diethyl ether (10 0 cm^3) added. The yellow product was collected by suction filtration. Yield. 0 050 g, 73 %. Microanalysis: Found (Calcd for C$_{29}$H$_{30}$Cl$_2$N$_2$OP$_2$Pd) C 50.8 (52.6), H 4.4 (4.5), N 3 8 (4.2) %. ^{31}P-\{^{1}H\} NMR (CDCl$_3$) δ(P) 80.1. IR (KBr disc, cm^{-1}): 3052w, 2976w, 2677w, 1670vs, 1479w, 1454w, 1436s, 1311s, 1248vs, 1186s, 1103vs, 1023w, 996s, 938w, 790w, 775w, 746s, 728w, 692vs, 623s, 608s, 537s, 517vs, 476w, 322s and 296s. FAB mass spectrum: *m/z* 626, [*M*-Cl]$^+$.

[Pd\{OPPh$_2$\}\{N(Me)C(O)N(Me)PPh$_2$\}]$_2$ 11. To a yellow solution of [Pd(OAc)$_2$] (0.150 g, 0.70 mmol) in dichloromethane (10.0 cm^3) was added solid [Ph$_2$PN(Me)]$_2$CO (0 320 g, 0 70 mmol) and the dark yellow solution stirred for *ca* 2 h. The solution was concentrated under reduced pressure to *ca* 1.0 cm^3 and diethyl ether (10.0 cm^3) added. The dark yellow product was collected by suction filtration. Yield: 0.251 g, 31 % Microanalysis: Found (Calcd for C$_{54}$H$_{52}$N$_4$O$_4$P$_4$Pd$_2$) C 55.5 (56.1), H 4.3 (4.5), N 4.3 (4.8) %. ^{31}P-\{^{1}H\} NMR (CDCl$_3$) δ(P) 71.2 and 84.4 IR

(KBr disc, cm^{-1}): 3052w, 2915w, 1630vs, 1610vs, 1480w, 1434s, 1325s, 1208w, 1105vs, 1010vs, 995vs, 948w, 815w, 744s, 692vs, 595w, 552vs, 535s, 508vs, 492s and 345w. FAB mass spectrum· m/z 1158, $[M]^{+}$.

[Pd{OPPh$_2$}{N(Et)C(O)N(Et)PPh$_2$}]$_2$ 12. To a yellow solution of [Pd(OAc)$_2$] (0.045 g, 0.2 mmol) in dichloromethane (5.0 cm^3) was added solid [Ph$_2$PN(Me)]$_2$CO (0 100 g, 0 02 mmol) and the dark yellow solution stirred for *ca* 2 h. The solution was concentrated under reduced pressure to *ca* 1 cm^3 and diethyl ether (10 cm^3) added. The dark yellow product was collected by suction filtration. Yield: 0.127 g, 51 %. Microanalysis: Found (Calcd for C$_{58}$H$_{60}$N$_4$O$_4$P$_4$Pd$_2$) C 56.8 (57.4), H 4 6 (5.0), N 4 0 (4.6) %. ^{31}P-{^{1}H} NMR (CDCl$_3$)· δ(P) 69.5 and 84.4. IR (KBr disc, cm^{-1}): 3053w, 2927w, 1672w, 1620vs, 1481w, 1435s, 1369w, 1319s, 1281s, 1219w, 1181s, 1103s, 1034s, 1022s, 996s, 746s, 695vs, 593w, 553vs, 529s, 505s, 472w and 328w. FAB mass spectrum: m/z 1214, $[M]^{+}$.

***cis*-[Mo(CO)$_4${Ph$_2$PN(Me)CON(Me)PPh$_2$}] 13.** To a partially dissolved solution of [Mo(CO)$_4$(pip)$_2$] (0.580 g, 1.50 mmol) in dichloromethane (20 0 cm^3) was added solid [Ph$_2$PN(Me)]$_2$CO (0 700 g, 1.50 mmol). The solution was heated to reflux for *ca* 15 min and allowed to cool to room temperature. The solution was concentrated under reduced pressure to *ca* 2 0 cm^3 and methanol (15 0 cm^3) added. The yellow product was collected by suction filtration. Yield. 0.725 g, 71 %. Microanalysis· Found (Calcd for C$_{31}$H$_{26}$N$_2$O$_5$P$_2$Mo) C 55 4 (56.0), H 3.8 (3.9), N 4 1 (4.2) %. ^{31}P-{^{1}H}NMR (CDCl$_3$): δ(P) 101.9 IR (KBr disc, cm^{-1}): 3056s, 2940s, 2024s, 1916vs, 1905vs, 1890vs, 1634vs, 1433s, 1412w, 1297vs, 1213w, 1088s, 962s, 818s, 752s, 742s, 692s, 584s, 568s, 515s, 411s, 382s and 334w. FAB mass spectrum: m/z 664, $[M]^{+}$.

***cis*-[Rh(cod){Ph$_2$PN(Et)CON(Et)PPh$_2$}]$^{+}$[ClO$_4$]$^{-}$ 14.** To a stirred solution of [RhCl(cod)]$_2$ (0 050 g, 0.10 mmol) in acetone (20.0 cm^3) was added AgClO$_4$ and the solution stirred for 15 min. The colourless precipitate was removed by filtration and washed with acetone (10.0 cm^3). To the combined filtrates and washings was added solid [Ph$_2$PN(Et)]$_2$CO (0.098 g, 0.20 mmol) and the solution stirred for *ca* 1 h. The solution was concentrated under reduced pressure to *ca* 1 0 cm^3 and diethyl ether (5.0 cm^3) added. The brown product was collected by suction filtration. Yield: 0 092 g, 58

%. Microanalysis: Found (Calcd for $C_{39}H_{42}ClN_2O_5P_2Rh$) C 57.7 (58.9), H 5.1 (5.3), N 3.4 (3.5) %. ^{31}P-$\{^1H\}$ NMR (CDCl$_3$): δ(P) 92 6, 88.0 IR (KBr disc, cm^{-1}) 3054s, 2967s, 1664vs, 1482s, 1459s, 1437vs, 1382s, 1249vs, 1095vs, 996s, 751s, 694vs, 622vs, 606s, 529s, 511s, 460s and 234vs. FAB mass spectrum: m/z 695 corresponds to [Rh(cod){Ph$_2$PN(Et)CON(Et)PPh$_2$-P,P'}]$^+$.

[{Ph$_2$P(AuCl)N(Et)CON(Et)P(AuCl)Ph$_2$}] 15. To a solution of [AuCl(tht)] (0.032 g, 0.10 mmol) in dichloromethane (10 0 cm^3) was added solid [Ph$_2$PN(Et)]$_2$CO (0 050 g, 0 10 mmol) and the colourless solution stirred for *ca* 15 min. The solution was concentrated under reduced pressure to *ca* 1 0 cm^3 and diethyl ether (5.0 cm^3) added. The colourless product was collected by suction filtration. Yield: 0.069 g, 72 % Microanalysis: Found (Calcd for $C_{29}H_{30}Cl_2N_2OP_2Au_2$) C 36.9 (36.6), H 3 6 (3 2), N 3.2 (2.9) %. ^{31}P-$\{^1H\}$ NMR (CDCl$_3$): δ(P) 75.7. IR (KBr disc, cm^{-1}): 3054s, 2963s, 2922s, 2677s, 2493s, 1655vs, 1479s, 1436vs, 1366vs, 1340vs, 1256vs, 1182s, 1128s, 1102vs, 1059s, 997w, 757s, 745s, 727vs, 708s, 691vs, 548s, 533s, 519s, 497s, 318s and 225vs. FAB mass spectrum: m/z 949, [M]$^+$.

[Ph$_2$PN(Et)]$_2$CS 16. A solution of chlorodiphenylphosphine (5 0 g, 4.1 cm^3, 22.7 mmol) in diethyl ether (20.0 cm^3) was added dropwise over a period of 45 min to a stirred solution of N,N'-diethylthiourea (3.00 g, 22.7 mmol) and triethylamine (4 60 g, 6.3 cm^3, 35 0 mmol) in diethyl ether (100 0 cm^3) and thf (20.0 cm^3) at −5 °C. The reaction mixture was then allowed to warm to room temperature and stirring continued for 72 h during which time triethylammonium hydrochloride separated from the colourless solution. A second solution of chlorodiphenylphosphine (5.0 g, 4.1 cm^3, 22.7 mmol) in diethyl ether (20.0 cm^3) was added to the reaction mixture and stirring continued for a further 48 h Triethylammonium hydrochloride was removed by suction filtration and the reduction of the solvent volume *in vacuo* results in the precipitation of the product as a white solid. Yield 2.94 g, 26 % Microanalysis: Found (Calcd for $C_{29}H_{30}N_2P_2S$) C 69.0 (69.6), H 6.0 (6.0), N 5.3 (5.6) % ^{31}P-$\{^1H\}$ NMR (CDCl$_3$): δ(P) 67 8 IR (KBr disc, cm^{-1}): 2976w, 2677w, 1663s, 1554vs, 1478s, 1435vs, 1383s, 1244s, 1174s, 1130m, 1092s, 1036s, 997s, 919m, 850m, 739vs, 694vs, 557vs, 514vs, 496vs and 376w FAB mass spectrum: m/z 468, [M-S]$^+$.

[PtCl₂{(Ph₂)PN(Me)CSN(Me)H}] 17. To a solution of [PtCl₂(cod)] (0 040 g, 0.10 mmol) in dichloromethane (5.0 cm³) was added solid [Ph₂PN(Me)]₂CS (0 050 g, 0.10 mmol) and the pale yellow solution stirred for *ca* 1 h. The solution was concentrated under reduced pressure to *ca* 1.0 cm³ and diethyl ether (10 cm³) added. The pale yellow product was collected by suction filtration. Yield: 0.050 g, 85 %. Microanalysis: Found (Calcd for $C_{15}H_{17}Cl_2N_2P_2SPt$) C 32.1 (32.4), H 2.9 (3.1), N 4 8 (5.1) %. $^{31}P\text{-}\{^1H\}$ NMR (CDCl₃): δ(P) 78.3, $^1J(^{195}Pt\text{-}^{31}P)$ 3967 Hz. . IR (KBr disc, cm⁻¹): 3222w, 3052w, 1577vs, 1482m, 1436vs, 1376s, 1325vs, 1218w, 1185w, 1142w, 1106vs, 1059m, 997m, 829s, 747s, 718m, 691s, 578s, 541m, 521m, 490s, 318w, 290m, 3235m, 221vs and 210vs. FAB mass spectrum: *m/z* 519, [*M*-Cl]⁺.

Chapter 3

The Preparation and Coordination Chemistry of Phosphorus (III) Derivatives of Dialkyl Hydrazines.

3.1 *Introduction.*

Since the discovery of bis(dihalophosphino)amines, $X_2P-N(R)-PX_2$[90-92], extensive research has been carried out on the main group and transition metal/organometallic chemistry of this type of ligand systems.[90-105] This is in sharp contrast to the corresponding studies of the dinitrogen-bridged diphosphines, bis(dihalophosphino)hydrazines, $X_2PN(R)N(R)PX_2$, which, until recent work by Katti and co-workers[47,48,49], has been limited to a few reports[21,40] The development of the chemistry of bis(dihalophosphino)hydrazine ligands is of particular significance because they have a similar chain length to that of dppe, a ligand which has proved adapt at forming five-membered chelate rings and has demonstrated significant applications in catalytic systems. The reactivity of the halide substituents on these ligands may also be utilised in the development of a wide range of $R'_2PN(R)N(R)PR'_2$-type of derivatives, allowing excellent control of the steric and electronic properties of any subsequent ligands. The studies reported by Katti and co-workers have centred on the synthesis and coordination chemistry of derivatives of bis(dichlorophosphino) dimethylhydrazine, $Cl_2PN(Me)N(Me)PCl_2$. We have studied the synthesis of derivatives of bis(dichlorophosphino) diethylhydrazine, $Cl_2PN(Et)N(Et)PCl_2$ and report on the effects changes in substituent groups have on the coordination chemistry of such ligands. We have also synthesised a number of derivatives of $Cl_2PN(Me)N(Me)PCl_2$ containing phenyl groups with substituents in the *ortho* position to investigate the possibility of these substituents occupying sites above and below metal centres in complexes thus limiting the available approach routes of reactants in catalytic systems

Results and discussion

3.2 *Synthesis of Cl$_2$PN(Et)N(Et)PCl$_2$*

As discussed in Chapter 1 Katti has reported the synthesis of Cl$_2$PN(Me)N(Me)PCl$_2$ from the reaction of 1,2-dimethylhydrazine dihydrochloride and phosphorus trichloride.[47] Employing a similar technique we were able to synthesise the analogous diphosphine, Cl$_2$PN(Et)N(Et)PCl$_2$ **18**, from the reaction of 1,2-diethylhydrazine dihydrochloride and phosphorus trichloride (Equation 3.1).

$$\text{HN(Et)N(Et)H.2HCl} \;+\; \text{excess PCl}_3 \longrightarrow \quad
\begin{array}{c}
\text{Et} \quad\quad \text{Et} \\
\diagdown \quad\quad \diagup \\
\text{N}-\text{N} \\
\diagup \quad\quad \diagdown \\
\text{Cl}_2\text{P} \quad\quad \text{PCl}_2
\end{array}$$
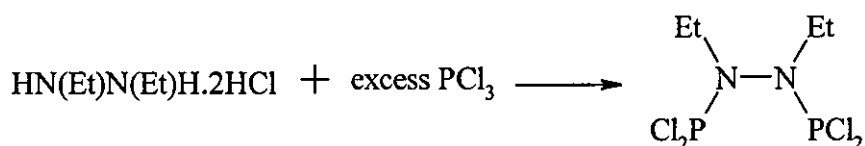
<div align="right">**18**   **Equation 3.1**</div>

Dropwise addition of PCl$_3$ to a finely ground sample of 1,2-diethylhydrazine dihydrochloride results in the formation of a viscous orange suspension. The reaction mixture is then heated under reflux for 96 hours and the excess PCl$_3$ removed *in vacuo* to leave a viscous orange oil. Kugelrohr distillation of the crude product leaves **18** as a colourless oil in good yield (72 %). The ^{31}P-$\{^{1}$H$\}$ NMR spectrum of **18** shows a singlet at δ(P) 156, an upfield shift of approximately 4 ppm from the value reported for Cl$_2$PN(Me)N(Me)PCl$_2$[47], and FAB^{+} mass spectrometry shows the expected parent-ion peak (m/z 290 $[M]^{+}$). Elemental analysis is in good agreement with the calculated values (Table 3 2) and the IR spectrum shows a band at 952 cm^{-1} that can be assigned to ν(PN). Having successfully synthesised Cl$_2$PN(Et)N(Et)PCl$_2$ we were then able to use this compound as a chloro precursor in nucleophilic substitution reactions and reactions with Grignard reagents to produce a range of aryloxy- and aryl-substituted phosphorus (III) hydrazides.

3.3 *Reaction of Cl$_2$PN(Et)N(Et)PCl$_2$ with Phenol.*

Reaction of Cl$_2$PN(Et)N(Et)PCl$_2$ with 4 equivalents of PhOH in the presence of Et$_3$N in hexane proceeds according to Equation 3.2 to yield the aryloxy-functionalised ligand (PhO)$_2$PN(Et)N(Et)P(OPh)$_2$ **19**.

$$\text{Et}_2\text{N-N(Et)}_2 \text{ structure: } Cl_2P\text{-N(Et)-N(Et)-}PCl_2 + 4PhOH \xrightarrow[\text{C}_6\text{H}_{14}]{4Et_3N} (PhO)_2P\text{-N(Et)-N(Et)-}P(OPh)_2 + 4NEt_3\cdot HCl$$
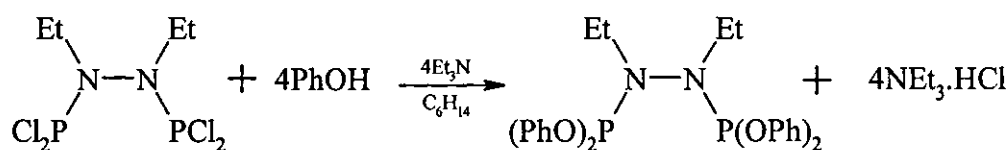
19   **Equation 3.2**

Dropwise addition of a hexane solution of phenol and triethylamine to a stirred hexane solution of $Cl_2PN(Et)N(Et)PCl_2$ results in the immediate precipitation of $[NEt_3H]Cl$ as the reaction proceeds. Stirring is continued for a further 12 hours. Removal of the ammonium salt by suction filtration and removal of the solvent *in vacuo* leaves **19** as a colourless viscous oil in good yield (81 %) The $^{31}P\text{-}\{^1H\}$ NMR spectrum of **19** consists of a single resonance at $\delta(P)$ 139, the difference in chemical shift between it and **18** (27 ppm) being comparable to that observed between $Cl_2PN(Me)N(Me)PCl_2$ and $(PhO)_2PN(Me)N(Me)P(OPh)_2$.[47,48] Elemental analysis is in agreement with calculated values (Table 3.2) and FAB^+ mass spectrometry shows the expected parent-ion peak (m/z 520 $[M]^+$) The IR spectrum of **19** shows bands which can be assigned to $\nu(PN)$ and $\nu(PO)$ (930 cm^{-1} and 1030 cm^{-1} respectively)

3.4 Reactions of Cl₂PN(Et)N(Et)PCl₂ with Grignard Reagents

Reaction of $Cl_2PN(Et)N(Et)PCl_2$ **18** with 4 equivalents of RMgBr (R= Ph or CH_2Ph), in diethyl ether, proceeds according to Equation 3 3 to yield the diphosphines $Ph_2PN(Et)N(Et)PPh_2$ **20** and $(PhCH_2)_2PN(Et)N(Et)P(CH_2Ph)_2$ **21**.

$$Cl_2P\text{-N(Et)-N(Et)-}PCl_2 + 4RMgBr \xrightarrow{(CH_3CH_2)_2O} R_2P\text{-N(Et)-N(Et)-}PR_2 + 4MgBrCl$$
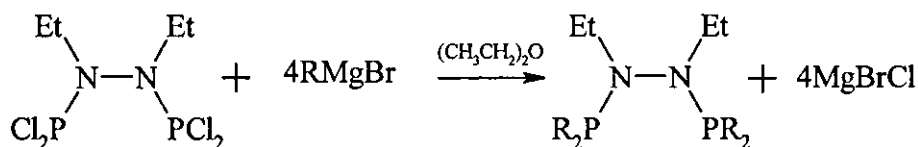
R = Ph (**20**), CH_2Ph (**21**)

Equation 3.3

Diethyl ether solutions of **18** were added dropwise to stirred solutions of PhMgBr and $CH_2PhMgBr$ in diethyl ether at 0 °C and the reaction mixtures stirred for a further 18 and 12 hours respectively. After this time deionized water was added slowly and the

layers separated. The diethyl ether layers were dried over $MgSO_4$ before being removed *in vacuo* to leave **20** and **21** as colourless and pale yellow solids in good yields (70 and 74% respectively) FAB^+ mass spectrometry shows peaks corresponding to the parent-ion peaks $[M]^+$ (m/z 456 for **20** and m/z 512 for **21**) and the IR spectra contain bands which can be assigned to v(PN) (970 cm^{-1} for **20** and 962 cm^{-1} for **21**) The ^{31}P-{^{1}H} NMR spectra of the two compounds show singlets at δ(P) 64.2 and 64.8 respectively, significantly further upfield than the value for **19** due to the lack of highly electronegative oxygen atoms close to the phosphorus centres Elemental analyses are in good agreement with calculated values (Table 3.2).

A series of ligands containing phenyl groups with substituents in the *ortho* position have also been successfully synthesised Reaction of the chloro precursor **18** with the grignard reagent *o*-anisylmagnesium bromide, 2-$CH_3OC_6H_4MgBr$, generates (*o*-$C_6H_4OCH_3$)$_2$PN(Et)N(Et)P(*o*-$C_6H_4OCH_3$)$_2$ **22**, while reaction of $Cl_2PN(Me)N(Me)PCl_2$ with *o*-anisylmagnesium bromide or *o*-tolylmagnesium chloride, 2-$CH_3C_6H_4MgCl$, yields (*o*-$C_6H_4OCH_3$)$_2$PN(Me)N(Me)P(*o*-$C_6H_4OCH_3$)$_2$ **23** and (*o*-$C_6H_4CH_3$)$_2$PN(Me)N(Me)P(*o*-$C_6H_4CH_3$)$_2$ **24** respectively (Equation 3.4 and 3.5).
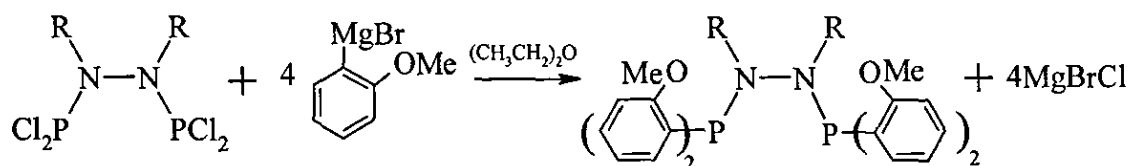
R = Et (**22**), Me (**23**)

Equation 3.4
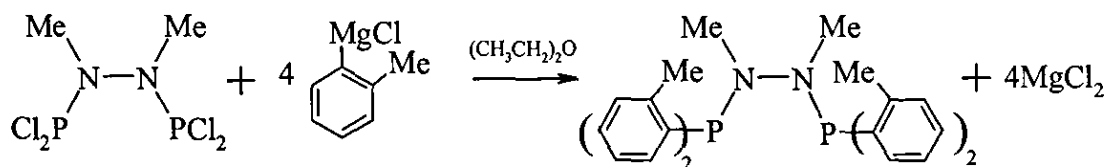
24   **Equation 3.5**

In the syntheses of **22** and **23** diethyl ether solutions of the chlorophosphines are added dropwise to stirred diethyl ether solutions of 2-$CH_3OC_6H_4MgBr$ (prepared previously from the reaction of 2-bromoanisole and magnesium turnings) and the

reaction mixtures stirred for 48 hours. Slow addition of deionized water results in the formation of two layers that are separated. The diethyl ether layers are then dried over $MgSO_4$ before being evaporated *in vacuo* to leave **22** and **23** as colourless oils. Trituration of the oils with light petroleum leaves the products **22** and **23** as colourless solids in yields of 67 and 81 % respectively. The $^{31}P-\{^1H\}$ NMR spectra of the two ligands show singlets at δ(P) 40.5 and 42.6 respectively and the FAB$^+$ mass spectra contain peaks corresponding to $[M]^+$ (m/z 576 for **22** and m/z 549 for **23**). The IR spectra of both compounds show a band which can be assigned to ν(PN) (933 cm^{-1} for **22** and 969 cm^{-1} for **23**) and elemental analyses are in agreement with calculated values (Table 3.1). The synthesis of **24** is achieved by using a similar technique to that employed in the synthesis of **22** and **23**, the only difference being that after addition of $Cl_2PN(Me)N(Me)PCl_2$ to the Grignard $2\text{-}C_6H_4CH_3MgCl$, the reaction mixture is heated to reflux for 4 h. The same work-up procedure was then employed to leave (*o*-$C_6H_4CH_3)_2PN(Me)N(Me)P(o\text{-}C_6H_4CH_3)_2$ **24** as a pale yellow solid in 65 % yield. Elemental analysis of the product was in good agreement with calculated values (Table 3.1) and the IR spectrum showed a band at 956 cm^{-1} that is characteristic of a ν(PN) stretch. As with **22** and **23** the $^{31}P-\{^1H\}$ NMR spectrum of **24** indicates the presence of a single phosphorus species, represented by a singlet at δ(P) 47.2 and the FAB$^+$ mass spectrum shows a peak which corresponds to the parent-ion (m/z 485 $[M]^+$).

3.5 *Coordination chemistry of $R_2PN(Et)N(Et)PR_2$*

Katti has reported the synthesis of various metal complexes in which diphosphine derivatives of $Cl_2PN(Me)N(Me)PCl_2$ act as *P,P'* chelates.[23,47-49] Here we describe the synthesis of metal complexes containing derivatives of $Cl_2PN(Et)N(Et)PCl_2$ acting as *P,P'* chelates, as well as further examples involving derivatives of $Cl_2PN(Me)N(Me)PCl_2$

The reaction of $(PhO)_2PN(Et)N(Et)P(OPh)_2$ **19** with equimolar quantities of $[PtCl_2(cod)]$ or $[PdCl_2(cod)]$ in dichloromethane proceeds according to Equation 3.6 to yield the five-membered, *P,P'* chelates *cis*-$[PtCl_2\{(PhO)_2PN(Et)N(Et)P(OPh)_2\}]$ **25** and *cis*-$[PdCl_2\{(PhO)_2PN(Et)N(Et)P(OPh)_2\}]$ **26** respectively.

Table 3.1 Elemental analysis data for complexes **18-24** (calculated values in parentheses).

Cpd	Formula	C	H	N
18	$Cl_2PN(Et)N(Et)PCl_2$	17 0 (16.6)	3.9 (3.5)	9.8 (9.7)
19	$(PhO)_2PN(Et)N(Et)P(OPh)_2$	70.0 (69.6)	5.5 (5.8)	5.2 (5.4)
20	$Ph_2PN(Et)N(Et)PPh_2$	72.9 (73.7)	6.5 (6 6)	5.9 (6.1)
21	$(PhCH_2)_2PN(Et)N(Et)P(CH_2Ph)_2$	74.3 (74 9)	7.4 (7.5)	5.2 (5.5)
22	$(o\text{-}C_6H_4OCH_3)_2PN(Et)N(Et)P(o\text{-}C_6H_4OCH_3)_2$	66 1 (66.6)	6.3 (6.6)	4.4 (4.8)
23	$(o\text{-}C_6H_4OCH_3)_2PN(Me)N(Me)P(o\text{-}C_6H_4OCH_3)_2$	65.1 (65.7)	5.9 (6.3)	4.8 (5 1)
24	$(o\text{-}C_6H_4CH_3)_2PN(Me)N(Me)P(o\text{-}C_6H_4CH_3)_2$	73 7 (74.4)	6 8 (7 1)	5.2 (5 8)
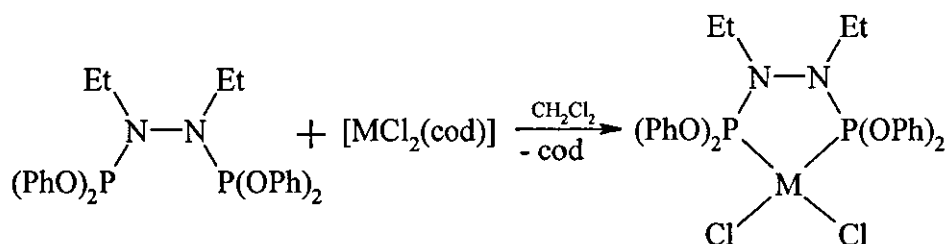
M = Pt (**25**), Pd (**26**)

Equation 3.6

Addition of the diphosphine **19** to a dichloromethane solution of [PtCl₂(cod)] results in the formation of a colourless solution. Stirring is continued for a further 2 hours, after which time diethyl ether is added and **25** is precipitated as a white solid in moderate yield (65 %). The same technique is employed in the synthesis of **26** and results in the product as a yellow solid in 50 % yield The $^{31}P\text{-}\{^1H\}$ NMR spectra of

the compounds show singlets, at δ(P) 92.3 and 116 6 respectively which both correspond to an upfield shift of approximately 3 ppm when compared to the analogous dimethyl complexes cis-[MCl$_2$\{(PhO)$_2$PN(Me)N(Me)P(OPh)$_2$\}].[49] The spectrum of **25** also shows satellites from coupling to [195]Pt. The magnitude of the coupling (5503 Hz) is in agreement with the value (5497 Hz) previously reported for the N,N'-dimethyl compound cis-[PtCl$_2$\{(PhO)$_2$PN(Me)N(Me)P(OPh)$_2$\}][49] and is indicative of a strong platinum-phosphorus interaction The IR spectra of **25** and **26** both show bands corresponding to ν(PN) and ν(PO) (928 and 1069 cm^{-1} respectively for **25** and 955 and 1070 cm^{-1} respectively for **26**) as well as two distinct ν(MCl) stretches (325 and 299 cm^{-1} for **25** and 325 and 296 cm^{-1} for **26**) which are indicative of a cis-MCl$_2$ geometry. FAB$^+$ mass spectrometry shows the expected parent-ion peaks and peaks corresponding to the loss of a chloride ion (m/z 786 [M]$^+$ and 750 [M − Cl]$^+$ for **25** and m/z 698 [M]$^+$ and 662 [M − Cl]$^+$ for **26**) and elemental analysis is in good agreement with calculated values (Table 3.5). Layering of a dichloromethane solution of **26** with diethyl ether gave yellow crystals of **26** suitable for X-ray crystallography. The solid state structure of cis-[PdCl$_2$\{(PhO)$_2$PN(Et)N(Et)P(OPh)$_2$\}] is shown in Figure 3.1 and selected bond lengths and angles are shown in Table 3.2. The X-ray structure of **26** contains two crystallographically independent molecules although the two molecules are structurally similar The five membered chelate rings result in P-Pd-P angles of less than 90° Both molecules are almost perfectly planar about the palladium [mean deviation from the PdP$_2$Cl$_2$ planes of 0.04 and 0.02 Å]. The PdP$_2$N$_2$ rings have a classic open envelope conformation. In the Pd(1)-P(1)-N(1)-N(2)-P(2) ring N(2) is out of the plane by 0 59 Å and in the Pd(2)-P(3)-N(3)-N(4)-P(4) ring N(3) and N(4) lie above the coordination plane by 0.41 and 0.72 Å respectively. The P-N, Pd-Cl and Pd-P bond lengths in **26** are in agreement with values previously reported for single bonds in the similar chelate complex cis-[PdCl$_2$\{(p-BrC$_6$H$_4$O)$_2$PN(Me)N(Me)P(OC$_6$H$_4$Br-p)$_2$\}][49], although the P-N bond lengths are considerably shorter than those observed in **31** and the chelate complexes described in Chapter 2.
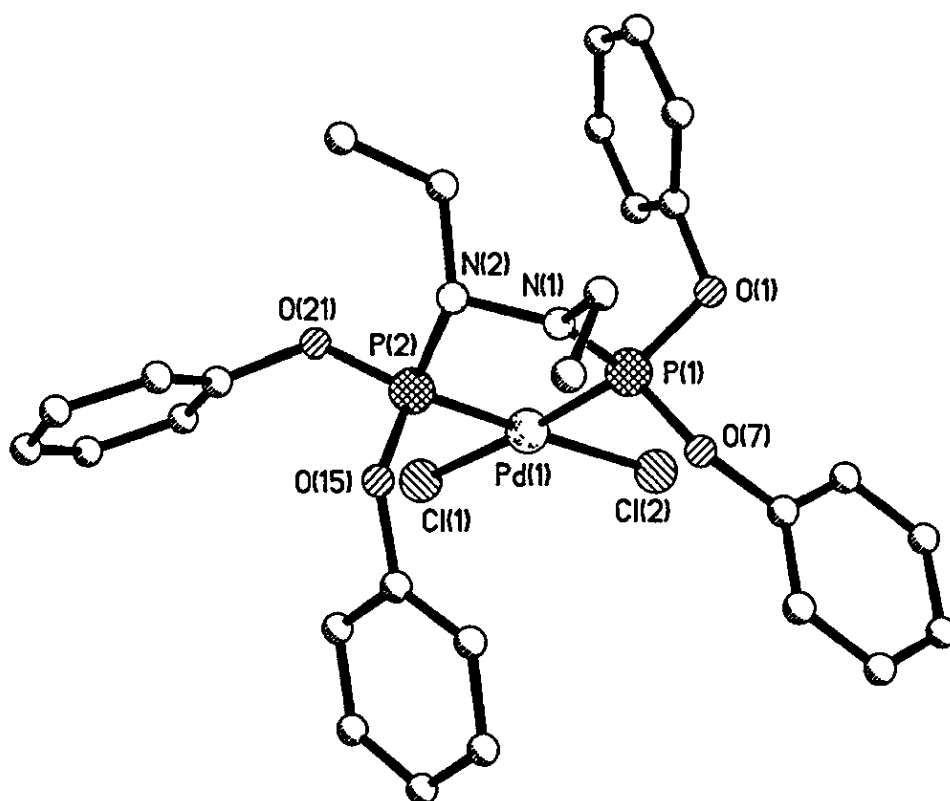
Figure 3.1 The solid state structure of cis-[PdCl₂{(PhO)₂PN(Et)N(Et)P(OPh)₂}] **26**.

Table 3.2 Selected bond lengths (Å) and angles (°) for **26**.

Bond	Length	Bond	Angle
Pd(1)-Cl(1)	2.343 (2) [2.342 (2)]	Cl(1)-Pd(1)-Cl(2)	93.20 (6) [94.17 (5)]
Pd(1)-Cl(2)	2.341 (2) [2.352 (14)]	P(1)-Pd(1)-P(2)	82.24 (6) [81 46 (5)]
Pd(1)-P(1)	2.199 (2) [2.207 (2)]	P(1)-Pd(1)-Cl(2)	90.30 (6) [91.46 (5)]
Pd(1)-P(2)	2.193 (2) [2.194 (2)]	P(2)-Pd(1)-Cl(1)	94.35 (6) [92.92 (6)]
P(1)-N(1)	1.654 (4) [1 662 (4)]	Pd(1)-P(1)-N(1)	107.9 (2) [108 3 (2)]
P(1)-O(1)	1.606 (4) [1.594 (3)]	Pd(1)-P(2)-N(2)	110.8 (2) [110.0 (2)]
P(1)-O(7)	1.579 (4) [1.587 (4)]	P(1)-N(1)-N(2)	119.5 (3) [119.4 (3)]
P(2)-N(2)	1.684 (4) [1.663 (4)]	P(2)-N(2)-N(1)	105.7 (3) [109.0 (3)]
P(2)-O(15)	1.582 (4) [1.582 (4)]	N(1)-P(1)-O(1)	109.9 (2) [107.4 (2)]
P(2)-O(21)	1.569 (4) [1.568 (4)]	N(2)-P(2)-O(21)	102.4 (2) [103.7 (2)]
N(1)-N(2)	1.434 (5) [1.432 (5)]	N(1)-P(1)-O(7)	100.2 (2) [102.7 (2)]

N B The values in parentheses are for the second crystallographically independent molecule

The ligand $Ph_2PN(Et)N(Et)PPh_2$ also reacts with equimolar quantities of $[PtCl_2(cod)]$ and $[PdCl_2(cod)]$ to yield five-membered P,P' chelates. The reactions proceed according to Equation 3.7 and result in the metal complexes *cis*-$[PtCl_2\{Ph_2PN(Et)N(Et)PPh_2\}]$ **27** and *cis*-$[PdCl_2\{Ph_2PN(Et)N(Et)PPh_2\}]$ **28**.

$$Et\diagdown N{-}N\diagup Et \text{ with } Ph_2P\diagup \diagdown PPh_2 \quad + \quad [MCl_2(cod)] \xrightarrow[-\ cod]{CH_2Cl_2} \quad Et\diagdown N{-}N\diagup Et,\ Ph_2P\diagdown M\diagup PPh_2,\ Cl\diagup \diagdown Cl$$
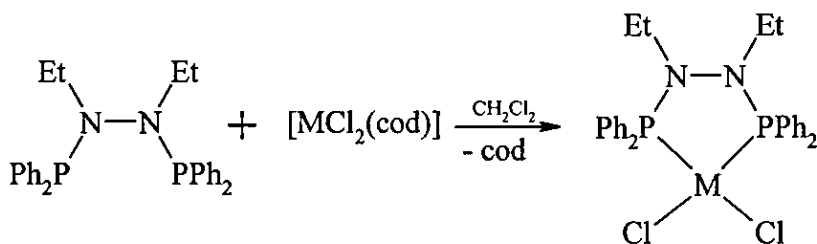
M = Pt (**27**), Pd (**28**)

Equation 3.7

Addition of the solid diphosphine **20** to dichloromethane solutions of $[PtCl_2(cod)]$ or $[PdCl_2(cod)]$ results in the formation of colourless or yellow solutions respectively. In both cases stirring is continued for a further 2 hours before the addition of diethyl ether. This results in the precipitation of *cis*-$[PtCl_2\{Ph_2PN(Et)N(Et)PPh_2\}]$ **27** as a colourless solid and the precipitation of *cis*-$[PdCl_2\{Ph_2PN(Et)N(Et)PPh_2\}]$ **28** as a pale yellow solid, both in 78 % yields. Elemental analysis for both compounds is in good agreement with calculated values (Table 3.5) and the $^{31}P\text{-}\{^1H\}$ NMR spectra show singlets at $\delta(P)$ 100.4 and 132.2 respectively. The $^{31}P\text{-}\{^1H\}$ NMR spectrum of **27** also shows satellites from coupling to ^{195}Pt, the magnitude of which (4055 Hz) is in agreement with values previously reported for Pt(II) complexes containing the phosphorus, of a P – N ligand, *trans* to a chloride[32] and indicates the expected ^1J interaction. However, due to the lack of a highly electronegative oxygen next to the phosphorus atom, this value is significantly smaller than the $^1J(^{195}Pt\text{-}^{31}P)$ value associated with **25**. The FAB^+ mass spectrum of each compound displays the parent-ion peak and a peak corresponding to the loss of a chloride ion (m/z 722 $[M]^+$ and 687 $[M$ - $Cl]^+$ for **27** and m/z 634 $[M]^+$ and 599 $[M - Cl]^+$ for **28**) and the IR spectra show bands characteristic of $\nu(PN)$ stretches (997 cm^{-1} for **27** and **28**) indicating an increase in the bond order. The IR spectra of **27** and **28** also show two distinct $\nu(MCl)$ stretches (314 and 290 cm^{-1} for **27** and 323 and 292 cm^{-1} for **28**), further evidence of the *cis* geometry of the complex.

The reaction of $Ph_2PN(Et)N(Et)PPh_2$ with equimolar quantities of [PtCl(Me)(cod)] in dichloromethane proceeds according to Equation 3.8 to give *cis*-[PtCl(Me){$Ph_2PN(Et)N(Et)PPh_2$}] **29**.

29
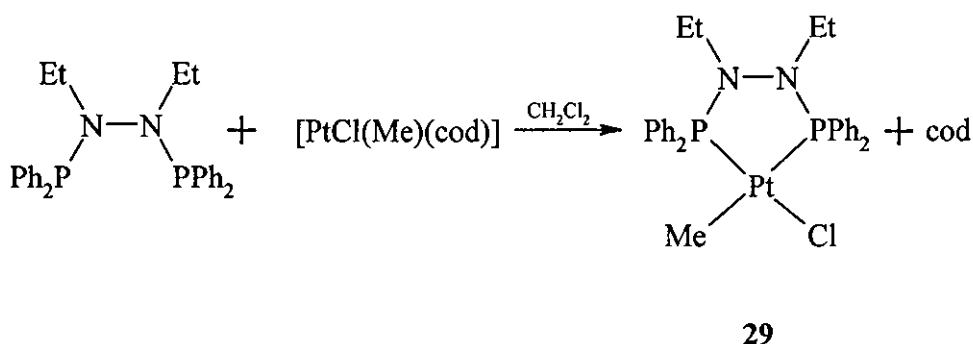
<div align="right">Equation 3.8</div>

Addition of the solid diphosphine **20** to a dichloromethane solution of [PtCl(Me)(cod)] followed by addition of diethyl ether results in the formation of **29** as a white solid in 79 % yield. The ^{31}P-{^1H} NMR spectrum of **29** (Figure 3 2) shows an AX type spectrum due to the chemical inequivalence of the phosphorus centres Both peaks in the spectrum are of equal magnitude and both show satellites due to coupling with ^{195}Pt The phosphorus atom *trans* to the chloride ligand in **29** is assigned to the peak at $\delta(P)$ 96.8 due to the larger $^1J(^{195}Pt-^{31}P)$ coupling associated with it (4577 Hz).
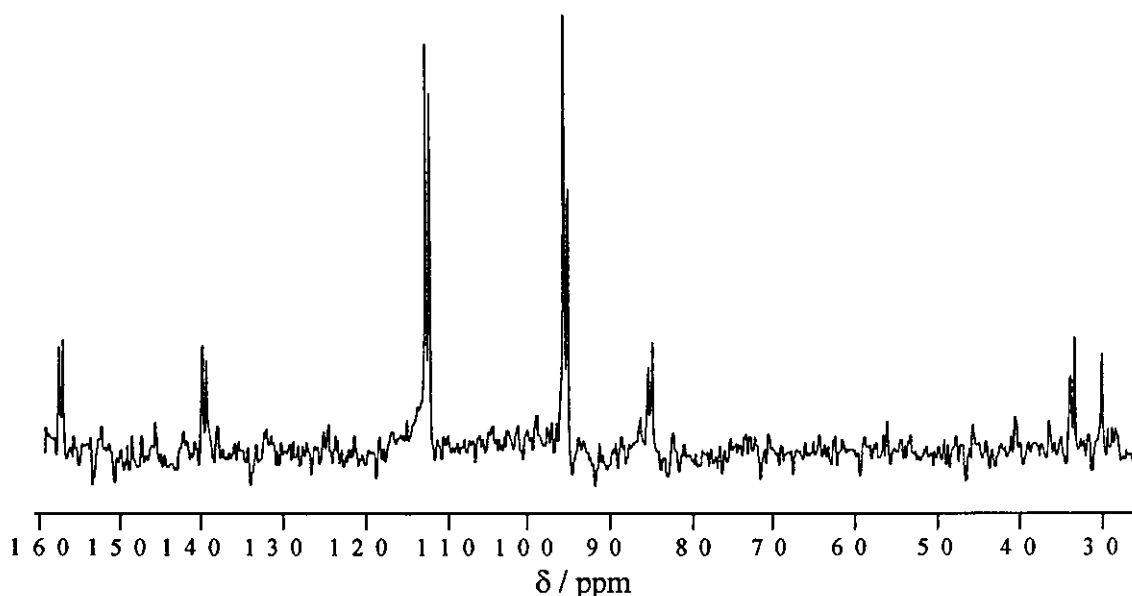
Figure 3.2 ^{31}P-{^1H} NMR spectrum of *cis*-[PtCl(Me){$Ph_2PN(Et)N(Et)PPh_2$}] **29.**

Consequently the phosphorus *trans* to the methyl group is assigned to the peak at δ(P) 114.2 and has a smaller $^1J(^{195}\text{Pt-}^{31}\text{P})$ coupling of 2016 Hz. The value of $^2J(^{31}\text{P-}^{31}\text{P})$ is 17 Hz which is in agreement with values reported previously for similar systems[32]. The FAB$^+$ mass spectrum of **29** shows the expected parent-ion peak (m/z 702 [*M*]$^+$) and a peak corresponding to the loss of a chloride ion (m/z 667 [*M* – Cl]$^+$). Elemental analysis is in agreement with calculated values (Table 3.5) and the IR spectrum shows a band at 997 cm^{-1} that is assigned to ν(PN)

The ligand $(\text{PhCH}_2)_2\text{PN(Et)N(Et)P(CH}_2\text{Ph})_2$ **21** reacts with [PtCl$_2$(cod)] in the same manner as **19** and **20** to give the five-membered metallacycle *cis*-[PtCl$_2$\{(PhCH$_2$)$_2$PN(Et)N(Et)P(CH$_2$Ph)$_2$\}] **30** as a colourless solid in 84 % yield. The $^{31}\text{P-}\{^1\text{H}\}$ NMR spectrum shows a single resonance at δ(P) 108.3 with satellites from coupling to ^{195}Pt [$^1J(^{195}\text{Pt-}^{31}\text{P})$ 4033 Hz]. This represents a downfield shift of 44 ppm from the value recorded for the free ligand **21**, which is comparable to the difference in shift observed between **20** and **27**. The FAB$^+$ mass contains the parent-ion peak (m/z 778 [*M*]$^+$) and elemental analysis is satisfactory. The IR spectrum shows a band at 988 cm^{-1} that is assigned to ν(PN), and indicates an increases in bond order when compared to the free ligand, as well as two ν(PtCl) stretches (317 and 285 cm^{-1}) that are indicative of a *cis*-PtCl$_2$ geometry.

The ligands containing *ortho* substituted phenyl groups, $(o\text{-C}_6\text{H}_4\text{OCH}_3)_2\text{P}$ N(Et)N(Et)P$(o\text{-C}_6\text{H}_4\text{OCH}_3)_2$ **22**, $(o\text{-C}_6\text{H}_4\text{OCH}_3)_2\text{PN(Me)N(Me)P}(o\text{-C}_6\text{H}_4\text{OCH}_3)_2$ **23**, and $(o\text{-C}_6\text{H}_4\text{CH}_3)_2\text{PN(Me)N(Me)P}(o\text{-C}_6\text{H}_4\text{CH}_3)_2$ **24**, also react successfully with equimolar quantities of [PtCl$_2$(cod)] to yield *P,P'* chelates (Equation 3.9 and 3 10).
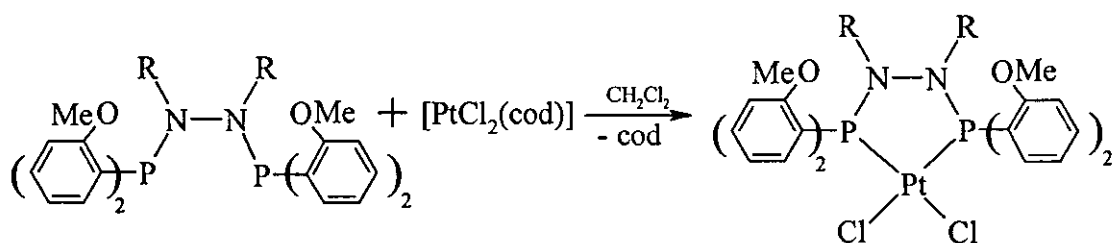
R = Et (**31**), Me (**32**)

Equation 3.9
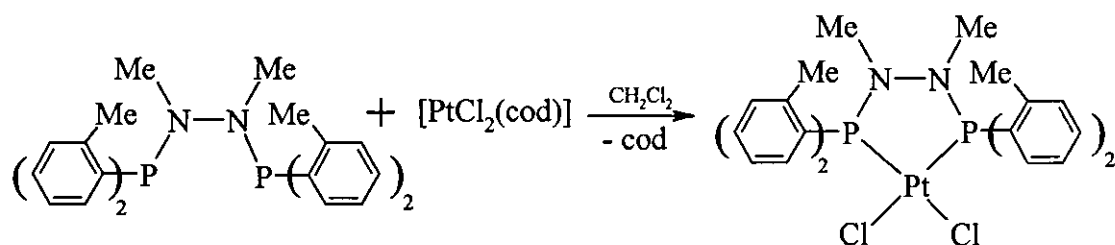
33

Equation 3.10

In each case, addition of the solid diphosphine to a dichloromethane solution of [PtCl$_2$(cod)] followed by addition of diethyl ether, results in the precipitation of the products cis-[PtCl$_2$\{(o-C$_6$H$_4$OCH$_3$)$_2$PN(Et)N(Et)P(o-C$_6$H$_4$OCH$_3$)$_2$\}] **31**, cis-[PtCl$_2$ \{(o-C$_6$H$_4$OCH$_3$)$_2$PN(Me)N(Me)P(o-C$_6$H$_4$OCH$_3$)$_2$\}] **32** and cis-[PtCl$_2$\{(o-C$_6$H$_4$CH$_3$)$_2$PN(Me)N(Me)P(o-C$_6$H$_4$CH$_3$)$_2$\}] **33** as colourless solids in moderate yields (70, 57 and 69 % respectively). The ^{31}P-\{^{1}H\} NMR spectra of all three products show singlets, at δ(P) 90.2, 88.5 and 110.3 respectively, representing downfield shifts of 45-65 ppm upon complexation, values comparable to those observed for **27** and **30**. All show satellites from coupling to ^{195}Pt and the magnitudes of the ^1J(^{195}Pt-^{31}P) couplings (4535 Hz for **31**, 4438 Hz for **32** and 4289 Hz for **33**) are consistent with the values observed for **25**, **27** and **30**, their relative sizes reflecting the nature of the substituents present, both in the *ortho* position in the ring and on the phosphorus atoms The FAB$^+$ mass spectra of the three complexes confirm the proposed structures. The spectra of **31** and **32** both show the expected parent-ions and peaks corresponding to the loss of a chloride ion (m/z 842 [M]$^+$ and 807 [M − Cl]$^+$ for **31** and m/z 814 [M]$^+$ and 779 [M − Cl]$^+$ for **32**) and although the spectrum of **33** fails to

Table 3.3 Selected IR data (cm^{-1}) for compounds **31**, **32** and **33**.

Compound	Formula	v(PN)	v(PtCl)
31	cis-[PtCl$_2$\{(o-C$_6$H$_4$OCH$_3$)$_2$PN(Et)N(Et)P(o-C$_6$H$_4$OCH$_3$)$_2$\}]	943	303, 280
32	cis-[PtCl$_2$\{(o-C$_6$H$_4$OCH$_3$)$_2$PN(Me)N(Me)P(o-C$_6$H$_4$OCH$_3$)$_2$\}]	965	301, 276
33	cis-[PtCl$_2$\{(o-C$_6$H$_4$CH$_3$)$_2$PN(Me)N(Me)P(o-C$_6$H$_4$CH$_3$)$_2$\}]	946	303, 286

show the expected parent-ion it does contain $[M - Cl]^+$ and $[M - 2Cl]^+$ ions (m/z 714 and 679 respectively) Further evidence in support of the *cis* chelate structure comes from the IR spectra which each show two ν(PtCl) stretches, as well as bands corresponding to ν(PN) (Table 3 3) Elemental analyses of all three products are in good agreement with calculated values (Table 3.5). Colourless crystals of *cis*-[PtCl$_2$\{(o-C$_6$H$_4$OCH$_3$)$_2$PN(Et)N(Et)P(o-C$_6$H$_4$OCH$_3$)$_2$\}] **31** suitable for X-ray crystallography were grown by layering a dichloromethane solution of **31** with diethyl ether. The molecular structure of **31**.CH$_2$Cl$_2$ is shown in Figure 3.3 and selected bond lengths and angles are shown in Table 3.4. The X-ray structure of **31** reveals that the molecule has crystallographic symmetry with a two-fold axis bisecting the N-N bond and passing through the Pt(1) atom Pt(1) is square planar with the PtP$_2$N$_2$ ring having the symmetry required geometry with N(1) above and N(2) below the coordination plane [both by 0.25 Å]. The Pt-P, P-N and Pt-Cl bond lengths are consistent the values previously reported for the *N,N'*-dimethyl compound *cis*-[PtCl$_2$\{(PhO)$_2$PN(Me)N(Me)P(OPh)$_2$\}][49] and the chelate complexes reported in Chapter 2 and are single in nature, although the P-N bonds are significantly longer than those in **26**. The structure of **31** also shows that the methoxy substituents on the phenyl ring do not occupy positions above and below the palladium atom as had been hoped.

The ligands **23** and **24** also react with the dimeric palladium species [\{Pd(C$_8$H$_{12}$OCH$_3$)(μ-Cl)\}$_2$] and NH$_4$PF$_6$ to yield the *cis-P,P'* chelates [Pd(C$_8$H$_{12}$OCH$_3$)\{(o-C$_6$H$_4$OCH$_3$)$_2$PN(Me)N(Me)P(o-C$_6$H$_4$OCH$_3$)$_2$\}]PF$_6$ **34**, and [Pd(C$_8$H$_{12}$OCH$_3$)\{(o-C$_6$H$_4$CH$_3$)$_2$PN(Me)N(Me)P(o-C$_6$H$_4$CH$_3$)$_2$\}]PF$_6$ **35** (Equation 3.10). In both cases solid NH$_4$PF$_6$ is added to a stirred, dichloromethane solution of the dimer [\{Pd(C$_8$H$_{12}$OCH$_3$)(μ-Cl)\}$_2$] and the reaction mixture stirred for 30 min A dichloromethane solution of the respective ligand is then added dropwise over a period of 10 minutes and results in the formation of a dark brown solution which is then stirred for a further 2 hours. Removal of the solvent *in vacuo* followed by addition of diethyl ether gives the products as light brown solids in good yields (65 and 70 % respectively).
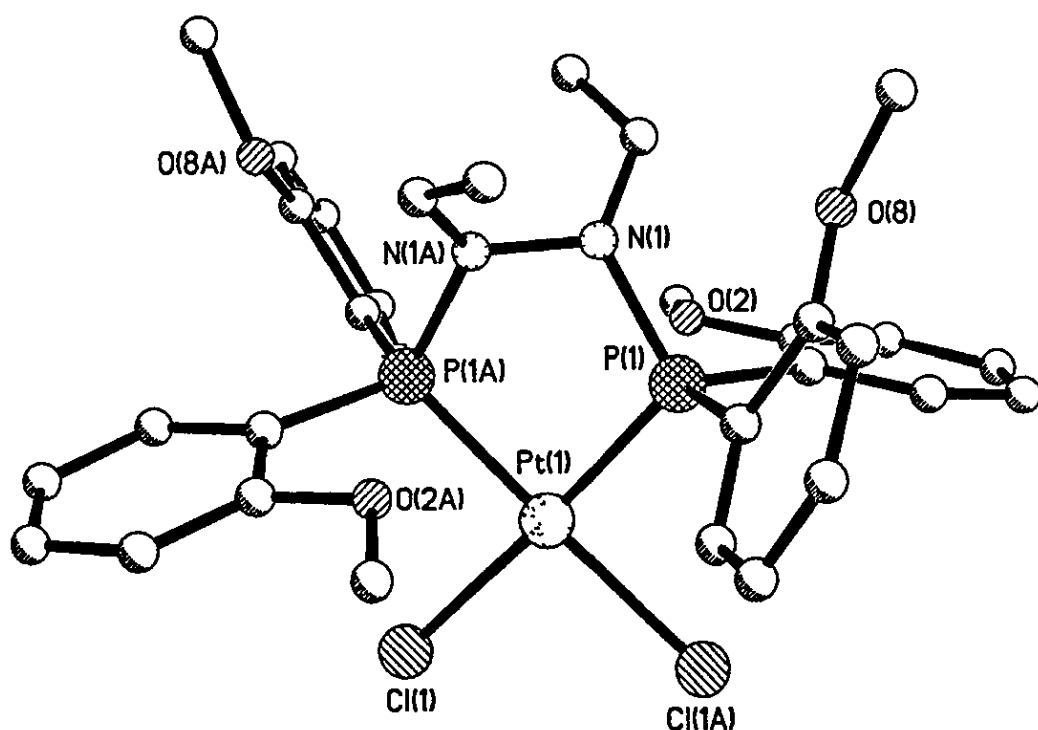
Figure 3.3 Solid state structure of *cis*-[PtCl$_2$\{(*o*-C$_6$H$_4$OCH$_3$)$_2$PN(Et)N(Et)P(*o*-C$_6$H$_4$OCH$_3$)$_2$\}].CH$_2$Cl$_2$.

Table 3.4 Selected bond lengths (Å) and angles (°) for **31**.CH$_2$Cl$_2$.

Bond	Length	Bond	Angle
Pt(1)-Cl(1)	2.396 (3)	Cl(1)-Pt(1)-Cl(1A)	91.1 (2)
Pt(1)-Cl(1A)	2.396 (3)	P(1A)-Pt(1)-P(1)	84.9 (2)
Pt(1)-P(1)	2.221 (4)	Pt(1)-P(1)-N(1)	108 0 (4)
Pt(1)-P(1A)	2 221 (4)	P(1)-Pt(1)-Cl(1A)	92.0 (12)
P(1A)-N(1A)	1.758 (13)	P(1)-N(1)-N(1A)	114 2 (4)
P(1)-N(1)	1.758 (13)	P(1A)-Pt(1)-Cl(1)	92.0 (2)
N(1A)-N(1)	1.37 (2)	Cl(1)-Pt(1)-P(1)	176.7 (14)

2 ... (structures) ... + ... Pd—Cl—Pd ... OMe MeO

$\xrightarrow[\text{DCM}]{2NH_4PF_6}$

... $]^+ PF_6^-$
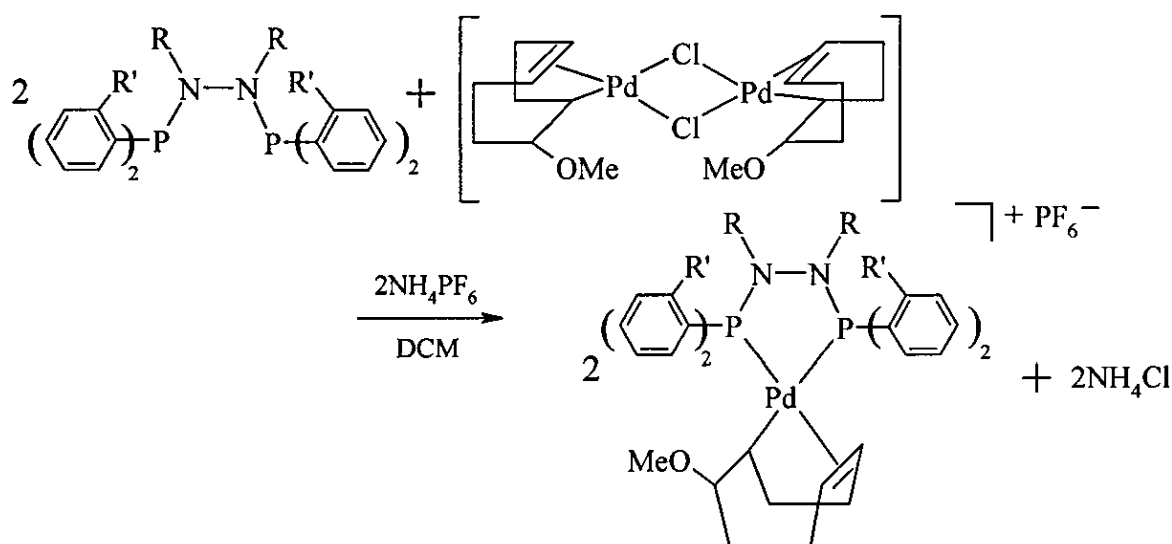
R = Me, R' = OMe (34)

R = Me, R' = Me (35)

Equation 3.11

The ^{31}P-$\{^1H\}$ NMR spectrum of each product shows an AX type pattern due to the phosphorus centres being chemically inequivalent The ^{31}P-$\{^1H\}$ NMR spectrum of **34** shows doublets at δ(P) 104.8 and 92.1 [$^2J(^{31}$P-^{31}P) 66 Hz] with the spectrum of **35** displaying doublets at δ(P) 113.4 and 105.2 [$^2J(^{31}$P-^{31}P) 66 Hz] The FAB$^+$ mass spectra of the complexes fail to show the expected parent-ion peak but both show peaks which can be assigned to the loss of a PF$_6^-$ ion (m/z 794 [M − PF$_6$]$^+$ for **34** and m/z 730 [M − PF$_6$]$^+$ for **35**). The IR spectra of both complexes show bands assigned to ν(PN) (950 cm^{-1} for **34** and 948 cm^{-1} for **35**) and elemental analyses are in good agreement with calculated values (Table 3.5).

3.6 Conclusions

Our results show that the ligand Cl$_2$PN(Et)N(Et)PCl$_2$ can be synthesised from the reaction of 1,2-diethylhydrazine dihydrochloride and phosphorus trichloride and is readily funtionalised to produce a range of aryloxy- and aryl-substituted phosphorus (III) hydrazides. The ^{31}P-$\{^1H\}$ NMR data for each ligand reflects the nature of the substituents present on the phosphorus atoms and correlates with the data reported for similar derivatives of the *N,N'*-dimethyl ligand Cl$_2$PN(Me)N(Me)PCl$_2$. Coordination

86

studies have shown that the ligands react successfully with Pt(II) and Pd(II) species to form five-membered P,P'-chelate rings, the data for such complexes once again being in agreement with the values reported for similar chelates of the ligands $R_2PN(Me)N(Me)PR_2$. Only very slight differences are observed in the $^{31}P-\{^1H\}$ NMR chemical shifts of analogous dimethyl and diethyl compounds, suggesting that a change in substituent on the nitrogen atom has little effect on the electronic properties of the ligands and complexes. Despite our studies there is still a great deal of scope for further investigation into the chemistry of bis(dihalophosphino)hydrazines The number of possible phosphorus substituents is only limited by the number of suitable alcohol and Grignard reagents available, while the coordination chemistry of these ligands with metals other than Pt(II) and Pd(II) also requires study. We were only able to acquire the X-ray structure of one complex containing *ortho*-substituted phenyl groups (**31**, Figure 3.4) and although that particular example shows that the methoxy substituents do not occupy positions above and below the palladium atom, the possibility of substituents doing so should not be discarded without further investigation.

Table 3.5 Elemental analysis data for complexes **25-35** (calculated values in parentheses).

Cpd	Formula	C	H	N
25	*cis*-[PtCl$_2${(PhO)$_2$PN(Et)N(Et)P(OPh)$_2$}]	42 4 (42 7)	3 9 (3 8)	3 4 (3 6)
26	*cis*-[PdCl$_2${(PhO)$_2$PN(Et)N(Et)P(OPh)$_2$}]	48 0 (48 2)	4.4 (4.3)	4 0 (4 0)
27	*cis*-[PtCl$_2${Ph$_2$PN(Et)N(Et)PPh$_2$}]	47 7 (47 4)	4.4 (4.1)	3 4 (3 8)
28	*cis*-[PdCl$_2${Ph$_2$PN(Et)N(Et)PPh$_2$}]	52 8 (53 1)	4 6 (4 8)	4 2 (4 4)
29	*cis*-[PtCl(Me){Ph$_2$PN(Et)N(Et)PPh$_2$}]	48 5 (49 6)	4 6 (4.7)	3 8 (3 9)
30	*cis*-[PtCl$_2${(PhCH$_2$)$_2$PN(Et)-N(Et)P(CH$_2$Ph)$_2$}]	48 8 (49 4)	4.7 (4 9)	3.1 (3 6)
31	*cis*-[PtCl$_2${(*o*-C$_6$H$_4$OCH$_3$)$_2$PN(Et)-N(Et)P(*o*-C$_6$H$_4$OCH$_3$)$_2$}]	45 1 (45 6)	4 4 (4 6)	2 8 (3 3)
32	*cis*-[PtCl$_2${(*o*-C$_6$H$_4$OCH$_3$)$_2$PN(Me)N(Me)P(*o*-C$_6$H$_4$OCH$_3$)$_2$}]	48 1 (48 8)	3 4 (3 9)	2 8 (3 2)
33	*cis*-[PtCl$_2${*o*- (C$_6$H$_4$CH$_3$)$_2$PN(Me)N(Me)P(*o*-C$_6$H$_4$CH$_3$)$_2$}]	47 5 (48 0)	4 3 (4 6)	3 5 (3 7)
34	[Pd(C$_8$H$_{12}$OCH$_3$){(*o*-C$_6$H$_4$OCH$_3$)$_2$PN(Me)N(Me)P(*o*-C$_6$H$_4$OCH$_3$)$_2$}]$^+$PF$_6^-$	49 2 (49 8)	5 0 (5 2)	3 4 (2 9)
35	[Pd(C$_8$H$_{12}$OCH$_3$){(*o*-C$_6$H$_4$CH$_3$)$_2$PN(Me)N(Me)P(*o*-C$_6$H$_4$CH$_3$)$_2$}]$^+$PF$_6^-$	52 8 (53 5)	5 6 (5 6)	3 1 (3 2)

Experimental

General experimental conditions and instrumentation were as set out on page 12 and described in Chapter 2. 1,2-diethylhydrazine dihydrochloride was crushed using a pestle mortar prior to use. [{Pd(C$_8$H$_{12}$OCH$_3$)(μ-Cl)}$_2$] was prepared using the literature procedure.[106] Phenol, phosphorus trichloride, PhMgBr, PhCH$_2$MgCl and 2-CH$_3$C$_6$H$_4$MgCl were used without further purification.

Cl$_2$PN(Et)N(Et)PCl$_2$ 18. Phosphorus trichloride (10.00 g, 72.7 mmol) was added to a finely crushed sample of 1,2-diethylhydrazine dihydrochloride (1.00 g, 6.2 mmol) at

room temperature under an atmosphere of nitrogen. The reaction mixture was heated under reflux for 96 h. The excess phosphorus trichloride was removed *in vacuo* to leave a viscous orange oil Distillation of the resulting oil *in vacuo* leaves compound **18** as a viscous, colourless oil. Yield: 1.3 g, 72 % Microanalysis: Found (Calcd for $C_4H_{10}Cl_4N_2P_2$) C, 17 0 (16.6); H, 3.5 (3 9); N, 9.7 (9 8) %. $^{31}P-\{^1H\}$ NMR (CDCl$_3$): $\delta(P)$ 156.3. IR (neat, cm^{-1}): 2978s, 2935s, 2555s, 2260s, 1451vs, 1379vs, 1355s, 1187vs, 1148vs, 1074vs, 1016vs, 952vs, 858w, 818w, 782w, 761w, 729vs, 612w, 507vs, 436vs, 404vs and 225w. FAB mass spectrum *m/z* 289, [M$^+$].

(PhO)$_2$PN(Et)N(Et)P(OPh)$_2$ 19. A solution of phenol (1 30 g, 13.8 mmol) and triethylamine (1.39 g, 1.9 cm^3, 13 8 mmol) in hexane (20 cm^3) was added dropwise over a period of 30 min to a solution of Cl$_2$PN(Et)N(Et)PCl$_2$ (1 00 g, 3 4 mmol) in hexane (20 0 cm^3) at room temperature. The reaction mixture was stirred for 12 h during which time triethylamine hydrochloride separated from the colourless solution. This precipitate was removed by suction filtration and the filtrate evaporated to dryness *in vacuo* to give a viscous, colourless oil. Yield: 1 45 g, 81 %. Microanalysis: Found (Calcd for $C_{28}H_{30}N_2O_2P_2$) C, 70.0 (69.6), H, 5.5 (5.8); N, 5 4 (5.2) %. $^{31}P-\{^1H\}$ NMR (CDCl$_3$): $\delta(P)$ 139.0. IR (neat, cm^{-1}) 2978vs, 2940s, 2350s, 1589s, 1444s, 1372vs, 1349s, 1170vs, 1111s, 1030s, 1009s, 930vs, 818w, 773w, 758m, 608w, 515s, 446m, 395s and 217w. FAB mass spectrum: *m/z* 520, [*M*]$^+$.

Ph$_2$PN(Et)N(Et)PPh$_2$ 20. A solution of **18** (1.00 g, 3.4 mmol) in diethyl ether (20.0 cm^3) was added dropwise over a period of 30 min to a stirred solution of 1M PhMgBr in diethyl ether (2 50 g, 14.0 cm^3, 13.6 mmol) at 0 °C and the reaction mixture stirred for 18 h. Deionized water (20.0 cm^3) was added slowly over 10 min and stirring continued for a further 1 h, after which the reaction mixture was transferred to a separatory funnel and the layers separated. The ether layer was dried over MgSO$_4$ and the drying agent then removed by suction filtration. The filtrate was evaporated to dryness *in vacuo* to give a white solid product. Yield: 1.1 g, 70 %. Microanalysis: Found (Calcd for $C_{28}H_{30}N_2P_2$) C, 72.9 (73.7); H, 6.5 (6.6); N, 5.9 (6.1) % $^{31}P-\{^1H\}$ NMR (CDCl$_3$): $\delta(P)$ 64.2. IR (KBr disc, cm^{-1}): 2973w, 1651s, 1484w, 1434vs, 1362s, 1320w, 1172vs, 1124s, 1057s, 1024s, 970s, 826s, 759s, 698s, 608w, 575s, 528w, 483w, 333s, 240vs and 230vs. FAB mass spectrum: *m/z* 456, [*M*]$^+$.

89

(PhCH$_2$)$_2$PN(Et)N(Et)P(CH$_2$Ph)$_2$ 21. A solution of **18** (1.00 g, 3.4 mmol) in diethyl ether (20.0 cm^3) was added dropwise over a period of 30 min to a stirred solution of 2M PhCH$_2$MgCl in diethyl ether (2.10 g, 6.8 cm^3, 13.7 mmol) at 0 ^{o}C and the reaction mixture stirred for 12 h. Deoinized water (20.0 cm^3) was added slowly over 10 min and stirring continued for a further 1 h, after which the reaction mixture was transferred to a separatory funnel and the layers separated The ether layer was dried over MgSO$_4$ and the drying agent then removed by suction filtration. The filtrate was evaporated to dryness *in vacuo* to give a pale yellow, solid product. Yield 1.3 g, 74 %. Microanalysis: Found (Calcd for C$_{32}$H$_{38}$N$_2$P$_2$) C, 74.3 (74 9); H, 7.4 (7.5); N, 5.2 (5.5) %. ^{31}P-{^{1}H} NMR (CDCl$_3$): δ(P) 64.8. IR (KBr disc, cm^{-1}): 3025w, 1600s, 1493vs, 1451vs, 1376s, 1210s, 1092s, 1062s, 1028s, 962s, 933s, 906s, 850vs, 823s, 764s, 697s, 585s, 569w, 497s, 478s, and 230vs FAB mass spectrum. *m/z* 512, [*M*]$^+$.

(*o*-C$_6$H$_4$OCH$_3$)$_2$PN(Et)N(Et)P(*o*-C$_6$H$_4$OCH$_3$)$_2$ 22. A solution of 2-bromoanisole (4.90 g, 3.3 cm^3, 26.5 mmol) in diethyl ether (80.0 cm^3) was added dropwise to a slurry of magnesium turnings (1.43 g, 59.0 mmol) and iodine (1 crystal) in diethyl ether (20.0 cm^3) and the reaction mixture stirred for 2.5 h. 60.0 cm^3 of the reaction solution was transferred to a round bottomed flask and a solution of Cl$_2$PN(Et)N(Et)PCl$_2$ (1 00 g, 3 4 mmol) in diethyl ether (25.0 cm^3) added dropwise over a period of 30 min. After stirring for 24 h, deionized water (25.0 cm^3) was added slowly over 10 min and stirring continued for a further 1 h, after which the reaction mixture was transferred to a separatory funnel and the layers separated. The ether layer was dried over MgSO$_4$ and the drying agent then removed by suction filtration. The filtrate was evaporated to dryness in vacuo to give a colourless oil. The product was washed with light petroleum (b.p. 60-80 ^{o}C) to give a solid product. Yield: 1.31 g, 67 %. Microanalysis: Found (Calcd for C$_{32}$H$_{38}$N$_2$O$_4$P$_2$) C, 66.1 (66 6); H, 6.3 (6.6); N, 4.4 (4.8) %. ^{31}P-{^{1}H} NMR (CDCl$_3$) δ(P) 40.5. IR (KBr disc, cm^{-1}): 3053m, 2941m, 2834m, 1655w, 1571s, 1472s, 1427vs, 1374w, 1270s, 1242vs, 1182m, 1160m, 1128m, 1099w, 1067w, 1027s, 933s, 793m, 757vs, 729w, 708w, 503w, 480w, 431w, 237vs and 218s. FAB mass spectrum: *m/z* 576, [*M*]$^+$.

(*o*-C₆H₄OCH₃)₂PN(Me)N(Me)P(*o*-C₆H₄OCH₃)₂ 23. A solution of 2-bromoanisole (4.90 g, 3.3 cm³, 26 5 mmol) in diethyl ether (80.0 cm³) was added dropwise to a slurry of magnesium turnings (1.43 g, 59.0 mmol) and iodine (1 crystal) in diethyl ether (20.0 cm³) and the reaction mixture stirred for 2.5 h. 60.0 cm³ of the reaction solution was transferred to a round bottomed flask and a solution of Cl₂PN(Me)N(Me)PCl₂ (1.00 g, 3.8 mmol) in diethyl ether (25.0 cm³) added dropwise over a period of 30 min. reaction After stirring for 24 h, deionized water (25.0 cm³) was added slowly over 10 min and stirring continued for a further 1 h, after which the reaction mixture was transferred to a separatory funnel and the layers separated. The ether layer was dried over MgSO₄ and the drying agent then removed by suction filtration. The filtrate was evaporated to dryness *in vacuo* to give a colourless oil The product was washed with light petroleum (b p. 60-80 °C) to give a solid product. Yield: 1.7 g, 81 % Microanalysis· Found (Calcd for $C_{30}H_{34}N_2O_4P_2$) C, 65.1 (65.7); H, 5.9 (6.3); N, 4.8 (5.1) %. ³¹P-{¹H} NMR (CDCl₃): δ(P) 42.6. IR (KBr disc, cm⁻¹): 3385s, 3059s, 3000s, 2935s, 2834s, 1583vs, 1571vs, 1460vs, 1429vs, 1268s, 1238s, 1159w, 1129s, 1092w, 1066s, 1042s, 969vs, 883w, 858w, 792s, 753vs, 692s, 611s, 574w, 498s, 472s, 428vs and 230vs. FAB mass spectrum: *m/z* 549, [*M*]⁺.

(*o*-C₆H₄CH₃)₂PN(Me)N(Me)P(*o*-C₆H₄CH₃)₂ 24. A solution of Cl₂PN(Me)N(Me)PCl₂ (1.00 g, 3.8 mmol) in diethyl ether (25 0 cm³) was added dropwise over a period of 30 min to a stirred solution of 1M 2-CH₃C₆H₄MgCl in diethyl ether (2 30 g, 15.2 cm³, 15.2 mmol) at 0 °C and the reaction mixture heated under reflux for 4 h. Deionized water (25.0 cm³) was added slowly over 10 min and stirring continued for a further 1 h, after which the reaction mixture was transferred to a separatory funnel and the layers separated. The ether layer was dried over MgSO₄ and the drying agent then removed by suction filtration. The filtrate was evaporated to dryness *in vacuo* to give a yellow oil. The product was washed with light petroleum (b.p 60-80 °C) to give a pale yellow solid. Yield: 1.2 g, 65 %. Microanalysis: Found (Calcd for $C_{30}H_{34}N_2P_2$) C, 73.7 (74.4); H, 6.8 (7.1); N, 5 2 (5 8) % ³¹P-{¹H} NMR (CDCl₃): δ(P) 47 2 IR (KBr disc, cm⁻¹): 3396w, 1815w, 1560s, 1520vs, 1439vs, 1377s, 1268w, 1198w, 1156s, 1130s, 1066s, 1030s, 956s, 897s, 845vs, 800s, 751s, 731vs, 718s, 607s, 562w, 487s, 455s, 396w, 292w and 230vs. FAB mass spectrum: *m/z* 485, [*M*]⁺.

cis-[PtCl₂{(PhO)₂PN(Et)N(Et)P(OPh)₂}] **25.** A solution of (PhO)₂PN(Et)N(Et)P(OPh)₂ (0.175 g, 0.34 mmol) in dichloromethane (10.0 cm³) was added dropwise to a solution of [PtCl₂(cod)] (0 130 g, 0 34 mmol) in dichloromethane (5 0 cm³) and the colourless solution stirred for *ca* 2h. The solution was concentrated under reduced pressure to *ca* 1.0 cm³ and diethyl ether (20.0 cm³) added. The white product was collected by suction filtration. Yield: 0.178 g, 65 %. Microanalysis: Found (Calcd for C₂₈H₃₀Cl₂N₂O₄P₂Pt) C, 42.4 (42.7); H, 3.9 (3.8); N, 3.4 (3 6) %. ³¹P-{¹H} NMR (CDCl₃): δ(P) 92.3, ¹*J*(¹⁹⁵Pt-³¹P) 5503 Hz. IR (KBr disc. cm⁻¹) 2991s, 1585vs, 1484vs, 1455vs, 1385s, 1348s, 1186vs, 1113vs, 1069vs, 1023s, 968vs, 822s, 763vs, 688s, 652s, 614w, 586s, 535w, 439w, 325s, 299m, 236vs and 227vs FAB mass spectrum: *m/z* 786, [*M*]⁺.

cis-[PdCl₂{(PhO)₂PN(Et)N(Et)P(OPh)₂}] **26.** A solution of (PhO)₂PN(Et)N(Et)P(OPh)₂ (0.182 g, 0.35 mmol) in dichloromethane (10.0 cm³) was added dropwise to a solution of [PdCl₂(cod)] (0.100 g, 0.35 mmol) in dichloromethane (5 0 cm³) and the yellow solution stirred for *ca* 2h. The solution was concentrated under reduced pressure to *ca.* 1 0 cm³ and diethyl ether (20.0 cm³) added. The yellow product was collected by suction filtration. Yield 0 123 g, 50 %. Microanalysis: Found (Calcd for C₂₈H₃₀Cl₂N₂O₄P₂Pd) C, 48.0 (48.2); H, 4.4 (4.3), N, 4.0 (4 0) %. ³¹P-{¹H} NMR (CDCl₃): δ(P) 116.6. IR (KBr disc, cm⁻¹): 2975s, 1585vs, 1484vs, 1455vs, 1377s, 1348w, 1177vs, 1119vs, 1070s, 1024s, 955vs, 822s, 763vs, 682s, 654s, 614w, 575s, 518w, 496w, 329s, 296s, 237vs and 225vs. FAB mass spectrum *m/z* 698, [*M*]⁺.

cis-[PtCl₂{Ph₂PN(Et)N(Et)PPh₂}] **27.** To a solution of [PtCl₂(cod)] (0 040 g, 0.11 mmol) in dichloromethane (5.0 cm³) was added solid Ph₂PN(Et)N(Et)PPh₂ (0.048 g, 0.11 mmol) and the colourless solution stirred for *ca* 2h. The solution was concentrated under reduced pressure to *ca* 1.0 cm³ and diethyl ether (10 0 cm³) added. The white product was collected by suction filtration Yield· 0 060 g, 78 %. Microanalysis Found (Calcd for C₂₈H₃₀Cl₂N₂P₂Pt) C, 47.7 (47.4); H, 4 4 (4.1); N, 3 4 (3.8) %. ³¹P-{¹H} NMR (CDCl₃). δ(P) 100.4, ¹*J*(¹⁹⁵Pt-³¹P) 4055 Hz. IR (KBr disc, cm⁻¹): 3053s, 2972s, 1572vs, 1480vs, 1436vs, 1380s, 1311w, 1182vs, 1104vs, 1027w,

997s, 921w, 872w, 749vs, 720vs, 692s, 656s, 630w, 578s, 556w, 527s, 507vs, 493w, 471w, 314s, 233vs and 225vs. FAB mass spectrum: m/z 722, $[M]^+$.

cis-[PdCl$_2$\{Ph$_2$PN(Et)N(Et)PPh$_2$\}] 28. To a solution of [PdCl$_2$(cod)] (0 030 g, 0.11 mmol) in dichloromethane (15 0 cm^3) was added solid Ph$_2$PN(Et)N(Et)PPh$_2$ (0 048 g, 0.11 mmol) and the yellow solution stirred for *ca* 2h. The solution was concentrated under reduced pressure to *ca* 1.0 cm^3 and diethyl ether (20 0 cm^3) added. The yellow product was collected by suction filtration Yield: 0 052 g, 78 %. Microanalysis Found (Calcd for C$_{28}$H$_{30}$Cl$_2$N$_2$P$_2$Pd) C, 52.8 (53.1); H, 4.6 (4.8); N, 4.2 (4.4) % ^{31}P-\{^{1}H\} NMR (CDCl$_3$). δ(P) 132 2 IR (KBr disc, cm^{-1}). 3053w, 2972s, 1618w, 1585w, 1479s, 1436vs, 1380s, 1312w, 1183w, 1118vs, 1101vs, 1026w, 997s, 918w, 750vs, 719vs, 691s, 654s, 609w, 574s, 522s, 490w, 292w and 225vs. FAB mass spectrum m/z 634, $[M]^+$.

cis-[PtMe(Cl)\{Ph$_2$PN(Et)N(Et)PPh$_2$\}]   29. To a solution of [PtMe(Cl)(cod)] (0.038g, 0.11 mmol) in dichloromethane (10.0 cm^3) was added solid Ph$_2$PN(Et)N(Et)PPh$_2$ (0.048 g, 0 11 mmol) and the colourless solution stirred for *ca* 2 h The solution was concentrated under reduced pressure to *ca* 1 0 cm^3 and diethyl ether (20.0 cm^3) added. The white product was collected by suction filtration Yield: 0.058 g, 79 %. Microanalysis: Found (Calcd for C$_{29}$H$_{33}$ClN$_2$P$_2$Pt) C, 48.5 (49 6), H, 4.6 (4.7); N, 3.8 (3.9) %. ^{31}P-\{^{1}H\} NMR (CDCl$_3$): δ(P$_A$ trans to CH$_3$) 114.2, ^{1}J(^{195}Pt-^{31}P$_A$) 2016 Hz, δ(P$_B$ trans to Cl) 96.8, ^{1}J(^{195}Pt-^{31}P$_B$) 4577 Hz. IR (KBr disc, cm^{-1}): 3054s, 2970s, 2874s, 1671w, 1479s, 1436vs, 1377s, 1312w, 1180s, 1122vs, 1103vs, 997w, 750vs, 717vs, 693vs, 652s, 580s, 554s, 524vs, 492s, 301w, 242s and 210vs. FAB mass spectrum: m/z 702, $[M]^+$.

cis-[PtCl$_2$\{(PhCH$_2$)$_2$PN(Et)N(Et)P(CH$_2$Ph)$_2$\}] 30. To a solution of [PtCl$_2$(cod)] (0.050 g, 0.13 mmol) in dichloromethane (15.0 cm^3) was added solid (PhCH$_2$)$_2$PN(Et)N(Et)P(CH$_2$Ph)$_2$ (0.068 g, 0.13 mmol) and the colourless solution stirred for *ca* 2 h. The solution was concentrated under reduced pressure to *ca* 2.0 cm^3 and diethyl ether (20.0 cm^3) added. The white product was collected by suction filtration. Yield: 0.087 g, 84 %. Microanalysis: Found (Calcd for C$_{32}$H$_{38}$Cl$_2$N$_2$P$_2$Pt) C, 48.8 (49.4), H, 4.7 (4.9), N, 3.1 (3.6) % ^{31}P-\{^{1}H\} NMR (CDCl$_3$): δ(P) 108 3, ^{1}J(^{195}Pt-

^{31}P) 4033 Hz, $^2J(^{31}P_A-^{31}P_B)$ 17 Hz. IR (KBr disc, cm^{-1}): 3026s, 2979s, 2926s, 1601s, 1495vs, 1452vs, 1386s, 1357w, 1260s, 1172vs, 1124s, 1073s, 988w, 917w, 857s, 838s, 808s, 790s, 773s, 755vs, 695vs, 610w, 582s, 569w, 535w, 472w, 317s, 235s and 229vs FAB mass spectrum: *m/z* 778, [*M*]$^+$.

cis-[PtCl₂{(o-C₆H₄OCH₃)₂PN(Et)N(Et)P(o-C₆H₄OCH₃)₂}] 31. To a solution of [PtCl₂(cod)] (0.100 g, 0.26 mmol) in dichloromethane (5.0 cm^3) was added solid (C₆H₄-o-OCH₃)₂PN(Et)N(Et)P(C₆H₄-o-OCH₃)₂ (0.154 g, 0.26 mmol) and the colourless solution stirred for *ca* 2 h. The solution was concentrated under reduced pressure to *ca* 2 0 cm^3 and diethyl ether (20 0 cm^3) added. The white product was collected by suction filtration. Yield: 0.107 g, 70 %. Microanalysis: Found (Calcd for C₃₂H₃₀Cl₂N₂O₄P₂Pt) C, 45.1 (45.6); H, 4.4 (4.5); N, 2.8 (3.3) %. ^{31}P-{^{1}H} NMR (CDCl₃): δ(P) 90 2, $^1J(^{195}Pt-^{31}P)$ 4535 Hz. IR (KBr disc, cm^{-1}): 3065w, 2937w, 2864w, 1588s, 1573s, 1477vs, 1463s, 1430vs, 1375w, 1282s, 1253s, 1182m, 1165m, 1109m, 1075m, 1045m, 1019s, 943w, 801s, 757s, 692m, 633m, 581m, 557m, 506m, 446w, 337w, 303w, 280w and 229s. FAB mass spectrum: *m/z* 842, [*M*]$^+$.

cis-[PtCl₂{(o-C₆H₄OCH₃)₂PN(Me)N(Me)P(o-C₆H₄OCH₃)₂}] 32. To a solution of [PtCl₂(cod)] (0 075 g, 0 20 mmol) in dichloromethane (5.0 cm^3) was added solid (C₆H₄-o-OCH₃)₂PN(Me)N(Me)P(C₆H₄-o-OCH₃)₂ (0 110 g, 0 20 mmol) and the colourless solution stirred for *ca* 2 h The solution was concentrated under reduced pressure to *ca* 2 0 cm^3 and diethyl ether (20 0 cm^3) added. The white product was collected by suction filtration. Yield: 0.101 g, 57 %. Microanalysis: Found (Calcd for C₃₀H₃₄Cl₂N₂O₄P₂Pt) C, 48.1 (48 8); H, 3 4 (3.9); N, 2 8 (3.2) %. ^{31}P-{^{1}H} NMR (CDCl₃): δ(P) 88.5, $^1J(^{195}Pt-^{31}P)$ 4438 Hz. IR (KBr disc, cm^{-1}): 3386s, 3067s, 2932s, 2833s, 1637w, 1587vs, 1571s, 1474vs, 1455vs, 1428vs, 1276s, 1251s, 1164w, 1136w, 1072w, 1016s, 965w, 800s, 762vs, 694w, 646s, 581s, 558s, 526w, 509w, 484w, 445s, 365w, 276w, 230s and 215vs. FAB mass spectrum: *m/z* 814, [*M*]$^+$

cis-[PtCl₂{(o-C₆H₄CH₃)₂PN(Me)N(Me)P(o-C₆H₄CH₃)₂}] 33. To a solution of [PtCl₂(cod)] (0.070 g, 0.19 mmol) in dichloromethane (5.0 cm^3) was added solid (C₆H₄-o-CH₃)₂PN(Me)N(Me)P(C₆H₄-o-CH₃)₂ (0.090 g, 0.19 mmol) and the colourless solution stirred for *ca* 1 h The solution was concentrated under reduced

pressure to *ca* 2.0 cm^3 and diethyl ether (15.0 cm^3) added. The white product was collected by suction filtration. Yield: 0.092 g, 69 %. Microanalysis· Found (Calcd for C$_{30}$H$_{34}$Cl$_2$N$_2$P$_2$Pt) C, 47.5 (48.0); H, 4.3 (4.6); N, 3.5 (3.7) %. ^{31}P-{^{1}H} NMR (CDCl$_3$): δ(P) 110.3, $^1J(^{195}$Pt-^{31}P) 4289 Hz. IR (KBr disc, cm^{-1}): 2894s, 1654w, 1591s, 1561s, 1447vs, 1379s, 1283s, 1203w, 1162w, 1133s, 1084s, 946w, 808s, 762vs, 723s, 684w, 576s, 554w, 531w, 515w, 494s, 455s, 420s, 303w, 286w, 235s and 230vs. FAB mass spectrum: *m/z* 714, [*M* - Cl]$^+$.

[Pd(C$_8$H$_{12}$OCH$_3$){(*o*-C$_6$H$_4$OCH$_3$)$_2$PN(Me)N(Me)P(*o*-C$_6$H$_4$OCH$_3$)$_2$}] **34.** To a stirred solution of [{Pd(C$_8$H$_{12}$OCH$_3$)(*μ*-Cl)}$_2$] (0 050 g, 0.09 mmol) in dichloromethane (10 0 cm^3) was added solid NH$_4$PF$_6$ (0.030 g, 0.18 mmol) and the reaction mixture stirred for a further 30 min A solution of (C$_6$H$_4$-*o*-OCH$_3$)$_2$PN(Me)N(Me)P(C$_6$H$_4$-*o*-OCH$_3$)$_2$ (0.100 g, 0.18 mmol) in dichloromethane (10 0 cm^3) was then added dropwise to the reaction mixture over a period of 10 min and the resulting dark brown solution stirred for 2 h. The solution was concentrated under reduced pressure to *ca* 5 0 cm^3 and diethyl ether (25.0 cm^3) added. The light brown product was collected by suction filtration. Yield: 0 109 g, 65 % Microanalysis: Found (Calcd for C$_{39}$H$_{49}$F$_6$N$_2$OP$_3$Pd) C, 52 8 (53 5); H, 5.6 (5.6); N, 3.1 (3.2) %. ^{31}P-{^{1}H} NMR (CDCl$_3$): δ(P) 104.8 and 92.1, $^2J(^{31}$P-^{31}P) 66 Hz. IR (KBr disc, cm^{-1}): 2933w, 1586m, 1574m, 1515m, 1474s, 1431s, 1275s, 1245s, 1164m, 1135m, 1075w, 1043w, 1018m, 950m, 839s, 797m, 756m, 737w, 657w, 616m, 580w, 557m, 523w, 501w, 436w and 358w. FAB mass spectrum: *m/z* 794, [*M*-PF$_6$]$^+$.

[Pd(C$_8$H$_{12}$OCH$_3$){(*o*-C$_6$H$_4$CH$_3$)$_2$PN(Me)N(Me)P(*o*-C$_6$H$_4$CH$_3$)$_2$}] **35.** To a stirred solution of [{Pd(C$_8$H$_{12}$OCH$_3$)(*μ*-Cl)}$_2$] (0.130 g, 0.23 mmol) in dichloromethane (10.0 cm^3) was added solid NH$_4$PF$_6$ (0.075 g, 0.46 mmol) and the reaction mixture stirred for a further 30 min. A solution of (C$_6$H$_4$-*o*-CH$_3$)$_2$PN(Me)N(Me)P(C$_6$H$_4$-*o*-CH$_3$)$_2$ (0.222 g, 0.46 mmol) in dichloromethane (10 0 cm^3) was then added dropwise to the reaction mixture over a period of 10 min and the resulting dark brown solution stirred for 2 h. The solution was concentrated under reduced pressure to *ca* 5 0 cm^3 and diethyl ether (25.0 cm^3) added The light brown product was collected by suction filtration. Yield: 0.280 g, 70 % Microanalysis: Found (Calcd for C$_{39}$H$_{49}$F$_6$N$_2$OP$_3$Pd) C, 52.8 (53.5); H, 5.6 (5 6); N, 3.1 (3.2) %. ^{31}P-{^{1}H} NMR (CDCl$_3$): δ 113.4 and

105.2, $^2J(^{31}P\text{-}^{31}P)$ 66 Hz. IR (KBr disc, cm^{-1}). 2924vs, 1624w, 1588s, 1523vs, 1448vs, 1381w, 1278s, 1186s, 1132s, 1081s, 1023s, 948w, 839vs, 806s, 757vs, 719s, 682w, 611w, 556vs, 538w, 508w, 488s, 469s, 280w, 242s and 229vs. FAB mass spectrum: m/z 730, $[M\text{-}PF_6]^+$.

Chapter 4

The Preparation and Coordination Chemistry of Phosphorus (III) Derivatives of Piperazine and Homopiperazine.

4.1 *Introduction*

One of the important roles occupied by ligands in catalytic metal complexes is to offer steric protection to the catalytically active site.[107] This requirement is achieved by incorporating bulky substituent groups into the ligand which hinder the approach of the polymerisation reactants and 'steer' them towards the reacting polymer chain. With this requirement in mind, we have studied the reactions of the cyclic amine compounds piperazine and homopiperazine with different chlorophosphines to ascertain the possibility of synthesising diphosphine chelates which would offer significant steric hindrance by forming umbrella-like ligands around a metal centre. Here we report on the synthesis of diphosphine derivatives of piperazine and homopiperazine and their reactions with different metal compounds.

Results and Discussion

4.2 *Synthesis of phosphorus (III) derivatives of piperazine*

Reaction of piperazine with two equivalents of the chlorophosphines Ph_2PCl, $(C_6H_4O_2)PCl$ and $(C_2H_4O_2)PCl$, in the presence of NEt_3, proceeds in thf to give **36, 37** and **38** respectively (Equation 4.1).
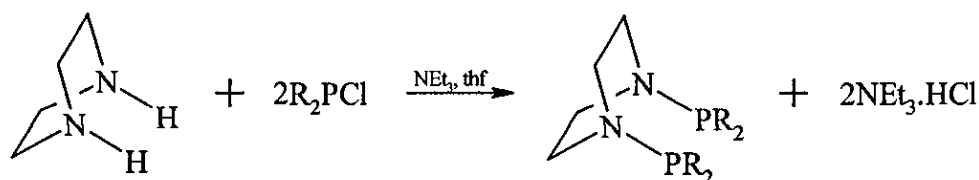
$R_2 = Ph_2$ (**36**), $C_6H_4O_2$ (**37**)

and $C_2H_4O_2$ (**38**)   **Equation 4.1**

Addition of chlorodiphenylphosphine in thf to a solution of piperazine in thf, at room temperature, results in the immediate precipitation of [Et₃NH]Cl as the reaction proceeds. Removal of the ammonium salt by filtration, reduction of the volume of thf *in vacuo* and addition of diethyl ether gives $Ph_2PN(C_2H_4)_2NPPh_2$ **36**. This method is an adaptation of a previously published literature method[52] and typically results in **36** in yields of 70-80 %. Air- and moisture- tolerant, **36** is readily soluble in both dichloromethane and thf . The $^{31}P\text{-}\{^1H\}$ NMR spectrum of **36** comprises a singlet at δ(P) 62.9. The possibility of this peak representing the mono-substituted amine was rejected after performing *in situ* ^{31}P NMR studies. Monitoring of the reaction mixture at regular intervals, immediately after completion of the chlorodiphenylphosphine addition, shows a phosphorus-containing species, with a chemical shift of δ(P) 35.1, to be the initial reaction product. This is assumed to be the mono-substituted amine and gradually decreases in intensity as the reaction proceeds, to leave **36** as the only phosphorus containing compound (Equation 4.2). FAB^+ mass spectrometry and elemental analysis (Table 4.1) both support the proposed identity of **36** as a diphosphine and the IR spectrum of **36** also supports this conclusion as there is no band associated with a ν(N-H) stretch The IR spectrum of **36** does however show bands corresponding to ν(CN) (1478 cm⁻¹) and ν(PN) (930 cm⁻¹).

δ(P) 35.1   δ(P) 62.9
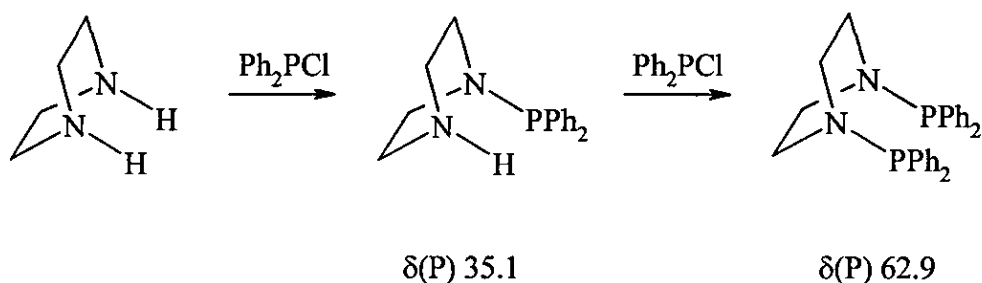
Equation 4.2

Formation of the ligands $(C_6H_4O_2)PN(C_2H_4)_2NP(C_6H_4O_2)$ **37** and $(C_2H_4O_2)PN(C_2H_4)_2NP(C_2H_4O_2)$ **38** is achieved by employing the same experimental technique used in the synthesis of **36** This results in both **37** and **38** being isolated as colourless, solid products in good yield (71 and 72 % respectively). The $^{31}P\text{-}\{^1H\}$ NMR spectrum of **37** comprises a singlet at δ(P) 144 2, the large downfield shift when compared to **36** reflecting the close proximity of the phosphorus centre to the strongly electronegative oxygen atoms. FAB^+ mass spectrometry shows the expected parent-

ion peak (m/z $[M]^+$ 362) and elemental analysis is in good agreement with calculated values (Table 4.1). The IR spectrum of **37** shows bands which can be attributed to $v(CN)$ (1479 cm^{-1}) and $v(PN)$ (918 cm^{-1}). The $^{31}P\text{-}\{^1H\}$ NMR spectrum of **38** also shows a singlet ($\delta(P)$ 137.9) which, like **37**, is shifted significantly downfield when compared to **36**. FAB$^+$ mass spectrometry again shows the parent-ion peak (m/z $[M]^+$ 266) and elemental analysis is in good agreement with calculated values (Table 4.1). The IR spectrum shows bands at 1438 and 952 cm^{-1} which are assigned to $v(CN)$ and $v(PN)$.

Table 4.1 Elemental analysis data for compounds **36-38** (calculated values in parentheses)

Compound	Formula	C	H	N
36	$Ph_2PN(C_2H_4)_2NPPh_2$	73.2 (74.0)	6.2 (6.2)	5.5 (6.2)
37	$(C_6H_4O_2)PN(C_2H_4)_2NP(C_6H_4O_2)$	52.2 (53.0)	4.3 (4.4)	7.3 (7.7)
38	$(C_2H_4O_2)PN(C_2H_4)_2NP(C_2H_4O_2)$	35.6 (36.1)	6.2 (6.0)	9.9 (10.5)

4.3 *Coordination chemistry of $R_2PN(C_2H_4)_2NPR_2$, $R_2 = Ph_2$, $C_6H_4O_2$ and $C_2H_4O_2$.*

The reactions of **36** and **37** with equimolar quantities of [PtCl$_2$(cod)] in dichloromethane proceed according to Equation 4.3 to yield the seven-membered, P,P' chelates *cis*-[PtCl$_2\{Ph_2PN(C_2H_4)_2NPPh_2\}$] **39** and *cis*-[PtCl$_2\{(C_6H_4O_2)PN(C_2H_4)_2NP(C_6H_4O_2)\}$] **40**.
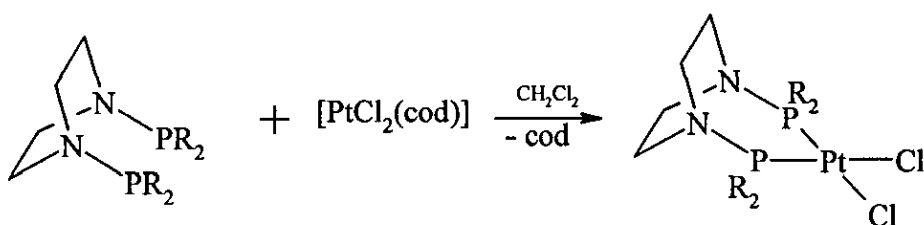
$R_2 = Ph_2$ (**39**), $C_6H_4O_2$ (**40**)

Equation 4.3

99

Addition of the solid diphosphines **36** and **37** to stirred dichloromethane solutions of [PtCl$_2$(cod)] results in the formation of colourless solutions. Stirring is continued for a further 2 hours, after which time diethyl ether is added and the products **39** and **40** are precipitated as colourless solids in good yield (79 and 89 % respectively) The ^{31}P-{^{1}H} NMR spectrum of both compounds show singlets with satellites from coupling to ^{195}Pt, the nature of the substituent groups on the phosphorus being reflected in the positions of the chemical shifts (δ(P) 53.5 and 99.6 respectively) and the magnitude of the $^1J(^{195}$Pt-^{31}P) coupling constants (3972 and 5480 Hz respectively). Both parameters for each compound are in agreement with values previously reported for similarly substituted phosphines when trans to a chloride in a Pt(II) complex[32,48] The IR spectra of **39** and **40** show bands which can be assigned to ν(CN) (1435 and 1477 cm^{-1} respectively) and ν(PN) (960 and 966 cm^{-1} respectively), the latter showing an increase in the P-N bond order when compared to the free ligand, and elemental analysis data is in agreement with the calculated values (Table 4.3). For **39** FAB$^+$ mass spectrometry shows the expected parent-ion peaks and a peak corresponding to the loss of a chloride ion (m/z 720 [M]$^+$ and 685 [M - Cl]), for **40**, however, it fails to show a parent-ion peak but instead fragmentation patterns consistent with the loss of chloride ions (m/z 597 [M - Cl]$^+$ and 566 [M - 2Cl]$^+$). (C$_6$H$_4$O$_2$)PN(C$_2$H$_4$)$_2$N P(C$_6$H$_4$O$_2$) **37** also reacts with [PtMe$_2$(cod)], in dichloromethane, to produce the P,P' chelate cis-[PtMe$_2${(C$_6$H$_4$O$_2$)PN(C$_2$H$_4$)$_2$NP(C$_6$H$_4$O$_2$)}] **41** (Equation 4.4).

R$_2$ = C$_6$H$_4$O$_2$ (**41**)
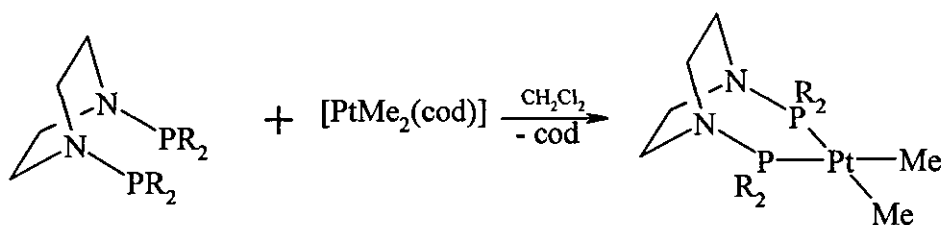
Equation 4.4

Addition of the solid ligand **37** to a stirred dichloromethane solution of [PtMe$_2$(cod)] results in a colourless solution. Addition of diethyl ether, after stirring for 2 hours, results in the precipitation of **41** as a colourless solid in moderate yield (63 %). The ^{31}P-{^{1}H} NMR spectrum of **41** show a singlet at δ(P) 154.9, a downfield shift of 10 7

ppm from the free ligand, with satellites from coupling to ^{195}Pt The value of the $^1J(^{195}$Pt-^{31}P) coupling constant (2977 Hz) is significantly smaller than that observed for the analogous dichloro- complex **40** but is consistent with values reported for similar complexes where phosphorus is *trans* to a methyl group[32]. Elemental analysis is in agreement with calculated values (Table 4.3)

The reaction of **36** with an equimolar quantity of [PdCl$_2$(cod)] in thf results in the bidentate, *P,P'* chelate complex *cis*-[PdCl$_2$\{Ph$_2$PN(C$_2$H$_4$)$_2$NPPh$_2$], **42** (Equation 4.5). The product was prepared and isolated using the same technique employed in the synthesis of its platinum analogue **39**, resulting in a yellow solid in 62 % yield.
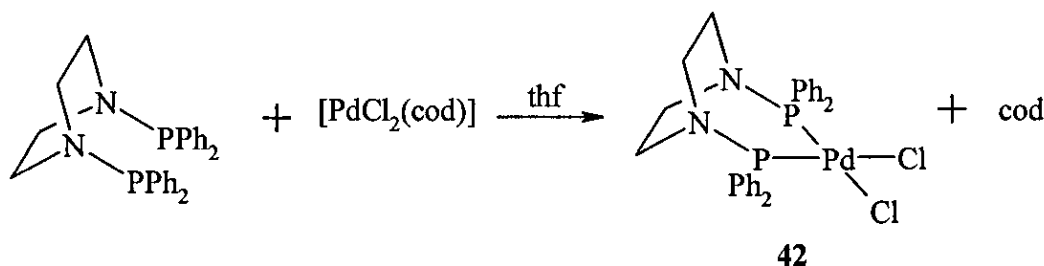
Equation 4.5

The ^{31}P-\{^{1}H\} NMR spectrum of **42** shows the anticipated singlet at δ(P) 101.7, a downfield shift of approximately 40 ppm when compared to the free ligand **36**. FAB$^+$ mass spectrometry showed a strong parent-ion peak and a peak corresponding to the loss of a chloride ion (*m/z* 632 [*M*]$^+$ and 597 [*M* - Cl]$^+$) and elemental analysis is in agreement with the calculated values (Table 4.3). Once again bands at 1435 cm^{-1} and 959 cm^{-1}, attributable to ν(CN) and ν(PN) respectively, are evident in the IR spectrum as are two ν(PdCl) stretches at 320 and 298 cm^{-1} which are indicative of a *cis*-PdCl$_2$ geometry. Slow diffusion of diethyl ether into a dichloromethane solution of **42** gives the product as yellow crystals. The X-ray structure of **42** contains two crystallographically independent molecules and shows the product to have the expected square planar geometry about the Pd centre (Figure 4.1). The bidentate nature of the co-ordination to the metal results in the formation of two 7-membered Pd-P-N-C-C-N-P ring systems that differ by which carbon atoms of the ligand backbone they incorporate. The N(C$_2$H$_4$)$_2$N backbone of the ligand adopts a boat conformation and forms an 'umbrella-like' structure around the Pd centre. Table 4.2 shows selected bond lengths and angles for **42**.
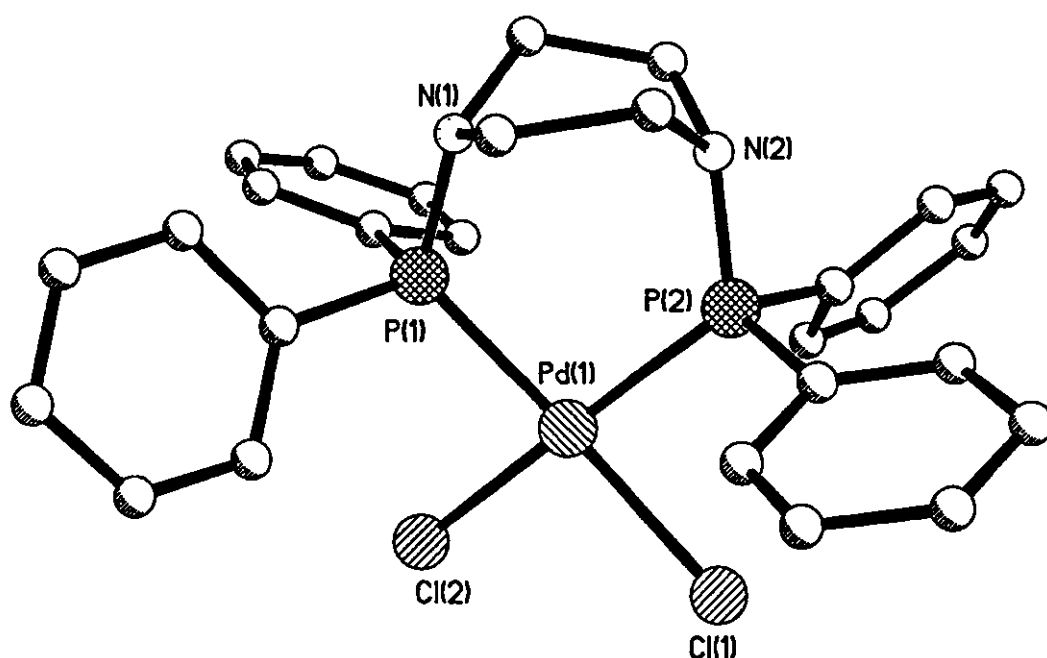
Figure 4.1 Solid state structure of *cis*-[PdCl₂{Ph₂PN(C₂H₄)₂NPPh₂}] **42**.

Table 4.2 Selected bond lengths (Å) and bond angles (°) for compound **42**.

Bond	Length	Bond	Angle
Pd(1)-P(1)	2.253 (5) [2.263 (5)]	P(1)-Pd(1)-P(2)	94.0 (2) [94.7 (2)]
Pd(1)-P(2)	2.256 (5) [2.246 (5)]	P(1)-Pd(1)-Cl(2)	88.9 (2) [87.2 (5)]
Pd(1)-Cl(1)	2.381 (5) [2.367 (5)]	P(2)-Pd(1)-Cl(1)	85 8 (2) [86.1 (2)]
Pd(1)-Cl(2)	2.390 (4) [2.387 (5)]	Cl(1)-Pd(1)-Cl(2)	92.1 (2) [92.0 (2)]
P(1)-N(1)	1.697 (14) [1 692 (14)]	Pd(1)-P(1)-N(1)	120.6 (6) [121.7 (6)]
P(2)-N(2)	1.675 (14) [1.71 (2)]	Pd(1)-P(2)-N(2)	123.3 (6) [121.5 (7)]

N B The values in parentheses are for the second crystallographically independent molecule.

The structure also reveals that the square planar palladium centre is distorted and in both of the two independent molecules the bite angle of the piperazine is larger than the ideal 90° [94.0 (2) and 94.7 (2)] and the Cl-Pd-Cl angles are also greater than 90° [92.1 (2) and 92.0 (2)]. The mean deviations of PdP₂Cl₂ from the plane are 0.14 Å for one of the molecules and 0.02 Å for the second. In both molecules the P-N, Pd-P and P-Cl bond lengths are all typical of single bonds and are comparable to those observed in Chapter 2 for compounds **9** and **10**.

Table 4.3 Elemental analysis data for complexes **39-43** (calculated values in parentheses).

Cpd	Formula	C	H	N
39	cis-[PtCl$_2$\{Ph$_2$PN(C$_2$H$_4$)$_2$NPPh$_2$]	45.9 (46.7)	3.7 (3.9)	3.2 (3 9)
40	cis-[PtCl$_2$\{(C$_6$H$_4$O$_2$)$_2$PN(C$_2$H$_4$)$_2$NP(C$_6$H$_4$O$_2$)$_2$\}]	30.4 (30.6)	2.8 (2.6)	4.3 (4 5)
41	cis-[PtMe$_2$\{(C$_6$H$_4$O$_2$)$_2$PN(C$_2$H$_4$)$_2$NP(C$_6$H$_4$O$_2$)$_2$\}]	36.3 (36.8)	3.9 (3.8)	4.6 (4.8)
42	cis-[PdCl$_2$\{Ph$_2$PN(C$_2$H$_4$)$_2$NPPh$_2$\}]	52.9 (53.3)	4.5 (4.5)	4.3 (4.4)
43	cis-[Mo(CO)$_4$\{Ph$_2$PN(C$_2$H$_4$)$_2$NPPh$_2$\}]	57.6 (58.0)	3.9 (4.3)	3.8 (4.2)

The reaction of **36** with [Mo(CO)$_4$(pip)$_2$] in dichloromethane proceeds, with displacement of the piperidines, to give cis-[Mo(CO)$_4$\{Ph$_2$PN(C$_2$H$_4$)$_2$NPPh$_2$\}], **43** (Equation 4.6).

43
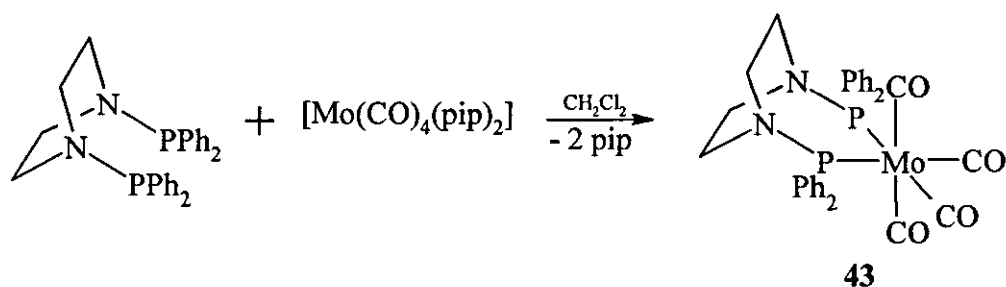
Equation 4.6

The [Mo(CO)$_4$(pip)$_2$] was suspended in dry dichloromethane and **36** added as a solid in one portion. The reaction mixture was then heated to reflux for 15 minutes, cooled and the solvent volume reduced *in vacuo* to *ca* 2 cm^3. Addition of methanol to the solution gave **43** as a yellow solid in approximately 70% yield. The ^{31}P-\{^{1}H\} NMR spectrum of **43** displays a singlet at δ(P) 97.2, a downfield shift of around 35 ppm upon complexation and similar in magnitude to the shift observed in Chapter 2 between compounds **1** and **13**. The IR spectrum of **43** shows four strong bands due to v(CO) (2021, 1917, 1901 and 1888 cm^{-1}), confirming the *cis* binding of the chelate and the terminal nature of the carbonyl ligands. FAB$^+$ mass spectrometry does not show the peak for the expected parent-ion but exhibits a fragmentation pattern consistent with the sequential loss of four carbonyl ligands (*m/z* 634 [*M* - CO]$^+$, 606 [*M* - 2CO]$^+$, 578 [*M* - 3CO]$^+$, 550 [*M* - 4CO]$^+$). Elemental analysis is in good

agreement with calculated values (Table 4 3) The complex can therefore be identified as possessing the expected octahedral geometry around the Mo centre and, as described previously for **42**, synthesis of the *P-P'* chelate results in the formation of two 7-membered ring systems which differ only by which carbon atoms of the ligand backbone they incorporate

Compounds **39-43** demonstrate the ability of $Ph_2PN(C_2H_4)_2NPPh_2$ and $(C_6H_4O_2)PN(C_2H_4)_2NP(C_6H_4O_2)$ to act as a bidentate chelating ligands and form seven-membered metallacycles. Reactions with compounds containing Au (I) and Ru (II) show that $Ph_2PN(C_2H_4)_2NPPh_2$, $(C_6H_4O_2)_2PN(C_2H_4)_2NP(C_6H_4O_2)_2$ and $(C_2H_4O_2)_2PN(C_2H_4)_2NP(C_2H_4O_2)_2$ can also act as a bridging ligands between two metal centres.

Reactions of the ligands **36, 37** and **38** with two equivalents of [AuCl(tht)] in dichloromethane proceed according Equation 4.7 to give the bimetallic gold species $[Ph_2P\{AuCl\}N(C_2H_4)_2NP\{AuCl\}Ph_2]$ **44** $[(C_6H_4O_2)P\{AuCl\}N(C_2H_4)_2NP\{AuCl\}(C_6H_4O_2)]$ **45** and $[(C_2H_4O_2)P\{AuCl\}N(C_2H_4)_2NP\{AuCl\}(C_2H_4O_2)]$, **46**.
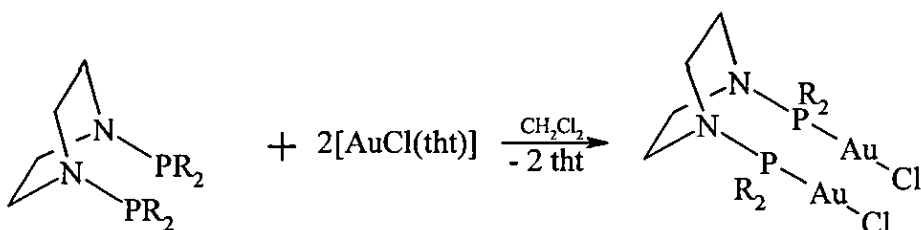
$$R = Ph \text{ (44)}, C_6H_4O_2 \text{ (45)}$$
$$\text{and } C_2H_4O_2 \text{ (46)}$$

Equation 4.7

Addition at room temperature of the solid ligands **36, 37** and **38** to dichloromethane solutions of 2 equivalents of [AuCl(tht)], followed by addition of diethyl ether, results in the precipitation of the products **44, 45** and **46** as colourless solids in varying yields (55, 86 and 76 % respectively). The elemental analysis values for each product are in good agreement with the calculated values (Table 4.4) and the $^{31}P-\{^1H\}$ NMR spectra all show singlets. The $^{31}P-\{^1H\}$ NMR spectrum of $[Ph_2P\{AuCl\}N(C_2H_4)_2NP\{AuCl\}Ph_2]$ **44** shows a singlet at $\delta(P)$ 80.7, while the chemical shifts of $[(C_6H_4O_2)P\{AuCl\}N(C_2H_4)_2NP\{AuCl\}(C_6H_4O_2)]$ **45**, $(\delta(P)$ 136 4)

and [(C$_2$H$_4$O$_2$)P{AuCl}N(C$_2$H$_4$)$_2$NP{AuCl}(C$_2$H$_4$O$_2$)], **46** (δ(P) 131.7) are significantly further downfield due to the phosphorus centres proximity to highly electronegative oxygen atoms. The FAB$^+$ mass spectrum of **45** shows the expected parent-ion peak (m/z [M]$^+$ 827), however, the FAB$^+$ mass spectra of **44** and **46** do not contain parent-ion peaks but both show strong peaks corresponding to [M – Cl]$^+$ (m/z 883 for **44** and m/z 695 for **46**). The IR spectra of all three compounds show bands corresponding to ν(CN) and ν(PN) (1434 and 966 cm^{-1} respectively for **44**, 1445 and 966 cm^{-1} respectively for **45** and 1445 and 967 cm^{-1} respectively for **46**).

Reaction of **36** with equimolar quantities of the chloro-bridged dimer [{RuCl(μ-Cl)(η^6-p-MeC$_6$H$_4$^{i}Pr)}$_2$] also gave a complex in which **36** acts as a bridging ligand. Addition of the solid diphosphine to a thf solution of [{RuCl(μ-Cl)(η^6-p-MeC$_6$H$_4$^{i}Pr)}$_2$] results in the formation of [{RuCl$_2$(η^6-p-MeC$_6$H$_4$^{i}Pr)}$_2$ {Ph$_2$PN(C$_2$H$_4$)$_2$NPPh$_2$}], **47**, which was isolated as a light brown solid in good yield (75 %) (Equation 4.8).

47
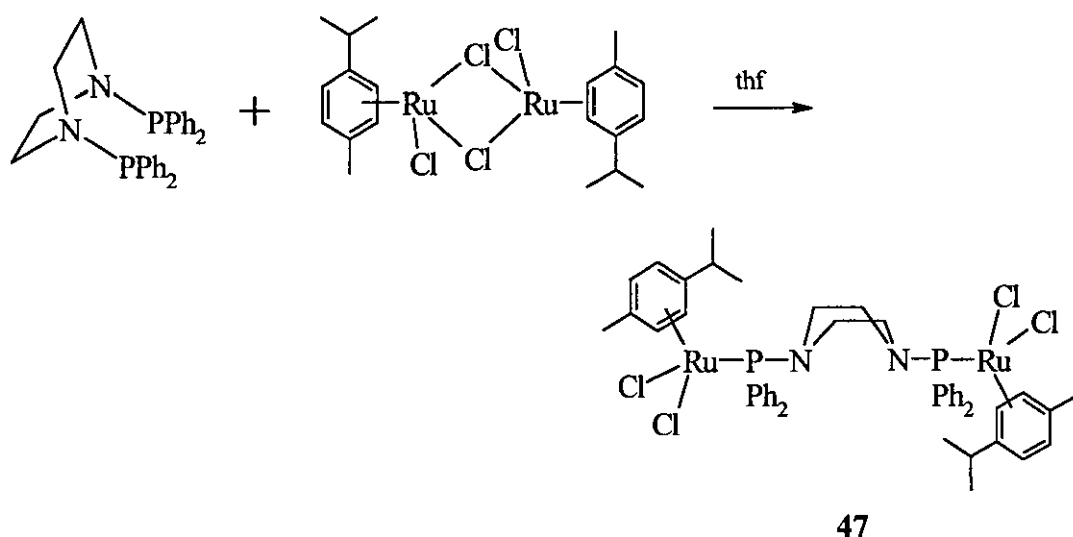
Equation 4.8

Elemental analysis is in good agreement with calculated values (Table 4.4) and the IR spectrum shows the bands which can be attributed to ν(CN) (1432 cm^{-1}) and ν(PN) (953 cm^{-1}). ^{31}P-{^{1}H} NMR studies show a singlet with a chemical shift 69.8 ppm, a downfield shift of only 7 ppm compared to the free ligand. FAB$^+$ mass spectrometry shows the expected parent-ion peak (m/z 1066 [M]$^+$), a peak assigned to [M-Cl]$^+$ (m/z

1031) and a strong peak corresponding to the loss of a $RuCl_2(\eta^6\text{-}p\text{-MeC}_6H_4{}^{i}Pr)$ fragment (m/z 760).

Table 4.4 Elemental analysis data for complexes **44** to **47** (calculated values in parentheses).

Cpd	Formula	C	H	N
44	$[Ph_2P\{AuCl\}N(C_2H_4)_2NP\{AuCl\}Ph_2]$	36.0 (36.6)	2.8 (3.1)	2.4 (3.1)
45	$[(C_6H_4O_2)_2P\{AuCl\}N(C_2H_4)_2NP\{AuCl\}(C_6H_4O_2)_2]$,	23.2 (23.2)	1.9 (1.9)	3.3 (3.4)
46	$[(C_2H_4O_2)_2P\{AuCl\}N(C_2H_4)_2NP\{AuCl\}(C_2H_4O_2)_2]$	13.3 (13.1)	2.2 (2.2)	3.8 (3 8)
47	$[\{RuCl_2(\eta^6\text{-}p\text{-MeC}_6H_4{}^{i}Pr)\}_2\{Ph_2PN(C_2H_4)_2NPPh_2\}]$	53.1 (54.0)	5.3 (5.3)	2.2 (2.6)

4.4 *Synthesis of phosphorus (III) derivatives of homopiperazine.*

Compounds **36, 37** and **38** demonstrate that piperazine reacts successfully with the chlorophosphines Ph_2PCl, $(C_6H_4O_2)PCl$ and $(C_2H_4O_2)PCl$ to produce bis substituted P – N ligand systems. An analogous set of ligands can be synthesised by reacting the same chlorophosphines with homopiperazine. Homopiperazine differs from piperazine by containing an extra CH_2 group, therefore forming a 7-membered nitrogen-carbon ring system. Reaction of homopiperazine with two equivalents of Ph_2PCl, $(C_6H_4O_2)PCl$ and $(C_2H_4O_2)PCl$, in the presence of NEt_3, proceeds in thf to give $Ph_2PN(C_5H_{10})NPPh_2$, **48**, $(C_6H_4O_2)PN(C_5H_{10})NP(C_6H_4O_2)$, **49** and $(C_2H_4O_2)$ $PN(C_5H_{10})NP(C_2H_4O_2)$, **50** respectively (Equation 4.9).
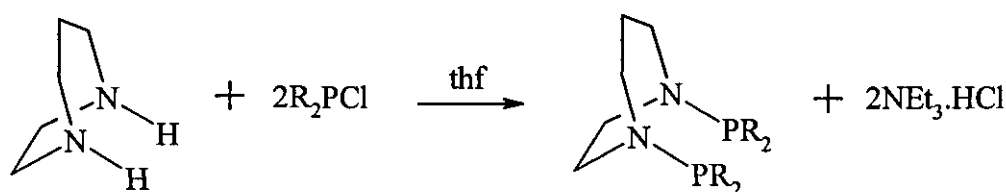
$$R_2 = Ph_2 \ (48), \ C_6H_4O_2 \ (49)$$
$$\text{and } C_2H_4O_2 \ (50)$$

Equation 4.9

Addition of thf solutions of each chlorophosphine to stirred solutions of homopiperazine, also in thf, resulted in the immediate precipitation of [Et₃NH]Cl as the reactions proceed. The reaction mixtures were then stirred for two hours after the completion of the chlorophosphine additions. *In situ* ^{31}P-$\{^1H\}$ NMR studies performed at this stage revealed that in each case only one phosphorus-containing species was present in the reaction mixtures. The ammonium salts were then removed by suction filtration and the filtrates evaporated to dryness *in vacuo* to leave **48, 49** and **50** as colourless solids The ^{31}P-$\{^1H\}$ NMR spectrum of $Ph_2PN(C_5H_{10})NPPh_2$ **48**, shows a singlet at $\delta(P)$ 65.7 and while the spectra of $(C_6H_4O_2)PN(C_5H_{10})NP(C_6H_4O_2)$, **49** and $(C_2H_4O_2)PN(C_5H_{10})NP(C_2H_4O_2)$, **50** also show singlets these are significantly further downfield, at $\delta(P)$ 148.3 and $\delta(P)$ 143 8 respectively, due to the phosphorus atom containing an oxygen substituent. The chemical shift values of all three ligands are slightly downfield from the values observed for the analogous piperazine derivatives, **36, 37** and **38**, suggesting that the addition of an extra CH_2 group into the ligand backbone causes a slight deshielding of the phosphorus centres. FAB^+ mass spectrometry confirms the proposed identities of the products as diphosphines, showing peaks corresponding to the expected parent-ions in each case (m/z $[M]^+$ 468 for **48**, $[M]^+$ 376 for **49** and $[M]^+$ 280 for **50**). For each of the products elemental analysis is in agreement with calculated values (Table 4.5) and the IR spectra show bands which can be assigned to $\nu(CN)$ and $\nu(PN)$ (1431 and 921 cm^{-1} respectively for **48**, 1459 and 916 cm^{-1} respectively for **49** and 1450 and 931 cm^{-1} respectively for **50**).

Table 4.5 Elemental analysis data for complexes **48, 49** and **50** (calculated values in parentheses).

Compound	Formula	C	H	N
48	$Ph_2PN(C_5H_{10})NPPh_2$	72.4 (74.3)	6.1 (6.4)	4 8 (5.9)
49	$(C_6H_4O_2)PN(C_5H_{10})NP(C_6H_4O_2)$	53.8 (54.3)	4.3 (4.8)	6.9 (7.4)
50	$(C_2H_4O_2)PN(C_5H_{10})NP(C_2H_4O_2)$	38.8 (38.6)	6.8 (6.4)	10.4 (10.0)

4.5 *Coordination chemistry of $R_2PN(C_5H_{10})NPR_2$, $R_2 = Ph_2$ and $C_6H_4O_2$*

The reactions of **48** and **49** with equimolar quantities of [PtCl₂(cod)] in dichloromethane proceed according to Equation 4.10 to yield the bidentate, *P,P'* chelates *cis*-[PtCl₂{Ph₂PN(C₅H₁₀)NPPh₂}] **51** and *cis*-[PtCl₂{(C₆H₄O₂)PN(C₅H₁₀) NP(C₆H₄O₂)}] **52**. Addition of the solid diphosphines **48** and **49** to dichloromethane solutions of [PtCl₂(cod)] results in the formation of colourless solutions which are stirred for a further 2 hours. After this time diethyl ether was added to the reaction mixture and the products **51** and **52** precipitated as colourless solids in excellent yield (92 and 84 % respectively).
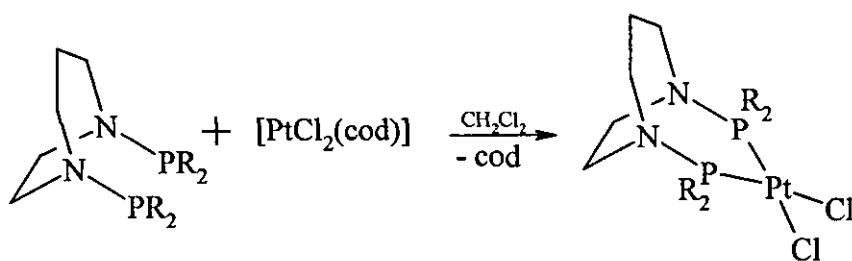
$R_2 = Ph_2$ (**51**), $C_6H_4O_2$ (**52**)

Equation 4.10

The ³¹P-{¹H} NMR spectra of the products show singlets, at δ(P) 64.1 and 102.3 respectively, with satellites from coupling to ¹⁹⁵Pt. As with **39** and **40** the magnitude of the couplings (4092 and 5466 Hz respectively) and the positions of the chemical shifts reflect the nature of the substituents on the phosphorus atoms. The IR spectra of **51** and **52** shows two bands indicating a *cis*-PtCl₂ geometry (300 and 277 cm⁻¹ for **51** and 306 and 279 cm⁻¹ for **52**) as well as bands corresponding to ν(CN) at 1436 and 1478 cm⁻¹ respectively, and ν(PN), at 936 and 951 cm⁻¹ respectively. The ν(CN) and ν(PN) values both represent an increase in frequency from the free ligand and indicate an increase in bond order upon complexation. Elemental analyses are in good agreement with calculated values (Table 4 6). FAB⁺ mass spectrometry studies on **51** show the parent-ion peak and a peak that can be assigned to the loss of a chloride ion (m/z [*M*]⁺ 734 and [*M* – Cl]⁺ 699). However, on **52** they fail to show the parent-ion peak but instead a peak corresponding to the loss of a chloride ion (m/z [*M* – Cl]⁺ 606).

$Ph_2PN(C_5H_{10})NPPh_2$ **48** and $(C_6H_4O_2)PN(C_5H_{10})NP(C_6H_4O_2)$, **49** also react successfully with equimolar quantities of $[PtMe_2(cod)]$ to give the P,P' chelates *cis*-$[PtMe_2\{Ph_2PN(C_5H_{10})NPPh_2\}]$ **53** and *cis*-$[PtMe_2\{(C_6H_4O_2)PN(C_5H_{10})N$ $P(C_6H_4O_2)\}]$ **54** (Equation 4.11). The same synthetic technique as that used in the formation of the dichloro analogues **51** and **52** was employed to give **53** and **54** as colourless solids in moderate yields (64 and 66 % respectively).

$$R = Ph\ (53),\ C_6H_4O_2\ (54)$$
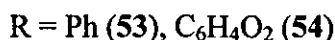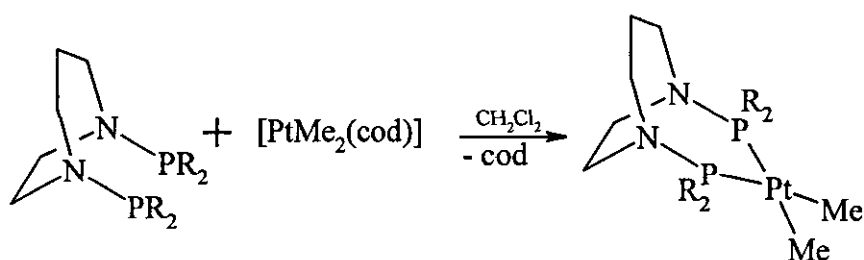
Equation 4.11

The resulting $^{31}P\text{-}\{^1H\}$ NMR spectra of both products show singlets (at $\delta(P)$ 89.1 for **53** and $\delta(P)$ 156.9 for **54**) with satellites from coupling to ^{195}Pt. In each case the magnitude of the coupling (2231 Hz for **53** and 2937 Hz for **54**) is, as anticipated, significantly smaller than the value observed for the analogous dichloro complexes but is in agreement with values previously reported for similar Pt(II) systems containing a phosphorus *trans* to a methyl group.[32] The $^{31}P\text{-}\{^1H\}$ NMR data for **54** is also in agreement with the values recorded for the analogous piperazine complex **41**. FAB^+ mass spectrometry studies on both **53** and **54** fail to show parent-ion peaks but instead show peaks which can be attributed to the loss of a methyl group (m/z $[M - CH_3]^+$ 678 for **53** and 586 for **54**). Elemental analyses are in good agreement with calculated values (Table 4.6) and the IR spectra show bands corresponding to $\nu(CN)$ and $\nu(PN)$ (1435 and 925 cm^{-1} respectively for **53** and 1480 and 919 cm^{-1} respectively for **54**).

The reactions of **48** and **49** with equimolar quantities of $[PdCl_2(cod)]$ in dichloromethane result in the formation of the bidentate, P,P' chelate complexes *cis*-$[PdCl_2\{Ph_2PN(C_5H_{10})NPPh_2\}]$ **55** and *cis*-$[PdCl_2\{(C_6H_4O_2)PN(C_5H_{10})NP(C_6H_4O_2)\}]$ **56** (Equation 4.12). Addition of the solid diphosphines **48** and **49** to dichloromethane solutions of $[PdCl_2(cod)]$ results in the formation of yellow solutions. Addition of

diethyl ether, after stirring for a further 2 hours, results in the precipitation of the products **55** and **56** as yellow solids in 87 and 94 % yields respectively.

$$R_2 = Ph_2 \ (\textbf{55}), \ C_6H_4O_2 \ (\textbf{56})$$
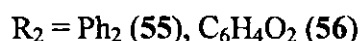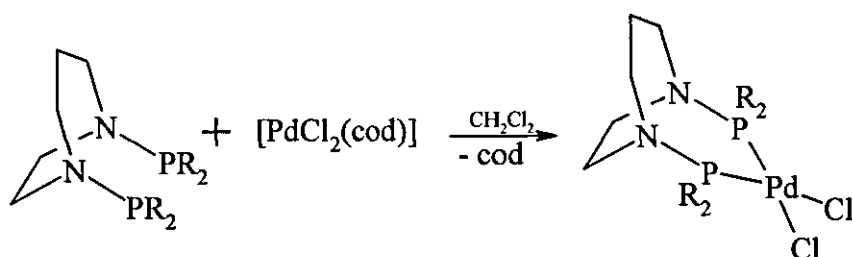
Equation 4.12

The $^{31}P\text{-}\{^1H\}$ NMR spectra of **55** and **56** show singlets at $\delta(P)$ 92.6 and 125.6, with the downfield shift between **55** and the free ligand **48** being comparable to that observed between the piperazine compounds **42** and **36**. FAB$^+$ mass spectrometry shows the expected parent-ion peaks (m/z $[M]^+$ 646 and m/z $[M]^+$ 553 respectively) and peaks due to the loss of a chloride ion (m/z $[M - Cl]^+$ 611 and $[M - Cl]^+$ 518 respectively). Elemental analyses are in good agreement with calculated values (Table 4 6).The IR spectrum of **55** shows two bands which can be assigned to $v(CN)$ and $v(PN)$ (1437 and 953 cm^{-1} respectively) as well as two distinct $v(PdCl)$ stretches at 312 and 289 cm^{-1} which indicate a *cis*-PdCl$_2$ geometry. The IR spectrum of **56** also shows bands which can be assigned to $v(CN)$ (1459 cm^{-1}), $v(PN)$ (916 cm^{-1}) and $v(PdCl)$ (306 and 276 cm^{-1}).

The complexes **51** to **56** demonstrate the ability of Ph$_2$PN(C$_5$H$_{10}$)NPPh$_2$, **48** and (C$_6$H$_4$O$_2$)PN(C$_5$H$_{10}$)NP(C$_6$H$_4$O$_2$), **49** to act as bidentate, *P,P'* chelating ligands in the same manner as previously described for the ligands Ph$_2$PN(C$_2$H$_4$)$_2$NPPh$_2$ **36** and (C$_6$H$_4$O$_2$)PN(C$_2$H$_4$)$_2$NP(C$_6$H$_4$O$_2$) **37** in complexes **39** to **43**. However, unlike **36** and **37**, which only form seven-membered metallacycles when acting as chelating ligands, **48** and **49** are able to form one seven- and one eight – membered metallacycle due to the extra CH$_2$ group in the ligand backbone (as demonstrated in Figure 4.2 for the reaction of the ligands with [PtCl$_2$(cod)]).

110
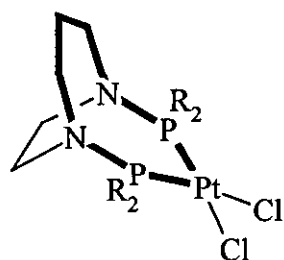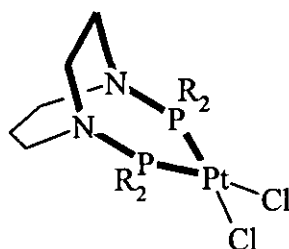
8-membered ring   7-membered ring

Figure 4.2 Different ring sizes in complexes containing the ligands **48** and **49**

As well as acting as chelates, **48** and **49**, like **36**, **37** and **38**, also demonstrate the ability to act as bridging ligands between two metal centres when reacted with two equivalents of [AuCl(tht)]. Reaction of the ligands with the [AuCl(tht)] in dichloromethane proceeds according to Equation 4.13 to give the bimetallic gold species [Ph$_2$P{AuCl}N(C$_5$H$_{10}$)NP{AuCl}Ph$_2$] and **57** [(C$_6$H$_4$O$_2$)P{AuCl}N(C$_5$H$_{10}$)N P{AuCl}(C$_6$H$_4$O$_2$)] **58**.
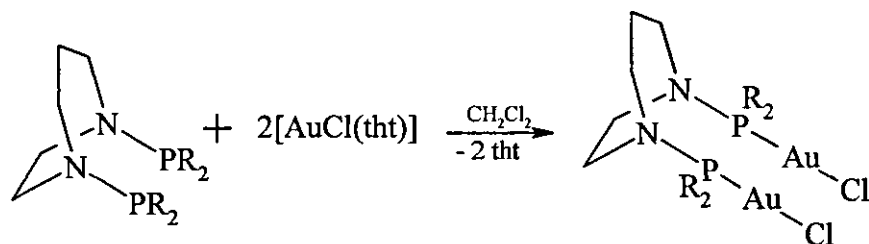
$R_2 = Ph_2$ (**57**), $C_6H_4O_2$ (**58**)

Equation 4.13

Employing the same technique used in the synthesis of **44**, **45** and **46** results in the isolation of **57** and **58** as colourless solids in good yields (76 and 81 % respectively). The $^{31}P-\{^1H\}$ NMR spectra of both **57** and **58** show singlets (at δ(P) 78.7 and δ(P) 139.9) which are comparable to the values reported for the complexes **44** and **45**. Elemental analyses are in good agreement with calculated values (Table 4.6). FAB$^+$ mass spectrometry studies on **57** and **58** failed to show a parent-ion peak and instead, in both cases, showed a peak corresponding to the loss of a chloride ion (m/z [M –

111

Cl]$^+$ 897 for **57** and 805 for **58**). The IR spectra of the products both show bands corresponding to ν(CN) and ν(PN) (1433 and 903 cm^{-1} respectively for **57** and 1441 and 908 cm^{-1} respectively for **58**).

Table 4.6 Elemental analysis data for complexes **51** to **58** (calculated values in parentheses).

Cpd	Formula	C	H	N
51	[PtCl$_2${Ph$_2$PN(C$_5$H$_{10}$)NPPh$_2$}]	46.4 (47.5)	3.9 (4.1)	3 4 (3.8)
52	[PtCl$_2${(C$_6$H$_4$O$_2$)PN(C$_5$H$_{10}$)NP(C$_6$H$_4$O$_2$)}]	31.5 (31 8)	2.9 (2 8)	3.9 (4 4)
53	[PtMe$_2${Ph$_2$PN(C$_5$H$_{10}$)NPPh$_2$}]	53.1 (53.6)	4.9 (5.2)	3.8 (4.0)
54	[PtMe$_2${(C$_6$H$_4$O$_2$)PN(C$_5$H$_{10}$)NP(C$_6$H$_4$O$_2$)}]	37.1 (37.9)	3.9 (4 0)	4.5 (4 7)
55	[PdCl$_2${Ph$_2$PN(C$_5$H$_{10}$)NPPh$_2$}]	53.3 (54.0)	4.8 (4 7)	4.2 (4 4)
56	[PdCl$_2${(C$_6$H$_4$O$_2$)PN(C$_5$H$_{10}$)NP(C$_6$H$_4$O$_2$)}]	35.9 (36.8)	3.6 (3.3)	4 6 (5.0)
57	[Ph$_2$P{AuCl}N(C$_5$H$_{10}$)NP{AuCl}Ph$_2$]	35 6 (37.4)	3.2 (3.2)	2.7 (3.0)
58	[(C$_6$H$_4$O$_2$)P{AuCl}N(C$_5$H$_{10}$)NP{AuCl}(C$_6$H$_4$O$_2$)]	23.8 (24.3)	2 1 (2.1)	3.2 (3.3)

4.6 *Conclusions.*

Both piperazine and homopiperazine are readily functionalised with chlorophosphines to produce new bis-substituted phosphine ligands. Subsequent reactions of these ligands with Pt(II), Pd(II) and Mo(0) result in the formation of 7- and 8-membered chelate rings. Further reactions with Au(I) and Ru(II) result in the ligands acting as bidentate bridging ligands. The spectroscopic data for derivatives of the two amines, which incorporate the same phosphorus substituents, is very similar suggesting that the extra CH$_2$ in the homopiperazine ligands has little effect on the electronic properties of the ligands and resulting complexes There is, however, a great deal of scope for further work involving these systems. Although Figure 4.1 confirms that the ligand **36** does indeed form an umbrella-like structure around the palladium centre, the steric properties of a ligand constitute only one of many parameters that have to be taken into consideration when designing an effective catalytic system. Further studies into the electronic properties of these types of ligands are required. As well as the possibility of forming new *bis*-substituted piperazine and

homopiperazine derivatives through reactions with various other chlorophosphines it may also be possible to isolate the *mono*-substituted intermediates and form unsymmetrical products via reaction with a second, different chlorophosphine. Further investigations on the reactions of the ligands with different metals can also be conducted.

Experimental

General experimental conditions and instrumentation were as set out on page 12 and as described in Chapters 2 and 3. [{RuCl(μ-Cl)(η^6-*p*-MeC$_6$H$_4^i$Pr)}$_2$][108] was prepared using the literature procedure and piperazine, homopiperazine, 1,2-phenylenephosphoro-chloridite and 2-chloro-1,3,2-dioxaphospholane were used without further purification.

Ph$_2$PN(C$_2$H$_4$)$_2$NPPh$_2$ 36. A solution of chlorodiphenylphosphine (5.1 g, 4.2 cm^3, 24.0 mmol) in thf (20 0 cm^3) was added dropwise over a period of 30 min to a stirred solution of piperazine (1.00 g, 12 0 mmol) and triethylamine (2.40 g, 3 3 cm^3, 24.0 mmol) in thf (30 cm^3) at room temperature. Stirring was continued for 24 h, during which time triethylammonium hydrochloride separated from the colourless solution. This precipitate was removed by suction filtration and the filtrate evaporated to dryness *in vacuo* to give a white solid product. Yield: 3.92 g, 75 %. Microanalysis: Found (Calcd. for C$_{28}$H$_{28}$N$_2$P$_2$) C 73.2 (74.0), H 6.2 (6.2), N 5.5 (6.2) %. ^{31}P-{^{1}H} NMR (CDCl$_3$): δ(P) 62.9. IR (KBr disc, cm^{-1}) 3065w, 2951w, 2830w, 2816w, 1583w, 1478s, 1431s, 1360m, 1307w, 1290m, 1250m, 1181m, 1156m, 1127m, 1080s, 1029w, 996w, 956w, 930m, 744m, 699m, 567m, 545s, 520m, 473m, 435s, 324w and 231s. FAB mass spectrum: *m/z* 455, [*M* + H]$^+$.

(C$_6$H$_4$O$_2$)PN(C$_2$H$_4$)$_2$NP(C$_6$H$_4$O$_2$) 37. A solution of 1,2-phenylenephosphoro-chloridite (4.65 g, 16.7 mmol) in thf (60.0 cm^3) was added dropwise over a period of 1 h to a stirred solution of piperazine (0.72 g, 8.3 mmol) and triethylamine (1.69 g, 2.3 cm^3, 16 7 mmol) in thf (70.0 cm^3). Stirring was continued for a further 2 h, during which time triethylammonium hydrochloride separated from the colourless solution. This precipitate was removed by suction filtration and the filtrate evaporated to

dryness *in vacuo* to give a white solid product. Yield: 2.15 g, 71 %. Microanalysis: Found (Calcd. for $C_{16}H_{16}N_2O_4P_2$) C 52.2 (53.0), H 4.3 (4.4), N 7.3 (7.7) %. $^{31}P-\{^1H\}$ NMR (CDCl$_3$): δ(P) 144.2. IR (KBr disc, cm^{-1}): 3066w, 2956w, 1610w, 1479vs, 1442m, 1373m, 1334m, 1260m, 1231s, 1144m, 1094m, 1009m, 918w, 818s, 725s, 740m, 677m, 611m, 561m, 512m, 428w, 375m and 237s. FAB mass spectrum *m/z* 363, $[M]^+$.

$(C_2H_4O_2)PN(C_2H_4)_2NP(C_2H_4O_2)$ 38. A solution of 2-chloro-1,3,2-dioxaphospholane (5.69 g, 4.0 cm^3, 45.0 mmol) in thf (70 0 cm^3) was added dropwise over a period of 1 h to a stirred solution of piperazine (1.93 g, 22.5 mmol) and triethylamine (4 54 g, 6.2 cm^3, 45.0 mmol) in thf (80.0 cm^3). Stirring was continued for a further 2 h, during which time triethylammonium hydrochloride separated from the colourless solution. This precipitate was removed by suction filtration and the filtrate evaporated to dryness *in vacuo* to give a white solid product. Yield: 4.31 g, 72 %. Microanalysis: Found (Calcd for $C_8H_{16}N_2O_4P_2$) C 35 6 (36.1), H 6.2 (6.0), N 9.9 (10.5) %. $^{31}P-\{^1H\}$ NMR (CDCl$_3$): δ(P) 137.9. IR (KBr disc, cm^{-1}): 3010w, 2959w, 2888w, 1560m, 1438m, 1378m, 1318m, 1218s, 1152m, 1086m, 1051m, 1005m, 952m, 866w, 752m, 679m, 582m, 549m, 416w and 237s. FAB mass spectrum: *m/z* 266, $[M]^+$.

cis-[PtCl$_2$\{Ph$_2$PN(C$_2$H$_4$)$_2$NPPh$_2$\}] 39. To a solution of [PtCl$_2$(cod)] (0.100 g, 0.26 mmol) in dichloromethane (5.0 cm^3) was added solid Ph$_2$PN(C$_2$H$_4$)$_2$NPPh$_2$ (0.120 g, 0 26 mmol) and the colourless solution stirred for *ca* 2 h. The solution was concentrated under reduced pressure to *ca* 1.0 cm^3 and diethyl ether (10.0 cm^3) added. The white product was collected by suction filtration. Yield: 0.152 g, 79 %. Microanalysis: Found (Calcd for $C_{28}H_{28}Cl_2N_2P_2Pt$) C, 45.9 (46.7), H 3 7 (3.9), N 3.2 (3.9) %. $^{31}P-\{^1H\}$ NMR (CDCl$_3$): δ(P) 53.5, $^1J(^{195}Pt-^{31}P)$ 3972 Hz IR (KBr disc, cm^{-1}): 3052s, 1618w, 1481s, 1435vs, 1369s, 1309s, 1261s, 1098vs, 960vs, 747s, 695vs, 550s, 519s, 284w, 230vs and 218vs. FAB mass spectrum: *m/z* 720, $[M]^+$.

cis-[PtCl$_2$\{(C$_6$H$_4$O$_2$)PN(C$_2$H$_4$)$_2$NP(C$_6$H$_4$O$_2$)\}] 40. To a solution of [PtCl$_2$(cod)] (0.100 g, 0.26 mmol) in dichloromethane (15.0 cm^3) was added solid (C$_6$H$_4$O$_2$)PN(C$_2$H$_4$)$_2$NP(C$_6$H$_4$O$_2$) (0.097 g, 0.26 mmol) and the colourless solution stirred for *ca* 2 h. The solution was concentrated under reduced pressure to *ca* 1.0

cm^3 and diethyl ether (15.0 cm^3) added. The white product was collected by suction filtration. Yield. 0.150 g, 89 %. Microanalysis: Found (Calcd for $C_{16}H_{16}Cl_2N_2O_4P_2Pt$) C, 30 4 (30.6), H 2.8 (2.6), N 4.3 (4.5) %. ^{31}P-$\{^1H\}$ NMR (CDCl$_3$): δ(P) 99.7, $^1J(^{195}Pt$-$^{31}P)$ 5480 Hz. IR (KBr disc, cm^{-1}): 3096w, 2925w, 1477s, 1373m, 1330m, 1263m, 1231s, 1134m, 1109s, 1047w, 1008m, 966vs, 936m, 862s, 760w, 697m, 626m, 583m, 542m, 421m, 334w and 306w. FAB mass spectrum: m/z 597, $[M$ - $Cl]^+$.

cis-$[PtMe_2\{(C_6H_4O_2)PN(C_2H_4)_2NP(C_6H_4O_2)\}]$ **41**. To a solution of $[PtMe_2(cod)]$ (0.080 g, 0.24 mmol) in dichloromethane (10.0 cm^3) was added solid $(C_6H_4O_2)PN(C_2H_4)_2NP(C_6H_4O_2)$ (0.087 g, 0.24 mmol) and the colourless solution stirred for ca 2 h. The solution was concentrated under reduced pressure to ca 1.0 cm^3 and diethyl ether (40.0 cm^3) added. The white product was collected by suction filtration. Yield: 0.089 g, 63 %. Microanalysis: Found (Calcd for $C_{18}H_{22}N_2O_4P_2Pt$) C, 36.3 (36 8), H 3.9 (3.8), N 4.6 (4.8) %. ^{31}P-$\{^1H\}$ NMR (CDCl$_3$): δ(P) 154.9, $^1J(^{195}Pt$-$^{31}P)$ 2977 Hz. IR (KBr disc, cm^{-1}): 2885w, 1480s, 1449w, 1373m, 1334m, 1262m, 1234s, 1198w, 1142m, 1098s, 1009m, 966s, 935m, 827s, 739s, 689m, 623m, 577m, 534m and 420m. FAB mass spectrum: m/z 587, $[M]^+$.

cis-$[PdCl_2\{Ph_2PN(C_2H_4)_2NPPh_2\}]$ **42**. To a solution of $[PdCl_2(cod)]$ (0.100 g, 0.35 mmol) in dichloromethane (5.0 cm^3) was added solid $Ph_2PN(C_2H_4)_2NPPh_2$ (0.160 g, 0.35 mmol) and the yellow solution stirred for ca 2 h. The solution was concentrated under reduced pressure to ca. 1.0 cm^3 and diethyl ether (10.0 cm^3) added. The yellow product was collected by suction filtration. Yield: 0.137 g, 62 %. Microanalysis: Found (Calcd for $C_{28}H_{28}Cl_2N_2P_2Pd$) C 52.9 (53.3), H, 4.5 (4.5), N 4.3 (4.4) %. ^{31}P-$\{^1H\}$ NMR (CDCl$_3$): δ(P) 101.7. IR (KBr disc, cm^{-1}): 3051w, 1571w, 1479s, 1435vs, 1308s, 1261s, 1180s, 1098vs, 1050s, 959vs, 924s, 745s, 691vs, 561s, 515vs, 501vs, 357s, 275s, 231s and 213vs. FAB mass spectrum: m/z 632, $[M]^+$.

cis-$[Mo(CO)_4\{Ph_2PN(C_2H_4)_2NPPh_2\}]$ **43**. To a partially dissolved solution of $[Mo(CO)_4(pip)_2]$ (0.500 g, 1 30 mmol) in dichloromethane (20.0 cm^3) was added solid $Ph_2PN(C_2H_4)_2NPPh_2$ (0.590 g, 1.30 mmol). The solution was heated to reflux for ca 15 min and allowed to cool to room temperature. The solution was concentrated under reduced pressure to ca 2.0 cm^3 and methanol (15.0 cm^3) added. The yellow product

115

was collected by suction filtration. Yield: 0 635 g, 72 %. Microanalysis: Found (Calcd for $C_{32}H_{28}N_2O_4P_2Mo$) C 57.6 (58.0) H 3.9 (4.3), N 3.8 (4.2) %. ^{31}P-{^1H} NMR (CDCl$_3$): δ(P) 97.2. IR (KBr disc, cm^{-1}): 3055w, 2962s, 2021vs, 1917vs, 1901vs, 1888vs, 1481s, 1435s, 1365s, 1260vs, 1089vs, 1021vs, 959vs, 801vs, 745s, 695vs, 586s, 554s, 523s, 385s, 247s, 230s and 224s. FAB mass spectrum: m/z 634, [M – CO]$^+$.

[Ph$_2$P(AuCl)N(C$_2$H$_4$)$_2$NP(AuCl)Ph$_2$] 44. To a solution of [AuCl(tht)] (0 071 g, 0.22 mmol) in dichloromethane (5.0 cm^3) was added solid Ph$_2$PN(C$_2$H$_4$)$_2$NPPh$_2$ (0.050 g, 0.11 mmol) and the colourless solution stirred for *ca.* 1 h The solution was concentrated under reduced pressure to *ca.* 1.0 cm^3 and diethyl ether (5 0 cm^3) added. The white product was collected by suction filtration. Yield: 0.054 g, 53 %. Microanalysis: Found (Calcd for $C_{28}H_{28}Cl_2N_2P_2Au_2$) C 36.0 (36.6), H 2.6 (3.1), N 2 4 (3.1) %. ^{31}P-{^1H} NMR (CDCl$_3$): δ(P) 80.7. IR (KBr disc, cm^{-1}): 3242w, 3005w, 1629w, 1479s, 1434vs, 1368s, 1261s, 1105vs, 1044s, 996w, 966s, 754s, 693vs, 578s, 536s, 495s, 333s, 246s, 230s and 207vs. FAB mass spectrum· m/z 883, [M – Cl]$^+$

[(C$_6$H$_4$O$_2$)P(AuCl)N(C$_2$H$_4$)$_2$NP(AuCl)(C$_6$H$_4$O$_2$)] 45. To a solution of [AuCl(tht)] (0.184 g, 0.58 mmol) in dichloromethane (15 0 cm^3) was added solid (C$_6$H$_4$O$_2$)PN(C$_2$H$_4$)$_2$NP(C$_6$H$_4$O$_2$) (0.104 g, 0.29 mmol) and the colourless solution stirred for *ca.* 1 h. The solution was concentrated under reduced pressure to *ca* 1.0 cm^3 and diethyl ether (30.0 cm^3) added. The white product was collected by suction filtration. Yield. 0.205 g, 86 %. Microanalysis: Found (Calcd for $C_{16}H_{16}Cl_2N_2O_4P_2Au_2$) C 23.2 (23.2), H 1.9 (1.9), N 3.3 (3.4) %. ^{31}P-{^1H} NMR (CDCl$_3$): δ(P) 136.4. IR (KBr disc, cm^{-1}): 3054w, 2928w, 2906w, 1445m, 1373m, 1261m, 1230s, 1138m, 1116s, 1094m, 1045w, 966s, 940m, 867s, 774m, 765m, 742s, 699m, 636m, 580m, 545w, 410w, 372w, 333m, 228m and 233m. FAB mass spectrum: m/z 827, [M]$^+$.

[(C$_2$H$_4$O$_2$)P(AuCl)N(C$_2$H$_4$)$_2$NP(AuCl)(C$_2$H$_4$O$_2$)] 46. To a solution of [AuCl(tht)] (0.160 g, 0.50 mmol) in dichloromethane (15.0 cm^3) was added solid (C$_2$H$_4$O$_2$)PN(C$_2$H$_4$)$_2$NP(C$_2$H$_4$O$_2$) (0 068 g, 0.25 mmol) and the colourless solution stirred for *ca* 2 h. The solution was concentrated under reduced pressure to *ca* 1.0

116

cm³ and diethyl ether (30.0 cm³) added. The white product was collected by suction filtration. Yield: 0.140 g, 76 %. Microanalysis: Found (Calcd for C$_8$H$_{16}$Cl$_2$N$_2$O$_4$P$_2$Au$_2$) C 13.3 (13.1), H 2.2 (2.2), N 3.8 (3.8) %. ^{31}P-{^{1}H} NMR (CDCl$_3$): δ(P) 131.7. IR (KBr disc, cm^{-1}): 2961w, 2904w, 1470w, 1445m, 1374m, 1336m, 1263m, 1229w, 1143m, 1111s, 1026s, 967s, 922s, 822m, 773s, 734m, 696s, 627m, 584m, 393w, 325m and 206m. FAB mass spectrum: *m/z* 695, [*M* - Cl]$^+$.

[{RuCl$_2$(η^6-*p*-MeC$_6$H$_4$^{i}Pr)}$_2${Ph$_2$PN(C$_2$H$_4$)$_2$NPPh$_2$}] 47. To a solution of [{RuCl(μ-Cl)(η^6-*p*-MeC$_6$H$_4$^{i}Pr)}$_2$] (0.250 g, 0.40 mmol) in thf (20.0 cm³) was added solid Ph$_2$PN(C$_2$H$_4$)$_2$NPPh$_2$ (0.185 g, 0.40 mmol) and the brown solution stirred for *ca* 12 h. The solution was concentrated under reduced pressure to *ca* 2.0 cm³ and diethyl ether (10 0 cm³) added. The red/brown product was collected by suction filtration and washed with diethyl ether (2 x 10.0 cm³). Yield: 0.299 g, 69 %. Microanalysis: Found (Calcd for C$_{48}$H$_{56}$Cl$_4$N$_2$P$_2$Ru$_2$) C 53.1 (54 0), H 5.3 (5.3), N 2 2 (2.6) %. ^{31}P-{^{1}H} NMR (CDCl$_3$)· δ(P) 69.8. IR (KBr disc, cm^{-1}): 3044m, 2964m, 2871m, 1586w, 1483s, 1432vs, 1374m, 1300w, 1261m, 1190m, 1119s, 1085vs, 1060s, 1030m, 953vs, 895m, 799w, 750s, 699vs, 682s, 560m, 527m, 483m, 444m, 346w, 291m, 212s, 233s, 227s and 218s FAB mass spectrum: *m/z* 1066, [*M*]$^+$.

Ph$_2$PN(C$_5$H$_{10}$)NPPh$_2$ 48. A solution of chlorodiphenylphosphine (6.87 g, 5.6 cm³, 31.2 mmol) in thf (50.0 cm³) was added dropwise over a period of 1 h to a stirred solution of homopiperazine (1.56 g, 15 6 mmol) and triethylamine (3.13 g, 4.3 cm³, 31.3 mmol) in thf (75 cm³) at room temperature. Stirring was continued for 2 h, during which time triethylammonium hydrochloride separated from the colourless solution This precipitate was removed by suction filtration and the filtrate evaporated to dryness *in vacuo* to give a white solid product Yield: 4.92 g, 68 %. Microanalysis: Found (Calcd for C$_{29}$H$_{30}$N$_2$P$_2$) C 73.4 (74.4), H 6.1 (6 4), N 5.2 (5.9) %. ^{31}P-{^{1}H} NMR (CDCl$_3$): δ(P) 65.7. IR (KBr disc, cm^{-1}): 3049m, 2920s, 2844m, 1584w, 1477m, 1431m, 1380w, 1362m, 1304w, 1287w, 1239w, 1167m, 1107s, 1091s, 1067m, 1049s, 1024m, 972s, 921s, 803w, 742s, 695s, 643m, 556w, 515m, 490m and 435m. FAB mass spectrum: *m/z* 468, [*M*]$^+$.

(C₆H₄O₂)PN(C₅H₁₀)NP(C₆H₄O₂) $(C_6H_4O_2)PN(C_5H_{10})NP(C_6H_4O_2)$ **49.** A solution of 1,2-phenylenephosphoro-chloridite (4.65g, 16.7 mmol) in thf (55.0 cm³) was added dropwise over a period of 1 h to a stirred solution of homopiperazine (0.84 g, 8.3 mmol) and triethylamine (1.69 g, 2.3 cm³, 16.7 mmol) in thf (85 0 cm³). Stirring was continued for a further 2 h, during which time triethylammonium hydrochloride separated from the colourless solution. This precipitate was removed by suction filtration and the filtrate evaporated to dryness *in vacuo* to give a white solid product. Yield: 2.58 g, 82 %. Microanalysis: Found (Calcd. for $C_{17}H_{18}N_2O_4P_2$) C 53.8 (54.3), H 4.3 (4.8), N 6.9 (7.4) %. ^{31}P-{^1H} NMR (CDCl₃): δ(P) 148.3. IR (KBr disc, cm⁻¹): 3061w, 2941w, 1477s, 1459m, 1373m, 1339m, 1315w, 1284w, 1233s, 1163m, 1116m, 1095m, 1052w, 1007w, 993m, 983m, 916m, 818s, 755m, 736m, 684m, 666m, 613m, 533w, 510m, 409w and 388w. FAB mass spectrum: *m/z* 376, [*M*]⁺.

(C₂H₄O₂)PN(C₅H₁₀)NP(C₂H₄O₂) $(C_2H_4O_2)PN(C_5H_{10})NP(C_2H_4O_2)$ **50.** A solution of 2-chloro-1,3,2-dioxaphospholane (5.69 g, 4.0 cm³, 45.0 mmol) in thf (55.0 cm³) was added dropwise over a period of 1 h to a stirred solution of homopiperazine (2.25 g, 22.5 mmol) and triethylamine (4.54 g, 6.2 cm³, 45.0 mmol) in thf (100 0 cm³). Stirring was continued for a further 2 h, during which time triethylammonium hydrochloride separated from the colourless solution. This precipitate was removed by suction filtration and the filtrate evaporated to dryness *in vacuo* to give a white solid product. Yield 4.91 g, 78 %. Microanalysis: Found (Calcd. for $C_9H_{18}N_2O_4P_2$) C 38.8 (38.6), H 6.8 (6.4), N 10.4 (10.0) %. ^{31}P-{^1H} NMR (CDCl₃)· δ(P) 143.8. IR (KBr disc, cm⁻¹)· 2959w, 2887w, 1450m, 1372w, 1317w, 1282w, 1199s, 1048s, 991m, 931m, 907m, 747m, 681m, 595w, 551m, 524m, 420w and 206m. FAB mass spectrum: *m/z* 376, [*M*]⁺.

cis-**[PtCl₂{Ph₂PN(C₅H₁₀)NPPh₂}]** *cis*-[PtCl₂{Ph₂PN(C₅H₁₀)NPPh₂}] **51.** To a solution of [PtCl₂(cod)] (0.100 g, 0.26 mmol) in dichloromethane (10.0 cm³) was added solid Ph₂PN(C₅H₁₀)NPPh₂ (0.125 g, 0 26 mmol) and the colourless solution stirred for *ca* 2 h. The solution was concentrated under reduced pressure to *ca* 1.0 cm³ and diethyl ether (40.0 cm³) added. The white product was collected by suction filtration. Yield: 0.180 g, 92 %. Microanalysis: Found (Calcd for $C_{29}H_{30}Cl_2N_2P_2Pt$) C, 46.4 (47.5), H 3.9 (4.1), N 3.4 (3.8) %. ^{31}P-{^1H} NMR (CDCl₃): δ(P) 64 1, $^1J(^{195}Pt$-$^{31}P)$ 4092 Hz. IR (KBr disc, cm⁻¹): 3056w, 3020w, 2941w, 2921w, 2864w, 1479m, 1465w, 1455w, 1436s, 1363w,

118

1274m, 1179s, 1098s, 1037s, 999m, 949w, 936m, 896m, 850w, 745s, 757m, 712m, 691s, 664m, 619w, 584m, 555m, 534m, 508s, 475m, 445w, 390w, 355w, 300m and 277m. FAB mass spectrum: m/z 734, $[M]^+$.

cis-[PtCl$_2$\{(C$_6$H$_4$O$_2$)PN(C$_5$H$_{10}$)NP(C$_6$H$_4$O$_2$)\}] 52. To a solution of [PtCl$_2$(cod)] (0.179 g, 0.48 mmol) in dichloromethane (15.0 cm^3) was added solid (C$_6$H$_4$O$_2$)PN(C$_2$H$_4$)$_2$NP(C$_6$H$_4$O$_2$) (0.180 g, 0.48 mmol) and the colourless solution stirred for *ca* 2 h. The solution was concentrated under reduced pressure to *ca* 1.0 cm^3 and diethyl ether (30.0 cm^3) added. The white product was collected by suction filtration. Yield: 0.104 g, 84 %. Microanalysis: Found (Calcd for C$_{17}$H$_{18}$Cl$_2$N$_2$O$_4$P$_2$Pt) C, 31.5 (31.8), H 2 9 (2.8), N 3.9 (4.4) %. ^{31}P-\{^{1}H\} NMR (CDCl$_3$): δ(P) 102.3, ^1J(^{195}Pt-^{31}P) 5466 Hz. IR (KBr disc, cm^{-1}): 2946w, 2885w, 2618w, 1478s, 1376w, 1330m, 1231s, 1156m, 114m, 1095m, 1053w, 1009m, 951m, 859s, 747m, 686w, 626m, 545m, 421w, 306m and 279m. FAB mass spectrum: m/z 606, $[M - Cl]^+$.

cis-[PtMe$_2$\{Ph$_2$PN(C$_5$H$_{10}$)NPPh$_2$\}] 53. To a solution of [PtMe$_2$(cod)] (0.100 g, 0.30 mmol) in dichloromethane (10 0 cm^3) was added solid Ph$_2$PN(C$_5$H$_{10}$)NPPh$_2$ (0.140 g, 0.30 mmol) and the colourless solution stirred for *ca* 2 h. The solution was concentrated under reduced pressure to *ca* 1.0 cm^3 and diethyl ether (30.0 cm^3) added. The white product was collected by suction filtration. Yield: 0.130 g, 64 %. Microanalysis: Found (Calcd for C$_{30}$H$_{36}$N$_2$P$_2$Pt) C, 53.1 (53 6), H 4.9 (5.2), N 3.8 (4.0) %. ^{31}P-\{^{1}H\} NMR (CDCl$_3$): δ(P) 89.1, ^1J(^{195}Pt-^{31}P) 2231 Hz. IR (KBr disc, cm^{-1}): 3054w, 2932w, 2856w, 1478w, 1460w, 1435s, 1360w, 1336w, 1306w, 1272w, 1179m, 1096s, 1028s, 999w, 925w, 880m, 841w, 753m, 696s, 647m, 619w, 578m, 550w, 528m, 504s, 468m, 441w, 387w and 351w. FAB mass spectrum: m/z 678, $[M - CH_3]^+$.

cis-[PtMe$_2$\{(C$_6$H$_4$O$_2$)PN(C$_5$H$_{10}$)NP(C$_6$H$_4$O$_2$)\}] 54. To a solution of [PtMe$_2$(cod)] (0.100 g, 0.30 mmol) in dichloromethane (10.0 cm^3) was added solid (C$_6$H$_4$O$_2$)PN(C$_2$H$_4$)$_2$NP(C$_6$H$_4$O$_2$) (0.114 g, 0.30 mmol) and the colourless solution stirred for *ca* 2 h The solution was concentrated under reduced pressure to *ca* 1.0 cm^3 and diethyl ether (35.0 cm^3) added. The white product was collected by suction filtration. Yield: 0.120 g, 66 %. Microanalysis: Found (Calcd for C$_{19}$H$_{24}$N$_2$O$_4$P$_2$Pt) C,

37.1 (37.9), H 3.9 (4.0), N 4 5 (4.7) %. ^{31}P-{^{1}H} NMR (CDCl$_3$) δ(P) 156.9, $^1J(^{195}$Pt-^{31}P) 2937 Hz. IR (KBr disc, cm^{-1}): 2942w, 2883w, 1655w, 1480s, 1375w, 1335m, 1234s, 1162m, 1113m, 1096m, 1054m, 1008m, 919m, 826s, 738s, 675m, 623m, 535m, 421w and 233w FAB mass spectrum: m/z 586, [$M-$CH$_3$]$^+$.

cis-[PdCl$_2${Ph$_2$PN(C$_5$H$_{10}$)NPPh$_2$}] 55. To a solution of [PdCl$_2$(cod)] (0.152 g, 0.53 mmol) in dichloromethane (20.0 cm^3) was added solid Ph$_2$PN(C$_5$H$_{10}$)NPPh$_2$ (0.250 g, 0.53 mmol) and the yellow solution stirred for ca 2 h The solution was concentrated under reduced pressure to $ca.$ 1.0 cm^3 and diethyl ether (40.0 cm^3) added. The yellow product was collected by suction filtration. Yield: 0.300 g, 87 % Microanalysis: Found (Calcd for C$_{29}$H$_{30}$Cl$_2$N$_2$P$_2$Pd) C 53 3 (54.0), H, 4.8 (4.7), N 4 2 (4.4) %. ^{31}P-{^{1}H} NMR (CDCl$_3$): δ(P) 92 6 IR (KBr disc, cm^{-1}): 3051w, 2921w, 1479w, 1453w, 1437s, 1375w, 1347w, 1282w, 1176m, 1098s, 1036s, 1000w, 953m, 896m, 855w, 820w, 755s, 711m, 697s, 660m, 619w, 580m, 548m, 528w, 505s, 484m, 312m and 289m. FAB mass spectrum: m/z 646, [M]$^+$.

cis-[PdCl$_2${(C$_6$H$_4$O$_2$)PN(C$_5$H$_{10}$)NP(C$_6$H$_4$O$_2$)}] 56. To a solution of [PdCl$_2$(cod)] (0.285 g, 1.00 mmol) in dichloromethane (25 0 cm^3) was added solid (C$_6$H$_4$O$_2$)PN(C$_5$H$_{10}$)NP(C$_6$H$_4$O$_2$) (0.378 g, 1.00 mmol) and the yellow solution stirred for ca 2 h. The solution was concentrated under reduced pressure to ca 1.0 cm^3 and diethyl ether (30.0 cm^3) added. The yellow product was collected by suction filtration. Yield: 0.520 g, 94 % Microanalysis: Found (Calcd for C$_{17}$H$_{18}$Cl$_2$N$_2$O$_4$P$_2$Pd) C, 35.9 (36 8), H 3.6 (3.3), N 4.6 (5.0) %. ^{31}P-{^{1}H} NMR (CDCl$_3$) δ(P) 125.6. IR (KBr disc, cm^{-1}): 3067w, 2954w, 1618m, 1595m, 1477s, 1459s, 1376m, 1330m, 1261m, 1230s, 1155s, 1095s, 1052m, 1008m, 916m, 903m, 847s, 748s, 683m, 624m, 540m, 421m, 336w, 306w, 276w and 232w. FAB mass spectrum: m/z 553, [M]$^+$.

[Ph$_2$P(AuCl)N(C$_5$H$_{10}$)NP(AuCl)Ph$_2$] 57. To a solution of [AuCl(tht)] (0.192 g, 0.60 mmol) in dichloromethane (15.0 cm^3) was added solid Ph$_2$PN(C$_5$H$_{10}$)NPPh$_2$ (0.140 g, 0.30 mmol) and the colourless solution stirred for ca 1 h. The solution was concentrated under reduced pressure to ca 1.0 cm^3 and diethyl ether (35.0 cm^3) added. The white product was collected by suction filtration. Yield: 0 214 g, 76 %. Microanalysis Found (Calcd for C$_{29}$H$_{30}$Cl$_2$N$_2$P$_2$Au$_2$) C 35.6 (37.4), H 3.2 (3.2), N 2.7

(3.0) %. ^{31}P-{^{1}H} NMR (CDCl$_3$): δ(P) 78 7. IR (KBr disc, cm^{-1}): 3052w, 2019w, 1479m, 1433s, 1371m, 1346w, 1319w, 1285w, 1267m, 1240w, 1168w, 1158s, 1106s, 1060m, 1023w, 995s, 903s, 753s, 737m, 693s, 666m, 579w, 562s, 549m, 527m, 483m, 364w and 327m. FAB mass spectrum: m/z 897, $[M$ - Cl$]^+$.

[(C$_6$H$_4$O$_2$)P(AuCl)N(C$_5$H$_{10}$)NP(AuCl)(C$_6$H$_4$O$_2$)] 58. To a solution of [AuCl(tht)] (0.140 g, 0.44 mmol) in dichloromethane (15.0 cm^3) was added solid (C$_6$H$_4$O$_2$)PN(C$_5$H$_{10}$)NP(C$_6$H$_4$O$_2$) (0.083 g, 0.22 mmol) and the colourless solution stirred for *ca* 1 h. The solution was concentrated under reduced pressure to *ca* 1.0 cm^3 and diethyl ether (30.0 cm^3) added. The white product was collected by suction filtration. Yield: 0.150 g, 81 %. Microanalysis: Found (Calcd for C$_{17}$H$_{18}$Cl$_2$N$_2$O$_4$P$_2$Au$_2$) C 23.8 (24.3), H 2.1 (2.1), N 3.2 (3.3) %. ^{31}P-{^{1}H} NMR (CDCl$_3$): δ(P) 139 9. IR (KBr disc, cm^{-1}): 2952w, 1655w, 1475s, 1441s, 1375m, 1329m, 1284w, 1229s, 1151m, 1114m, 1094m, 1051m, 1006m, 908m, 867s, 776m, 764m, 744m, 686m, 637m, 556w, 423w, 393w, 332m and 224w. FAB mass spectrum: m/z 805, $[M$ - Cl$]^+$.

Chapter 5

Catalytic Studies of Diphosphinoamine Ligands

5.1 *Introduction*

Using the Catalyst Evaluation services at BP Chemicals Ltd and St. Andrews University, tests were performed on a number of the prepared ligands to ascertain their ability to promote the palladium catalysed formation of polyketone from CO and ethene. A total of six ligands were screened. The diphenylphosphine derivatives of N,N'-dimethylurea, $[\{Ph_2PN(Me)\}_2CO]$, N,N'-dimethylthiourea, $[\{Ph_2PN(Me)\}_2CS]$, N,N'-diethylthiourea, $[\{Ph_2PN(Et)\}_2CS]$, and hydrazine, $[Ph_2PN(C_2H_4)_2NPPh_2]$, were all tested at the CATS service at St. Andrews University and two palladium complexes containing diphosphine derivatives of N,N'-dimethylhydrazine, $[Pd(C_8H_{12}OCH_3)\{(C_6H_4\text{-}o\text{-}OCH_3)_2PN(Me)N(Me)P(C_6H_4\text{-}o\text{-}OCH_3)_2\}]^+PF_6^-$ and $[Pd(C_8H_{12}OCH_3)\{(C_6H_4\text{-}o\text{-}CH_3)_2PN(Me)\ N(Me)\ P(C_6H_4\text{-}o\text{-}CH_3)_2\}]^+PF_6^-$, were tested at BP Chemicals Ltd, Sunbury-on-Thames.

5.2 *Results and discussion*

Test results involving all six ligands were poor and showed little or no production of polymeric material. The results of the screenings conducted at CATS are summarised in Table 5.1. The test with dppe was carried out in order to check the protocol of the experiments and, other than in this control, polymeric material was not formed in any of the other experiments, only low levels of oligomeric materials, with n = 0-2. Metallic looking residues were apparent in all cases in addition to varying amounts of $Ph_2P(O)OMe$ and other unidentified ligand decomposition products within the reaction medium. The ligands would appear to be unstable to the methanol reaction medium and rapidly undergo some form of methanolysis of the P-N bond. Reducing the temperature of the reaction from 85 °C to 65 °C (experiment 8) did not influence the ligand stability. One small noteworthy observation is that in experiments involving the ligand with a piperazine backbone (5, 6 and 8) the diester oligomers are

Expt	Ligand	Observations	Relative amounts by GCMS (Arbitrary Units)							
			n = 0		n = 1			n = 2		
			Methylpropionate	Diethylketone	Keto-ester	Diester	Diketone	Keto-ester	Diester	Diketone
7	dppe	Reaction medium a solid mass of polymer, weight 6 8 g	0 8	5.7	8.4	2.4	2.3	1.7	0.6	0.4
1	$\{Ph_2PN(Me)\}_2CO$	Darkly coloured solid residue Traces of $Ph_2P(O)OMe$ together with other ligand decomposition fragments	3.8	0.6	6 3	0.5	0.1	0.6	0.3	-
4	$\{Ph_2PN(Me)\}_2CO$	Darkly coloured solid residue Traces of $Ph_2P(O)OMe$ together with other ligand decomposition fragments	1.2	0.2	1.2	2.3	-	-	0.6	-
3	$\{Ph_2PN(Me)\}_2CS$	Darkly coloured solid residue Traces of $Ph_2P(O)OMe$	0.2	0.3	-	-	-	-	-	-
2	$\{Ph_2PN(Et)\}_2CS$	Darkly coloured solid residue Traces of $Ph_2P(O)OMe$ and larger amounts of $Ph_2P(S)OMe$ or $Ph_2P(O)SMe$	2.7	-	2.1	0.5	-	-	-	-
5	$Ph_2PN(C_2H_4)_2NPPh_2$	Darkly coloured solid residue Large amounts of $Ph_2P(O)OMe$	0.1	-	0.1	2 2	-	-	0.6	-
6	$Ph_2PN(C_2H_4)_2NPPh_2$	Darkly coloured solid residue Large amounts of $Ph_2P(O)OMe$	0.2	-	0.3	5.5	-	-	1.1	-
8	$Ph_2PN(C_2H_4)_2NPPh_2$	Darkly coloured solid residue Large amounts of $Ph_2P(O)OMe$	-	-	0.2	2.8	-	0.5	1.7	-

Table 5.1 Test results from the Catalyst Evaluation Service at St. Andrews University.

formed in preference to the normally observed keto-esters, with a diester:keto-ester ratio of 20:1.

Unfortunately, the tests conducted at BP Chemicals Ltd on the diphosphine derivatives of N,N'-dimethylhydrazine failed to give sufficient amounts of polymeric material to conduct any detailed analysis.

5.1 *Conclusions.*

The test results show that the particular ligands used do not promote the palladium-catalysed formation of polyketone from CO and ethylene under the conditions employed. It would be of interest to carry out further experiments in aprotic solvents to determine whether the ligand breakdown observed might be avoided. Also further tests with ligands containing different diphosphine groups would give a greater indication as to whether the relevant ligand backbones (i.e. urea, thiourea, hydrazine and piperazine) or the phosphine substituents exert a greater influence on the ability of the ligands to promote catalytic activity.

Experimental

St Andrews University· In all cases, with the exception of experiments 6 and 8, a 250 cm^3 batch autoclave fitted, with a glass liner and magnetic stirrer bar for mixing, was used. The catalysts were prepared *in-situ* from Pd(OAc)$_2$ (5.0 x 10^{-5} mol), (P-P) (5 0 x 10^{-5} mol) and p-toluenesulfonic acid (11 x 10^{-5} mol) in 10 cm^3 of methanol as solvent (catalyst concentration 5.0 x 10^{-3} mol dm^{-3}). The batch autoclave experiments were charged with an initial 45 bar of CO/ethene (1:1) and the reactions carried out at 85 °C for 17 h.

In experiment 6 the catalyst concentration was reduced to 2.0 x 10^{-3} mol dm^{-3} and the reaction time to 5 h.

In experiment 8 the catalyst concentration was reduced to 2 0 x 10^{-3} mol dm^{-3} (prepared *in-situ* from [Pd(MeCN)$_2$(p-tolSO$_3$)$_2$] (1.0 x 10^{-4} mol) and (P-P) (1 2 x 10^{-4}) in 50 cm^3 methanol). The reaction temperature and time were also reduced to 65 °C and 5 h, respectively.

BP Chemicals Ltd CO/ethene/propene termonomers were prepared as follows: dichloromethane (80 cm³) was charged into a dry 300 cm³ autoclave under nitrogen. This was cooled to –78 °C and then propene (12.0 g) was condensed in. The stirred autoclave was then heated to a temperature of 70 °C and pressurised to 45 bar using a 1:1 mixture CO and ethene. A solution of borane in 10 cm³ dichloromethane was introduced, followed by more dichloromethane (10 cm³). The procatalyst was then introduced as a solution in 10 cm³ dichloromethane, followed by a further 10 cm³ dichloromethane, thus bringing the total volume of this solvent in the autoclave to 120 cm³. The pressure was adjusted to 50 bar by addition of 1:1 CO/ethene and maintained at this pressure throughout the polymerisation by addition of the aforementioned gas mixture on demand from a ballast vessel of known volume After 3 h the pressure was released and the polymerisation mixture cooled to room temperature. Any resultant white polymer was isolated by filtration, washed with methanol and dried under reduced pressure.

Appendix

Single Crystal X-ray Crystallography Data.

Details of data collections and refinements for;

cis-[PtCl$_2$\{\{Ph$_2$PN(Me)\}$_2$CO\}]

cis-[PtCl$_2$\{\{Ph$_2$PN(Et\}$_2$CO\}]

cis-[PdCl$_2$\{\{Ph$_2$PN(Me)\}$_2$CO\}]

cis-[PdCl$_2$\{\{Ph$_2$PN(Et)\}$_2$CO\}]

[Pd\{OPPh$_2$\}\{N(Me)C(O)N(Me)PPh$_2$\}]$_2$

[Pd\{OPPh$_2$\}\{N(Et)C(O)N(Et)PPh$_2$\}]$_2$.CH$_2$Cl$_2$

cis-[Mo(CO)$_4$\{Ph$_2$PN(Me)C(O)N(Me)PPh$_2$\}]

[Ph$_2$P\{AuCl\}N(Et)C(O)N(Et)P\{AuCl\}Ph$_2$].CHCl$_3$

[PtCl$_2$\{(Ph$_2$)PN(Me)CSN(Me)H-P,S\}].dmso CHCl$_3$

cis-[PdCl$_2$\{(PhO)$_2$PN(Et)N(Et)P(OPh)$_2$\}]

cis-[PtCl$_2$\{(C$_6$H$_4$-o-OCH$_3$)$_2$PN(Et)N(Et)P(C$_6$H$_4$-o-OCH$_3$)$_2$\}].CH$_2$Cl$_2$

cis-[PdCl$_2$\{Ph$_2$PN(C$_2$H$_4$)$_2$NPPh$_2$\}]
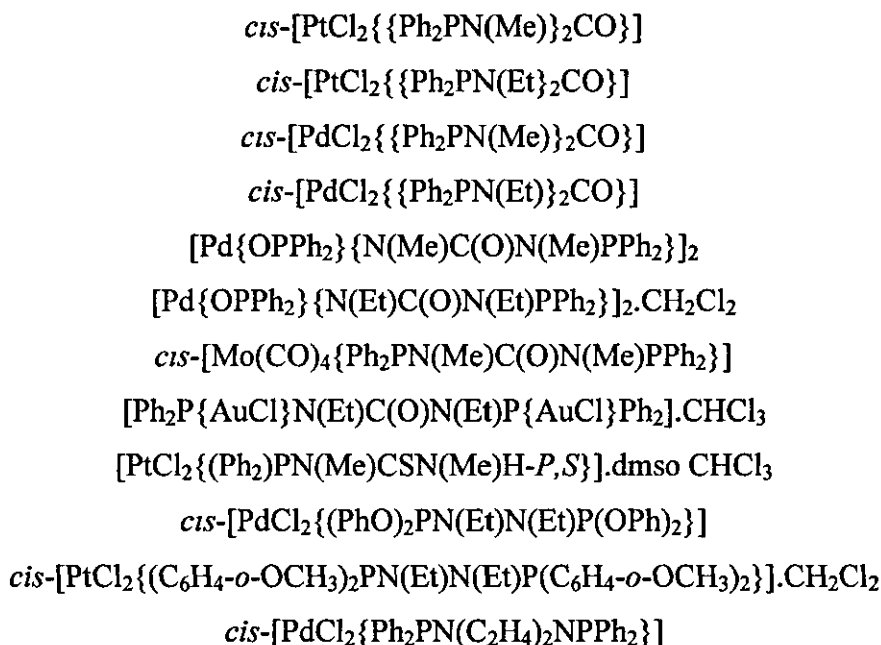
All crystallographic work on the above was carried out at Loughborough University.

Compound	3	4	9
Empirical Formula	$C_{27}H_{26}Cl_2N_2OP_2Pt$	$C_{29}H_{30}Cl_2N_2OP_2Pt$	$C_{27}H_{26}Cl_2N_2OP_2Pd$
Formula Weight	722.4	750 5	633.7
Colour/size (mm)	Clear / 0.16 x 0.16 x 0.28	Clear / 0.08 x 0 1 x 0.2	Yellow / 0.05 x 0.05 x 0.1
Crystal System	Orthorhombic	Triclinic	Monoclinic
Space Group	$P2_1cn$	P1	$P2_1/c$
a (Å)	10.0447 (5)	9.8640 (4)	9.90760 (10)
b (Å)	14 4768 (7)	10.8209 (4)	14.6999 (2)
c (Å)	18.5427 (9)	15.1644 (6)	19 0506 (2)
α (°)	90	78.4300 (10)	90
β (°)	90	80.0560 (10)	101.70
γ (°)	90	66.6640 (10)	90
Volume (Å^3)	2696.4 (2)	1448.16 (10)	2716.94 (5)
Z	4	2	4
Density (calc., Mg/cm^3)	1.780	1.721	1.549
μ (mm^{-1})	5.544	5.165	1.021
F (000)	1408	736	1280
Ind. Refl.	3199	6504	3916
Final R1/wR2	0.0209 / 0.0389	0 0257 / 0.0590	0.0263 / 0 0576
Goodness of fit on F^2	0.828	0.978	0.964
Largest Diff. Peak/Hole (eÅ^{-3})	0 525, -0.600	1.971, -1.570	0.380, -0.492

Compound	10	11	12.CH$_2$Cl$_2$
Empirical Formula	C$_{37}$H$_{42}$Cl$_4$N$_2$OP$_2$Pd	C$_{56}$H$_{56}$Cl$_4$N$_4$O$_4$P$_4$Pd	C$_{59}$H$_{62}$Cl$_2$N$_4$O$_4$P$_4$Pd
Formula Weight	947.3	1327.5	1298.7
Colour/size (mm)	Yellow / 0.06 x 0 2 x 0.2	Yellow / 0.06 x 0.1 x 0.2	Yellow / 0.1 x 0.15 x 0.15
Crystal System	Monoclinic	Triclinic	Monoclinic
Space Group	P2$_1$/c	P1	P2$_1$/n
a (Å)	14.2866 (3)	11.6946 (3)	10 4350 (2)
b (Å)	27 6453 (5)	15.4866 (6)	18.7436 (3)
c (Å)	9.7662 (2)	18.5407 (3)	15.69190 (10)
α (°)	90	76.1840 (10)	90
β (°)	92.6320 (10)	71.8340 (10)	94.3620 (10)
γ (°)	90	72.8060 (10)	90
Volume (Å^3)	3853.16 (13)	3007.91 (12)	3060.28 (8)
Z	4	2	2
Density (calc., Mg/cm^3)	1.633	1.486	1.409
μ (mm^{-1})	1.326	0.930	0.826
F (000)	1904	1364	1324
Ind. Refl.	9018	8562	4475
Final R1/wR2	0.0470 / 0.1041	0.0430 / 0.1130	0.1033 / 0.2379
Goodness of fit on F^2	0.969	1 022	0.891
Largest Diff. Peak/Hole (eÅ^{-3})	0.893, -1.100	2.305, -0.463	1.707, -3.409

Compound	13	15.CHCl$_3$	17.dmso.CHCl$_3$
Empirical Formula	C$_{31}$H$_{26}$MoN$_2$O$_5$P$_2$	C$_{50}$H$_{51}$Au$_2$Cl$_5$N$_2$OP$_2$	C$_{18}$H$_{23}$Cl$_5$N$_2$OPPtS$_2$
Formula Weight	664.42	1068.7	750.8
Colour/size (mm)	Clear / 0.04 x 0.15 x 0.2	Clear / 0.1 x 0.1 x 0 3	Clear / 0.16 x 0.14 x 0.06
Crystal System	Monoclinic	Monoclinic	Triclinic
Space Group	P2$_1$/c	P2$_1$/c	P1
a (Å)	12.05470 (10)	14.5596 (5)	11.4044 (5)
b (Å)	17.0186 (2)	15.4267 (5)	11.5628 (5)
c (Å)	14.662	16.1541 (5)	11.9275 (5)
α (°)	90	90	69.23
β (°)	94 4850 (10)	98.36	71.9290 (10)
γ (°)	90	90	74.8710 (10)
Volume (Å^3)	2998.72 (4)	3589 8 (2)	1377.76 (10)
Z	4	4	2
Density (calc., Mg/cm^3)	1.472	1.977	1.810
μ (mm^{-1})	0.586	8.652	5.800
F (000)	1352	2024	726
Ind. Refl.	4303	8391	3885
Final R1/wR2	0.0251 / 0.0609	0.0354 / 0.0752	0 0503 / 0.1149
Goodness of fit on F^2	0.950	0.849	0.622
Largest Diff. Peak/Hole (eÅ^{-3})	0.227, -0.264	1.245, -1.011	2.564, -4.492

Compound	26	31.CH$_2$Cl$_2$	42
Empirical Formula	C$_{28}$H$_{30}$Cl$_2$N$_2$O$_4$P$_2$Pd	C$_{33}$H$_{39}$Cl$_5$N$_2$O$_4$P$_2$Pt	C$_{28}$H$_{28}$Cl$_5$N$_2$P$_2$Pd
Formula Weight	697.8	961.9	631.8
Colour/size (mm)	Yellow / 0.15 x 0.2 x 0.2	Clear / 0.08 x 0.1 x 0.12	Clear / 0.04 x 0.1 x 0.1
Crystal System	Monoclinic	Monoclinic	Monoclinic
Space Group	P2$_1$/n	C2/c	P2$_1$/n
a (Å)	22.2887 (4)	24.3478 (7)	11.2228 (11)
b (Å)	8 8062 (2)	14.2665 (3)	27.882 (3)
c (Å)	32.0433 (5)	14.7842 (4)	17.936 (2)
α (°)	90	90	90
β (°)	105.61	111.4580 (10)	96.646 (3)
γ (°)	90	90	90
Volume (Å^3)	6057.3 (2)	4779 5 (2)	5574.9 (9)
Z	8	4	8
Density (calc., Mg/cm^3)	1.530	1.373	1 505
μ (mm^{-1})	0.931	3.316	0.922
F (000)	2832	1964	2560
Ind. Refl.	8687	5551	8047
Final R1/wR2	0.0449 / 0.0728	0.0874 / 0.1953	0.0827 / 0.1570
Goodness of fit on F^2	1.009	0.964	0.880
Largest Diff. Peak/Hole (eÅ^{-3})	0.338, -0.328	3.119, -4.798	1.112, -1.319

References.

1   L. H. Pignolet (Ed.), *Homogeneous Catalysis with Metal Phosphine Complexes*, Plenum Press, New York, 1983.

2   R. B. King, *Transition Metal Organometallic Chemistry An Introduction*, Academic Press, New York, 1969.

3   C. A. McAuliffe in *Comprehensive Coordination Chemistry*, eds. G. Wilkinson, R. D. Gillard and J. A. McCleverty, Pergamon Press, Oxford, 1987, Volume 2, p. 989.

4   A. Pidcock in *Transition Metal Complexes of Phosphorus, Arsenic and Antimony Ligands*, ed. C. A. McAuliffe, MacMillan, London, 1973, p. 3.

5   C. A. Tolman, *Chem Rev.*, 1977, **77**, 313.

6   G. Booth, *Adv. Inorg Chem Radiochem.*, 1964, **6**, 1.

7   G. R. Dobson, I. W. Stolz and R. K. Sheline, *Adv Inorg Chem Radiochem*, 1965, **8**, 1.

8   R. G. Hayter in *Preparative Inorganic Reactions*, ed. W. L. Jolley, Vol 2, Wilet-Interscience, New York, 1965, p. 228.

9   W. Levason and C. A. McAuliffe, *Adv Inorg Chem Radiochem*, 1972, **14**, 173.

10 G. Wilkinson, F. G. A. Stone and E. W. Abel (Eds.), *Comprehensive Organometallic Chemistry*, Pergamon Press, Oxford, 1982.

11 C. A. McAuliffe and W. A. Levason, *Phosphine, Arsine and Stibine Complexes of the Transition Elements*, Elsevier, Amsterdam, 1979.

12 R. J. Puddephatt, *Chem Soc Rev.*, 1983, 99.

13 I. Haiduc and I. Silaghi-Dumitrescu, *Coord Chem Rev.*, 1986, **74**, 127.

14 B. Chaudret, B. Delavaux and R. Poilblanc, *Coord Chem Rev.*, 1988, **88**, 191.

15 R. B. King, *Acc Chem Res.*, 1980, **13**, 243.

16 R. Keat, L. M. Muir, K. W. Muir and D. S. Rycroft, *J Chem Soc., Dalton Trans.* 1981, 2192.

17 H. –J. Chen, J. F. Barendt, R. C. Haltiwanger, T. G. Hill and A. D. Norman, *Phosphorus, Sulfur, Silicon and Relat Elem.*, 1986, **26**, 155.

18 J. S. Field, R. J. Haines and C. N. Sampson, *J. Chem Soc., Dalton Trans*, 1987, 1933.

19 H. Nöth and L. Meinel, *Z. Anorg Allg Chem.*, 1967, **349**, 225.

20 T. T. Bopp, M. D. Havlicek and J. W Gilje, *J Am. Chem Soc*, 1971, **93**, 3051.

21 M. D. Havlicek and J. W. Gilje, *Inorg Chem.*, 1972, **11**, 1624.

22 H. Noth and R. Ullman, *Chem Ber*, 1974, **107**, 1019.

23 K. V. Katti, V. S. Reddy and P. R. Singh, *Chem Soc Rev*, 1995, **24**, 97.

24 K. Utvary, E. Freundlinger and V. Gutmann, *Monatsch Chem.*, 1966, **97**, 348.

25 A Weisz and K. Utvary, *Monatsch Chem*, 1968, **99**, 2498.

26 N. Weferling and R. Schmutzler, *Am Chem. Soc, Symp Series, No 171, Phosphorus Chemistry* (L. D. Quin and J. G. Verkade, Ed.), 1981, 425.

27 N. Weferling, R. Schmutzler and W. S. Sheldrick, *Liebigs Ann Chem.*, 1982, 167.

28 G. Bettermann, R. Schmutzler, S. Pohl and U. Thewalt, *Polyhedron*, 1987, **6**, 1823.

29 R. Vogt and R. Schmutzler, *Z Naturforsch., Teil B*, 1989, **44**, 690.

30 W. Krueger, R. Schmutzler, H. M. Schiebel and V. Wray, *Polyhedron*, 1989, **8**, 293.

31 R. Vogt, P. G. Jones, A. Kolbe and R. Schmutzler, *Chem Ber.*, 1991, **124**, 2705.

32 P. Bhattacharyya, A. M. Z. Slawin, M. B. Smith, D. J. Williams and J. D. Woollins, *J. Chem Soc, Dalton Trans.*, 1996, 3647.

33 P. B. Hitchcock, S. Morton and J. F. Nixon, *J Chem Soc, Dalton Trans*, 1985, 1295.

34 M. Gruber, P. G. Jones and R. Schmutzler, *Chem Ber.*, 1990, **123**, 1313.

35 T. Q. Ly, A. M. Z. Slawin and J. D. Woollins, *Polyhedron*, 1999, **18**, 1761.

36 D. J. Birdsall, J. Green, T. Q. Ly, J. Novosad, M. Necas, A. M. Z. Slawin, J. D. Woollins and Z. Zak, *Eur J Inorg Chem.*, 1999, 1445.

37 M. Gruber and R. Schmutzler, *Phosphorus, Sulfur, Silicon and Relat Elem.*, 1993, **80**, 181.

38 M. Gruber and R. Schmutzler, *Phosphorus, Sulfur, Silicon and Relat Elem.*, 1993, **80**, 195.

39 M. Gruber and R. Schmutzler, *Phosphorus, Sulfur, Silicon and Relat. Elem*, 1993, **80**, 205

40 H. Noth and R. Ullmann, *Chem Ber*, 1976, **109**, 1942.

41 K. V. Katti, P. R. Singh and C. L. Barnes, *Inorg. Chem.*, 1992, **31**, 4588.

42 K. V. Katti, P. R. Singh, W. A. Volkert, A. R. Ketring and K. K. Katti, *Appl Radiat. Isot.*, 1992, **43**, 1151.

43 K. V. Katti, Y. W. Ge, P. R. Singh, S. V. Date and C. L Barnes, *Organometallics*, 1994, **13**, 541.

44 K. V. Katti, P. R. Singh and C. L. Barnes, *J. Chem. Soc , Dalton Trans* , 1993, 2153.

45 P. R. Singh, H Jimenez, K. V. Katti, W. A. Volkert and C. L. Barnes, *Inorg Chem.*, 1994, **33**, 736.

46 M. W. Wang, E. W. Volkert, P. R. Singh, K. K. Katti, P. Lusiak, K. V. Katti and C. L Barnes, *Inorg Chem.*, 1994, **33**, 1184.

47 V. S. Reddy and K. V. Katti, *Inorg Chem.*, 1994, **33**, 2695.

48 V. S. Reddy, K. V. Katti and C. L. Barnes, *Chem. Ber ,* 1994, **127**, 1355.

49 V. S. Reddy, K. V. Katti and C. L. Barnes, *Inorg Chem* , 1995, **34**, 5483.

50 V. S. Reddy, K. V. Katti and C. L. Barnes, *Chem Ber.*, 1994, **127**, 979.

51 V. S. Reddy, K. V. Katti and C. L. Barnes, *Inorg Chem* , 1995, **34**, 1273.

52 C. J. Thomas and M. N. S. Rao, *Z Anorg Allg. Chem.*, 1993, **619**, 433.

53 C. A., 1974, **80**, 134777.

54 M. J. Baker, M. F. Giles, A. G. Orpen, M. J. Taylor and R. J. Watt, *J Chem Soc , Chem. Commun.*, 1995, 197.

55 A. Sen, *Acc Chem Res.*, 1993, **26**, 303.

56 E. Drent, J. A. M. van Broekhaven and M. J. Doyle, *J. Organomet Chem* , 1991, **417**, 235.

57 A. Sen, *Adv Polym. Sci.*, 1986, **73174**, 125.

58 J Gillet, *J Polymer Photophysics and Photochemistry*, 1985, 261.

59 A. Sen, *A Chemtech*, 1986, 48.

60 Numerous patents by Shell. Representative examples: U S. Patent 4 904 744, 1990; Eur. Pat. Appl. 400 719, 1990; Eur. Pat. Appl. 373 725, 1990.

61 W. Reppe and A Magin, U. S. Pat. 2 577 208, 1951.

62 W. Reppe and A. Magin, *Chem. Abstr* , 1952, **46**, 6143.

63 T. M. Shyrne and H. V. Holler, U. S. Pat. 3 984 388, 1976.

64 T. M. Shyrne and H. V. Holler, *Chem. Abstr* , 1976, **85**, 178219.

65 A. Gough, British Pat. 1 081 304, 1967.

66 A. Gough, *Chem Abstr.*, 1967, **67**, 100569.

67 A. Sen and Ta-Wang Lai, *J Am Chem Soc*, 1982, **104**, 3520.

68 A. Sen and Ta-Wang Lai, *Organometallics*, 1984, **3**, 866.

69 E. Drent, Eur. Pat. Appl. 121 965, 1984.

70 E Drent, Eur. Pat Appl. 181 014, 1986.

71 J. A. M. van Broekhaven, E. Drent and E. Kler, Eur. Pat. Appl. 213 671, 1987.

72 J. A. M. van Broekhaven and E. Drent, Eur. Pat. Appl. 235 865, 1987.

73 E. Drent and P. H. M. Budzelaar, *Chem Rev.*, 1996, **96**, 663.

74 P. W. N. M. van Leeuwen, C. F Roobeek and H. J. Van der Heijden, *J. Am Chem Soc.*, 1994, **116**, 12117.

75 Z. Jiang, G. M. Dahlen, K. Houseknecht and A. Sen, *Macromolecules*, 1992, **25**, 2999.

76 B. A. Markies, D. Krius, M. P. H. Ruetveld, K. A. N. Verterk, J. Boersma, H. Kooijman, M. Lakın, A. L. Spek and G. Van Koten, *J Am Chem. Soc.*, 1995, **349**, 399.

77 H. Noth, *Z Naturforsch*, 1982, **37b**, 1491.

78 D. Matt, F. Ingold, F. Balegroune and D. Grandjean, *J Organomet Chem.*, 1990, **349**, 399.

79 N. W. Alcock, P. Bergamini, T. M. Gomes-Carniero, R. D. Jackson, J. Nicholls, A. G. Orpen, P. G. Pringle, S. Sostero and O. Traverso, *J Chem Soc, Chem Commun.*, 1990, 980.

80 T. Q. Ly, A. M. Z Slawin and J. D. Woollins, *J Chem Soc, Dalton Trans.*, 1997, 1611.

81 S M. Aucott, Ph.D. Thesis, Loughborough University, 1999.

82 N. Burford, S. Mason, R. E. Spence, J. M. Whelan, J F. Richardson and R. Rogers, *Organometallics*, 1992, **11**, 2241.

83 S. Okaya, H. Shimomura and Y. Kushi, *Chem Lett.*, 1992, 2019

84 R. Uson, A Laguna and M. Laguna, *Inorg. Synth.*, 1989, **26**, 85.

85 D. Drew and J. R Doyle, *Inorg. Synth.*, 1991, **28**, 346.

86 J. X. McDermott, J. F. White and G. M Whiteside, *J. Am. Chem Soc.*, 1976, **60**, 6521.

87 H. C. Clark and L. E. Manzer, *J. Organomet. Chem.*, 1973, **59**, 411.

88 J. D. Woollins (Ed.), *Inorganic Experiments*, VCH, Weinheim, 1994.

89 G. Giordano and R. H. Crabbtree, *Inorg Synth.*, 1979, **19**, 218.

90 J. F. Nixon, *J. Chem Soc A*, 1968, 2689.

91 A. R. Davies, A. T. Dronsfield, R. N. Haszeldine and D. R. Taylor, *J Chem Soc , Perkın Trans.*, 1973, **1**, 379.

92 R. Jefferson, J. F. Nixon, T. M. Painter, R. Keat and L. Stubbs, *J Chem Soc , Dalton Trans.*, 1973, 1414.

93 M. S. Balakrishna, V. S. Reddy, S. S. Krishnamurthy, J. C. T. R. Burckett St. Laurent and J. F. Nixon, *Coord Chem Rev.*, 1994, **1**, 129.

94 J. S. Field, R. J. Haines, J. Sundermeyer and S. F. Woollam, *J. Chem Soc , Dalton Trans* , 1993, 2735.

95 F. A. Cotton, W. H. Ilsley and W. Kaim, *J Am Chem. Soc.*, 1980, **102**, 1918.

96 J. S. Field, R. J. Haines and J. A. Jay, *J. Organomet Chem.*, 1978, **100**, 236.

97 D. R Derringer, P. E. Fanwick, J. Moran and R. A. Walton, *Inorg Chem ,* 1989, **28**, 1384.

98 J. I. Dulebohn, D. L. Ward and D. G. Nocera, *J Am Chem Soc.*, 1990, **112**, 2969.

99 J. Ellermann, F. A. Knoch and K. J. Meier, *Z Naturforsch , B*, 1990, **45**, 1657.

100 D. S. Dumond and M G. Rıchardson, *J Am Chem Soc.*, 1988, **100**, 7547.

101 A. Tarassoli, H. -J. Chen, M. L Thompson, U. S. Ullured, R. C. Haltiwanger and A. D. Norman, *Inorg Chem.*, 1986, **25**, 4152.

102 E. O. Fischer, W. Kellar, B. Z. Gasser and U. Schubert, *J. Organomet Chem ,* 1980, **199**, C24.

103 J. T. Mague and M. P. Johnson, *Organometallics*, 1990, **9**, 1254.

104 J. T. Mague and Z. Lin, *Organometallıcs*, 1992, **11**, 4139.

105 R. P. Kamalesh Babu, S. S. Krishnamurthy and M. Nethali, *J Organomet Chem.*, 1993, **454**, 157.

106 E. Rotondo, *Inorg Chem.*, 1976, **15**, 2102.

107 G. J. P. Britovsek, V. C. Gibson and D. F. Wass, *Angew Chem Int Ed.*, 1999, **38**, 428.

108 M. A. Bennett, T. N. Huang, T. W. Matheson and A. R. Smıth, *Inorg Synth ,* 1982, **21**, 74.